# THE EFFECTS OF SYNAPTIC MODULATION ON THE VIBROTACTILE RESPONSES OF SOMATOSENSORY CORTICAL NEURONS STUDIED BY MICROINJECTION, MICROSTIMULATION AND A COMPUTATIONAL MODEL

by

**Bige Vardar**

B.S. in Bioengineering, Istanbul Technical University, 2010

B.S. in Bioengineering, Montana State University, 2010

M.S. in Pharmaceutical Sciences, University of Copenhagen, 2012

Submitted to the Institute of Biomedical Engineering

in partial fulfillment of the requirements

for the degree of

Doctor

of

Philosophy

Boğaziçi University

2019

# THE EFFECTS OF SYNAPTIC MODULATION ON THE VIBROTACTILE RESPONSES OF SOMATOSENSORY CORTICAL NEURONS STUDIED BY MICROINJECTION, MICROSTIMULATION AND A COMPUTATIONAL MODEL

**APPROVED BY:**

| | |
|---|---|
| Prof. Dr. Burak Güçlü<br>(Thesis Advisor) | ..... |
| Prof. Dr. Can Yücesoy | ..... |
| Prof. Dr. Hale Saybaşılı | ..... |
| Prof. Dr. Neslihan Serap Şengör | ..... |
| Assist. Prof. Dr. İsmail Devecioğlu | ..... |

**DATE OF APPROVAL:** 9 May 2019

*To my beloved mother, Dr. Zeynep VARDAR, and father, Dr. Burak VARDAR*

*Annem Dr. Zeynep VARDAR ve babam Dr. Burak VARDAR'a*

# ACKNOWLEDGMENTS

I would like to take this opportunity to thank all my colleagues who helped and supported me throughout this project.

My special gratitude goes to Prof. Dr. Burak Güçlü, who gave me the opportunity to conduct this study, as well as his great help and guidance throughout the experimental work and writing. His feedback and advice were invaluable. During last 6 years working with him, I have gained a lot experience and confidence.

I thank to Prof. Dr. Can Yücesoy, Prof. Dr. Hale Saybaşılı, Prof. Dr. Neslihan Serap Şengör and Assist. Prof. Dr. İsmail Devecioğlu for being in my thesis committee and for their precious comments.

I am thankful to all Tactile Research Lab members (Sevgi Öztürk, Elçin Tunçkol, Deniz Kılınç, Sedef Yusufoğulları, İpek Karakuş, Samet Kocatürk, Ürün Eşen, Begüm Devlet) for their great kindness, advice and assistance as well as their great support in the lab.

I am grateful to my dearest family and friends, Damla Dinçer, Pırıl Yüksel, Toprak Yazır, and Orkun Akcan, for their everlasting support, and for making my life easier throughout the PhD work. I know it would not be the same without you. Lastly, I owe a sincere and earnest thankfulness to Mert Zeydanlı for keeping my mind off of work, sharing his office and helping me getting through the long hours of swimming.

This work was supported by Boğaziçi University Research Fund Grant no: 17XP2 (PI: Prof. Dr. Burak Güçlü)

# ACADEMIC ETHICS AND INTEGRITY STATEMENT

I, Bige Vardar, hereby certify that I am aware of the Academic Ethics and Integrity Policy issued by the Council of Higher Education (YÖK) and I fully acknowledge all the consequences due to its violation by plagiarism or any other way.

Name :

Signature:

Date:

# ABSTRACT

## THE EFFECTS OF SYNAPTIC MODULATION ON THE VIBROTACTILE RESPONSES OF SOMATOSENSORY CORTICAL NEURONS STUDIED BY MICROINJECTION, MICROSTIMULATION AND A COMPUTATIONAL MODEL

In this thesis, we studied the effects of synaptic modulation on the vibrotactile responses of somatosensory cortical neurons by three different methods: microinjection, microstimulation and a computational model. First, we recorded single-unit spikes evoked by sinusoidal (duration: 500 ms; frequency: 5, 40, and 250 Hz; amplitude: 100 $\mu$m) stimulation of the glabrous skin. The changes in the responses were studied with microinjection of aCSF (sham), bicuculline, AMPA and NMDA near the isolated neurons in anesthetized rats. All drugs increased average firing rates only during vibrotactile stimulation, and increased entrainment as measured by the vector strength of spike phases. The results suggest that three inhibitory factors shape the spike responses of the neurons. In a different experiment, we electrically stimulated Basal forebrain (BF), the main source of cortical cholinergic inputs, of anesthetized rats while recording single-unit (n=87) spike activity in the SI cortex. The vibrotactile responses were measured with and without BF stimulation (0.5-ms bipolar pulses (50 $\mu$A) at 100 Hz for 0.5 s). BF activation had short-term and long-lasting significant effects on entrainment, but being effective only at 5-Hz mechanical stimulation. BF activation did not cause significant main effects (regardless of cell type and layer) on the firing rate measures. Long-lasting effects of cholinergic activation on entrainment are dependent on cell type and layer, probably due to the projection pattern from BF. Lastly, a preliminary computational model was generated mimicking the vibrotactile responses observed in the first experiment. By changing the model parameters, the effects of synaptic inputs can be simulated. Overall, this thesis may help to understand clinical conditions regarding excitation-inhibition balance and cholinergic modulation.

**Keywords: Somatosensory, Attention, Cholinergic, GABAergic, Glutamatergic.**

# ÖZET

## SİNAPTİK MODÜLASYONUN BEDENDUYUSU KORTİKAL NÖRONLARININ TİTREŞİMSEL YANITLARI ÜZERİNDEKİ ETKİSİNİN MİKROENJEKSİYON, MİKROUYARIM VE HESAPLAMALI MODEL İLE İNCELENMESİ

Bu tez çalışmasında, sinaptik modülasyonun bedenduyusu kortikal nöronlarının titreşimsel yanıtları üzerindeki etkisini üç yöntem ile inceledik: mikroenjeksiyon, mikrouyarım ve hesaplamalı model. İlk olarak, kılsız deri üzerine uygulanan sinuzoidal titreşimlere (süre: 500ms; frekans: 5, 40, 250 Hz; genlik: 100$\mu$m) yanıt veren tekil nöronlardan kayıt aldik. Aksiyon potansiyellerindeki değişimi nöronların çevresine mikroenjeksiyon yöntemiyle verilen suni beyin omurilik sıvısı, bikukulin, AMPA ve NMDA ile inceledik. Tüm ilaçlar, ortalama aksiyon potansiyeli sayılarını (OAPS) ve vektör gücünü(VG) sadece mekanik uyaranın geldiği zaman aralığında arttırmıştır. Sonuçlar göstermektedir ki nöron aktivitesi üç baskılama faktörü ile şekillenmektedir. Farklı bir deneyde, kortikal kolinerjik girdi merkezi olan basal önbeyin (BO) bölgesini elektriksel olarak uyarırken arka ayak bölgesine ilişkin bedenduyusu korteksindeki tekil nöronlardan (n=87) kayıt aldık. Nöron kayıtlari BO uyarımının (10ms ara ile 50 tane 0.5-ms'lik bipolar darbe (50$\mu$A)) olduğu ve olmadığı durumlarda yapılmıştır. BO aktivasyonu, VG üzerinde istatistiksel olarak anlamlı kısa ve uzun süreli etki yaratmıştır. Bu etki, sadece 5-Hz'lik mekanik uyaranda gözlemlenmiştir. BO aktivasyonu (nöron tipi ve kortikal katmandan bağımsız) OAPS'de bir değişiklik yaratmamıştır. Kolinerjik aktivasyonun VG üzerindeki uzun süreli etkisi nöron tipine ve kortikal katmana bağlıdır. Son olarak, ilk çalışmada elde edilen deneysel veri kullanılarak bir hesaplamalı model yapılmıştır. Model parametreleri değiştirilerek, sinaptik girdilerin etkileri modellenebilir. Sonuç olarak, bu tez çalışması etkinleştirme-baskılama dengesi ve kolinerjik modülasyona bağlı klinik durumları anlamakta yardımcı olabilir.

**Anahtar Sözcükler: Beden duyusu, Dikkat, Kolinerjik, GABAerjik, Glutamaterjik.**

# TABLE OF CONTENTS

# LIST OF FIGURES

# LIST OF TABLES

# LIST OF SYMBOLS

| | |
|---|---|
| $R_b$ | Background average firing rate |
| $R_o$ | Average firing rate during initial 100-ms period of the stimulus |
| $R_d*$ | Average firing rate during the remaining portion of the stimulus |
| $R_d$ | Average firing rate during entire mechanical stimulus(500-ms) |
| $k_{1e}$ | Self-decay constant for excitatory neuron |
| $k_{1i}$ | Self-decay constant for inhibitory neuron |
| $k_{2e}$ | Refractory period for excitatory neuron |
| $k_{2i}$ | Refractory period for inhibitory neuron |
| $\tau_e$,$\tau_i$ | Decay constant for excitatory neuron and inhibitory neuron |
| $w_{ee}$ | Excitatory synaptic weight onto excitatory neuron |
| $w_{ei}$ | Excitatory synaptic weight onto inhibitory neuron |
| $w_{ie}$ | Inhibitory synaptic weight onto excitatory neuron |
| $w_{ii}$ | Inhibitory synaptic weight onto inhibitory neuron |
| $w_{te}$ | Thalamic synaptic weight onto excitatory neuron |
| $w_{ti}$ | Thalamic synaptic weight onto inhibitory neuron |
| d | Varying parameter in activation function P |
| C | Maximum peak response |
| $\sigma$ | Time-to-peak |
| P | Activation function |
| E | Excitatory neuron |
| I | Inhibitory neuron |
| Th | Thalamic neuron |
| $T_0$ | Basal Thalamic rate |
| $\alpha$2-$\alpha$10 | Subunits of nicotinic acetylcholine receptors |
| $\beta$2-$\beta$10 | Subunits of nicotinic acetylcholine receptors |
| Ch1-Ch4 | Groups of cholinergic cells |
| M1-M4 | Subunits of muscarinic acetylcholine receptors |

# LIST OF ABBREVIATIONS

| | |
|---|---|
| CNS | Central Nervous System |
| SI | Primary Somatosensory Cortex |
| M1 | Primary Motor Cortex |
| mPFC | Medial Prefrontal Cortex |
| GZ | Granular |
| PGZ | Perigranular |
| DZ | Dysgranular Zones |
| RF | Receptive field |
| VF | Von Frey |
| VP | Ventroposterior |
| VPL | Ventroposterior Lateral |
| Po | Posterior |
| RS | Regular Spiking |
| FS | Fast Spiking |
| IB | Intrinsically Bursting |
| LTS | Low-threshold spiking |
| $GABA_A$ | $\alpha$-aminobutyric acid type A |
| $GABA_B$ | $\alpha$-aminobutyric acid type B |
| $GABA_C$ | $\alpha$-aminobutyric acid type C |
| NMDA | N-methyl-D-aspartate |
| AMPA | $\alpha$-amino-3-hydroxy-5-methyl-4-isoxazoleproprionate |
| AFR | Average firing rate |
| VS | Vector Strength |
| IP | Intraperitoneally |
| aCSF | Artificial cerebrospinal fluid |
| SP | Spike-phase |
| PSTH | Peristimulus time histogram |
| E1a/b | Short-latency excitatory components |

| | |
|---|---|
| E2 | Long latency excitatory component |
| I1 | Post-excitatory inhibitory phase |
| IPSP | Inhibitory postsynaptic potential |
| EPSP | Excitatory postsynaptic potential |
| RA | Rapidly adapting |
| SA | Slowly adapting |
| FA | Fast adapting |
| RA1 | Rapidly-Adapting type 1 |
| SA1 | Slowly Adapting type 1 |
| RA2 | Rapidly-Adapting type 2 |
| SA2 | Slowly Adapting type 2 |
| BF | Basal forebrain |
| NB | Nucleus Basalis of Meynert |
| ML | Medio-lateral |
| AP | Anterior Posterior |
| DV | Dorsal-Ventral |
| E | Excitation |
| I | Inhibition |
| ACh | Acetylcholine |
| AChE | Acetylcholine esterase |
| ADHD | Attention Deficit Hyperactivity Disorder |
| WHO | World Health Organization |
| AD | Alzhemier's Disease |
| PDD | Parkinson's Disease Dementia |
| nAChRs | Nicotinic acetylcholine receptors |
| mAChRs | Muscarinic acetylcholine receptors |
| ITI | Inter-trial interval |
| GP | Globus pallidus |
| SI | Substantia innominate |
| ICMS | Intracortical microstimulation |
| Ca | Caudal |

| | |
|---|---|
| ax | Axon |
| ISI | Inter-spike Interval |
| LTMR | Low-threshold mechanoreceptor |
| LTP | Long-term potentiation |
| VPL | Ventral posterolateral nucleus of the thalamus |
| VPM | Ventral posteromedial nucleus of the thalamus |
| SII | Secondary somatosensory cortex |

# 1. INTRODUCTION

## 1.1 Motivation

Although the acetylcholine (ACh) is the one of the first molecules discovered as a neurotransmitter, its function in the brain has not been demonstrated well yet [1]. For example, abnormalities in the cholinergic system due to the change in ACh levels or abnormal function in receptor expression has been associated with several neurodegenerative and cognitive diseases such as Alzhemeier's disease (AD), Parkinson's disease (PDD) and Attention deficit hyperactivity disorder (ADHD) as well as psychiatric diseases such as the schizophrenia [1–3]. However, due to lack of evidence for the function of ACh in the brain, there is no known treatments for the diseases mentioned yet. In 2015, World Health Organization (WHO) stated that around 47.5 million people are affected by AD, the estimated number will be 135.5 million in 2050 [4]. However, recently one of major pharmaceutical company, Pfizer, declared that they suspended AD and PDD researches requiring more basic knowledge about the origin of the diseases [5]. Moreover, recent focus has been on ADHD since this disease starts in the early childhood and the symptoms has been affecting patients' life throughout their adulthood [3]. ADHD is a neurobehavioral disorder, prevalence of this disease is approximately around 5% worldwide [6]. Furthermore, the most widely used concept for drugs used in the treatments are based on reducing the symptoms (i.e. inhibiting acetylcholinesterase (AChE) to increase level of ACh), not for the treatment of the disease. Thus, the cholinergic hypothesis stating that the cause of the diseases are based on deficiency of ACh in the CNS should be further tested in the brain [7, 8]. The brain regions important for attentional processing regarding with cholinergic system were determined in the vast amount of psychophysical and neuroimaging experiments in both animals and humans. These regions appears to be the parietal, somatosensory, and frontal regions. Although it is not easy to explain cognitive functions (such as attention) physiologically, sensory systems can be useful models because physiological activation of neural circuits is possible (using a peripheral stimuli). Thus, with the

result of physiological experiments, we can integrate information between molecular level and behavior. Attentional processing was studied mostly in visual cortex. Yet, the current knowledge points out that no matter it is bottom- up or top-down attentional process, change of attention in one sensory modality is leading a shift of attention in another sensory modality. Since the current knowledge of tactile attention stems from behavioral studies, there is lack of empirical data on intracortical mechanism of tactile information. These knowledge will make comparisons possible with one another sensory modality, and their interaction in between. To note the original aspects of this PhD work:

i. Study was be on the somatosensory system, specifically hindlimb area of primary somatosensory system. This will give us advantage of immobilization of the specific body part and application of controllable vibrotactile stimulus, thus generating novel stimulation of bottom-up processing.

ii. With the application of different compounds into the cortex (via microinjection of glutamergic and GABAergic compounds or via electrical stimulation to induce cholinergic input to the cortex), the functional properties of the neuron responding to each drug in specific layer were revealed. This will not only make contribution to the understanding of neural mechanisms of attention related processes but also reveal the effects of drugs on the spatial and temporal parameters of cortico-cortical and horizontal connections within specific column.

iii. It is important to note that distribution of niconitic and muscarinic receptor types in the hindlimb representation of the primary somatosensory cortex were also revealed with the help of post-experiment immunohistochemistry.

iv. In the future part after this PhD work, electrophysiological data can be integrated with behavioral studies in which rats are required to do attention task. Same vibrotactile parameters can be used in the custom-made operant chamber which will allow us to compare the differences between anesthetized and behaving animal. Investigation of the effects of drugs in behaving animal might be possible as well with help of chronic implantation where drugs are injected into

the associated area or the electrical stimulation of the cortex are possible.

## 1.2 General Introduction

General introduction about the sense of touch, mechanoreceptors and how the tactile processing is mediated in the central nervous sytem are given in this section. Moreover, in the concept of this PhD thesis, the general information about the attention and how it is connected to cholinergic system are reviewed in this section. Therefore, related literature for each chapter is summarized and given in the introduction section of each chapter.

### 1.2.1 The Sense of Touch

Skin is the largest organ of the body mediating our sense of touch and is composed of several layers; epidermis, dermis, subcutaneous tissue (Figure 1.1(a)). Each layer includes a wide variety of sensory receptors such as thermoreceptors (mediating temperature related information), mechanoreceptors, nociceptors, pruriceptors, and nociceptors [9]. Epidermis is the outer layer of the skin which protects the underlying skin layers and body. Dermis is middle layer containing nerve endings, hair follicles, blood vessels and touch receptors. Moreover, subcutaneous tissue includes fat and connective tissues protecting underlying tissue from damage and serving as a layer of insulator. The somatic system is responsible for all the feelings we are surrounded with such as feeling hot, cold, pressure, itch, vibrations, rough or smooth surfaces, etc. The somatosensory system is defined with three important functions: proprioception, interoception and exteroception [10]. *Proprioception* comes from the feeling of one's self. This awareness of this feeling is provided with receptors found in the skeletal muscle, joint capsules.. *Interoception* is the feeling and function of the organ of the body and its internal state. Although these are not conscious sensations, the receptors in the viscera are responsible for regulating, and conveying the information. Lastly, *exteroception* is defined as direct interaction with external world upon the body, and consists of all

receptors in the skin. Within the somatosensory system, there are four main types of receptors: mechanoreceptors, thermoreceptors, pain receptors, and proprioceptors. Specifically, we focus on the mechanoreceptors found in the glabrous and hairy skin (Figure 1.1(b)) [10]) since they are specialized for discriminitive touch, understanding the texture or the shape of an object, and mediating the grip control, reaching and locomotion via sensory feedback to central nervous system (CNS) [9–11].

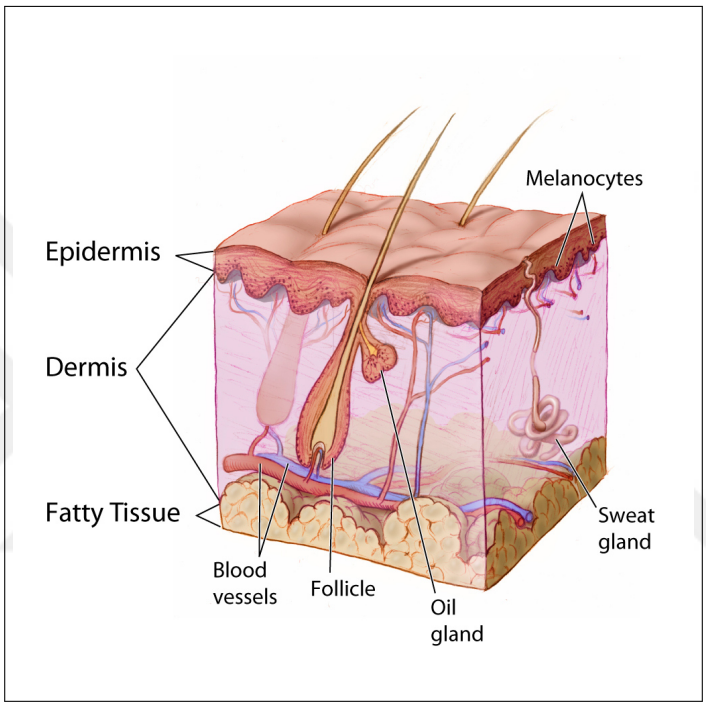


(a)

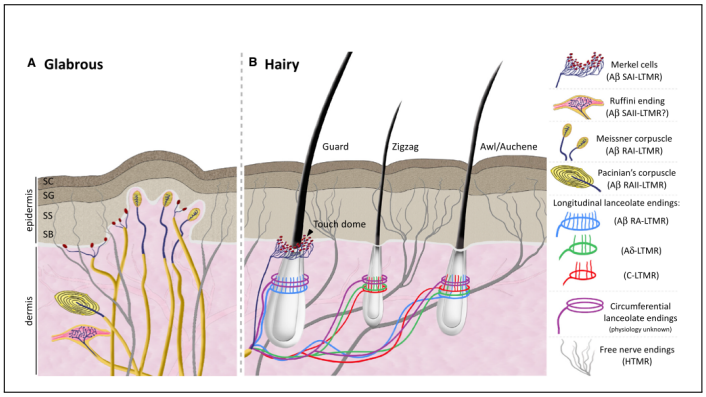


(b)

**Figure 1.1** a) Skin anatomy illustrating the different layers of skin (epidermis, dermis, subcutaneous tissue) b) Illustration of different types of mechanoreceptors found in the glabrous and hairy skin. Reproduced from Abraira 2013 and Bliss 2010 [12, 13].

### 1.2.2 Mechanoreceptors and associated nerve fibers in the glabrous skin

There are four types of mechanoreceptors in the glabrous skin; Merkel's disks, Meissner's corpuscles, Ruffini's corpuscles, and Pacinian corpuscles (Figure 1.1(b)). Although each receptor responds differently to skin deformations depending on its morphology, innervation pattern, the depth in the skin and response properties such as adaptation and tuning frequency, all together forms the combined information for the understanding of the sense of touch [10, 11]. These receptors are defined as low-threshold mechanoreceptors (LTMR) since they respond even to the weakest mechanical deformation of the skin. All low-threshold mechanoreceptors are innervated by large myelinated axons (A$\beta$) for fast information transmission for tactile perception. These fibers are divided into two types depending on the functional characteristics of their natural response to sustained indentation of the skin: slowly adapting (SA) and rapidly adapting (RA). These are also further subdivided two types in each unit, depending on the size and location in the skin: rapidly adapting type 1 (RA-1), rapidly adapting type 2 (RA-2), slowly adapting type 1 (SA-1), slowly adapting type 2 (SA-2). Afferents associated with Meisnner's corpuscles (RA-1) and Pacinian corpuscles (FA-2 in human, RA-2 in other mammals) are called RA since they respond only at onset and offset of the ramp-and-hold stimuli whereas afferents associated with Merkel cells (SA-1) and Ruffini endings (SA-2) are defined as SA since they have a sustained discharge during

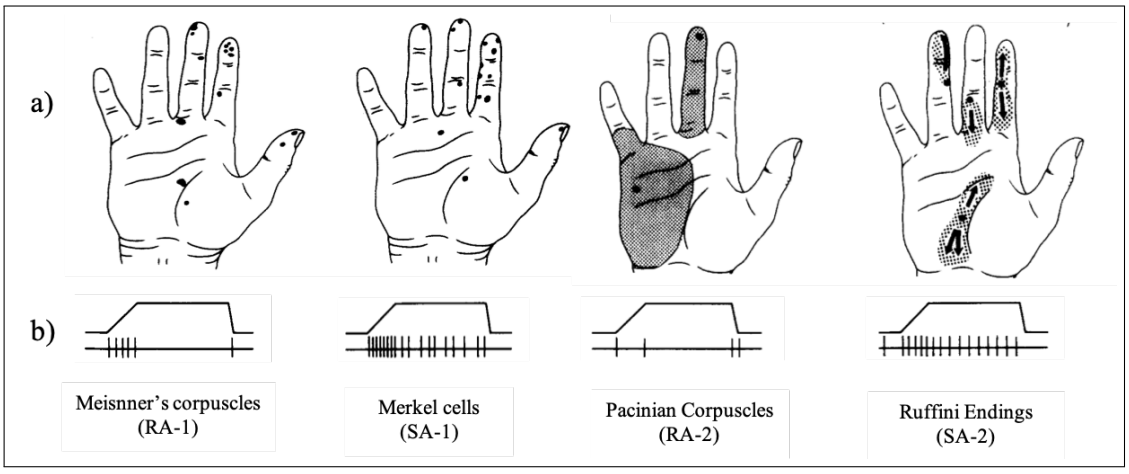


**Figure 1.2** a) Innervation density and RF representations of RA and SA afferents. b) Response properties to ramp-and-hold stimuli of each cutaneous mechanoreceptors. Reproduced from Johansson and Vallbo 1983, and Abriara and Ginty 2013 [12, 14].

all period of the stimuli. Their response properties along with variable receptive field (RF) size with associated end organ are shown in Figure 1.2. RA-1 and SA-1 afferents have small receptive fields (2-3mm diameter for SA-1, 3-5mm diamater for RA-1 [15]) with distinctive borders located mostly at fingertips (Figure 1.2a). Populations of SA1 afferents are required to obtain the shape of the objects when they are indented to skin or scanned over the skin [16–18]. On the other hand, RA-1 fibers innervate multiple corpuscles leading to lower spatial resolutions compared to SA-1. In addition to these, RA-2 afferents associated with Pacinian corpuscles have three distinct features; large receptive fields covering the entire palm, transient response to sustained stimuli and sensitivity to high frequency vibrations.

Meissner's corpuscles are located between the dermal papillae beneath the epidermis of the fingers, palms, and soles (Figure 1.1(b)) [21, 22]. They are formed of myelinated and unmyelinated afferents in the shape of cylindirical coil encapsulating the sensory nerve ending (Shown in Figure 1.3(a) and 1.3(b)) [19, 23]. They form

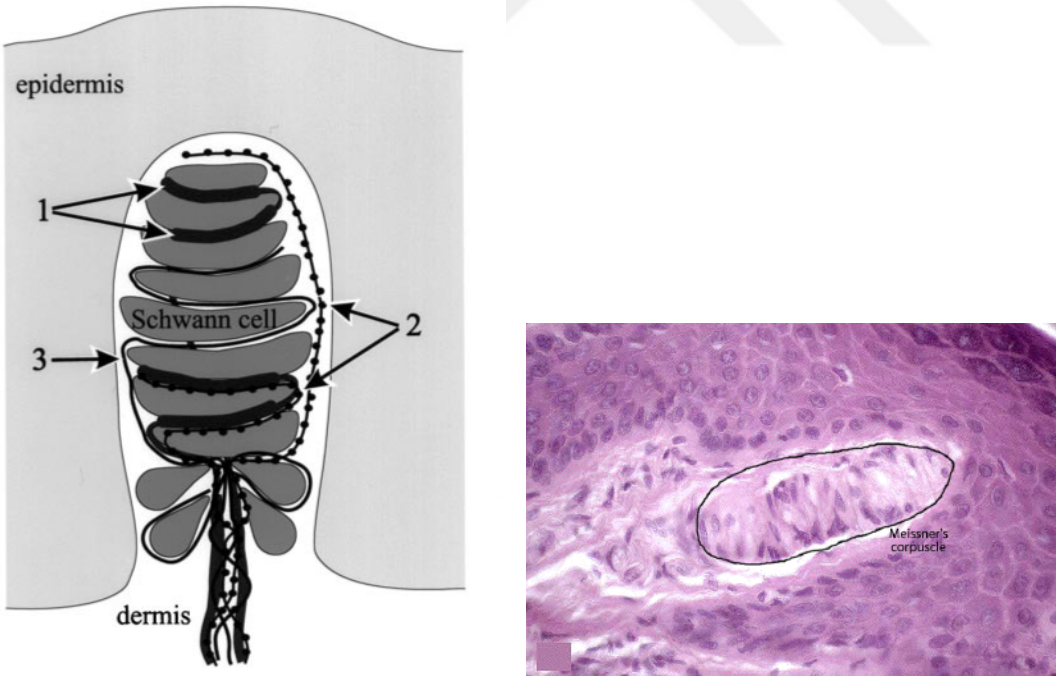


(a) (b)

**Figure 1.3** Anatomy of the Meissner corpuscles. a) Schematic drawing of an Meissner's corpuscles just beneath the surface of the skin and illustration of three types of innervation: 1) myelinated afferent, 2) unmyelinated varicose afferent, 3) unmyelinated varicose afferent [19]. b) High power view of a Meissner's corpuscle. Adopted from [20].

approximately 45% of the mechanoreceptors found in the glabrous skin [11]. Each Meissner corpuscles innervate approximately 2 to 5 afferents whereas an afferent axon innervate 10 to 20 Meissner's corpuscles. They are usually responsible for sensitivity of a light touch. They have the lowest threshold for sensing the vibrations between 10 and 50 Hz. They have been found in higher density at finger pads [11].

Merkel's discs are also known as Merkel cells. They are located in the epidermis where they are aligned with papillae which is beneath the dermal ridges (Figure 1.1(b)) and 1.4). They are found in both glabrous and hairy skin and responsible for 25% of mechanoreceptors found in the hand which are densely found in the fingertips, lips and external genitalia [24]. They have small receptive fields (Figure 1.2). They are mainly activated through light pressure. They play a major role for sensing the ridges, edges, rough textures and also in static discrimination of shapes. As shown in Figure 1.4(b), each Merkel cell (diameter=10$\mu$m) has several branches innervating a single nerve fiber (SA-1). In addition, Merkel endings are usually found as clusters of 50-70 innervating a single myelinated axon [25]. Moreover, due to synaptic junction between the nerve-ending and Merkel cell, it has been thought that Merkel cells have

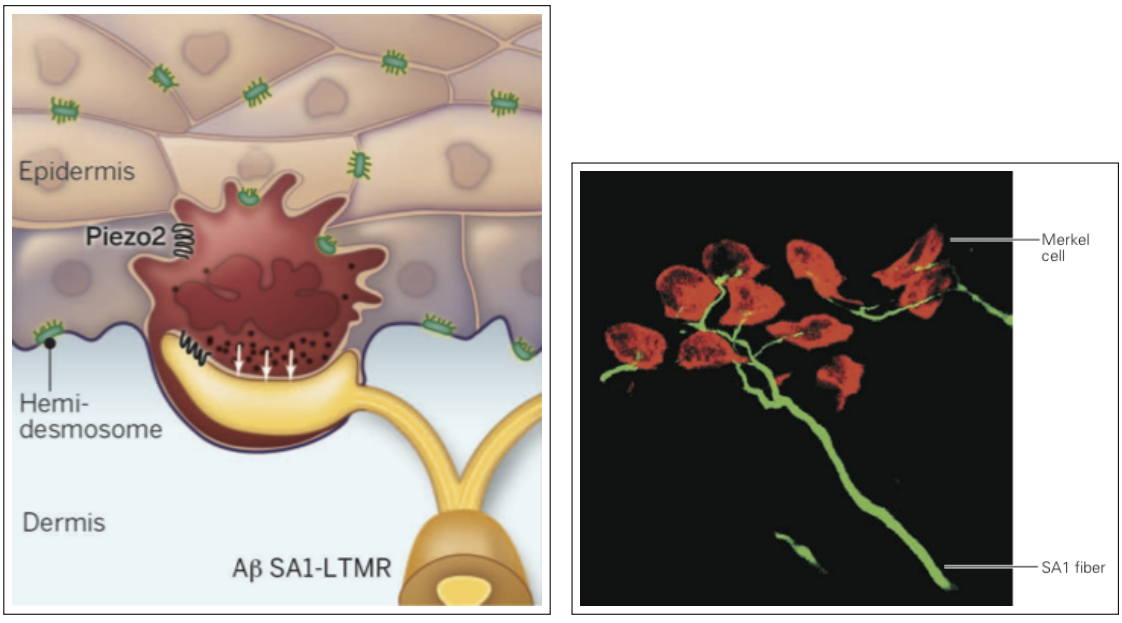


(a) (b)

**Figure 1.4** a) Low threshold mechanoreceptor (LTMR) Merkel cells in the glabrous skin [9] b)Merkel's discs (Merkel cells) with branches innervating SA-1 fiber located in the hairy skin. Adopted from Gardner 2012 [11].

mechanoreceptive ion channel located on the cell rather than in the nerve ending [26] (Figure 1.4(a). They respond to low freqeuncy vibrations between 5 and 10 Hz. They are extremely sensitive to small indentations such as 1$\mu$m. They produce action potential at highest when the skin is deformed with sharper objects. Firing rate reduces when exploring curves or flat surfaces [10, 11].

Pacinian corpuscles are located in the subcutaneous tissue (Figure 1.1(b)) and they are also found in the deeper layers of gut in some mammals (i.e. mesenteries of the gut) [11, 24]. They form 10-15% of the cutenous receptors in the hand. They are large encapsulated nerve endings formed with Schwann cells. Their location, morphology

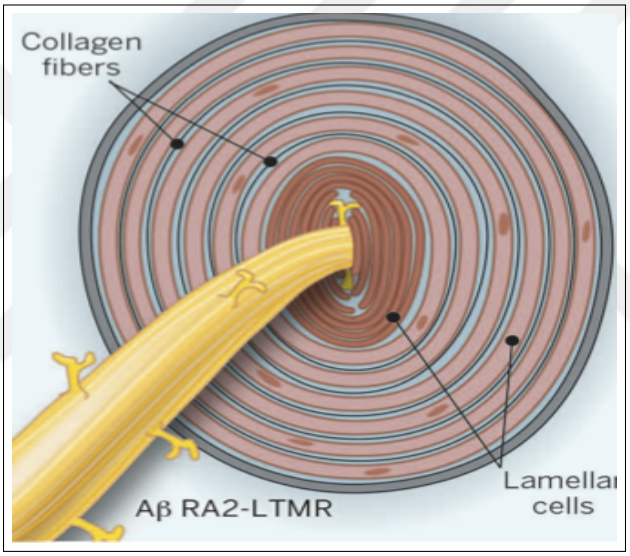


(a)

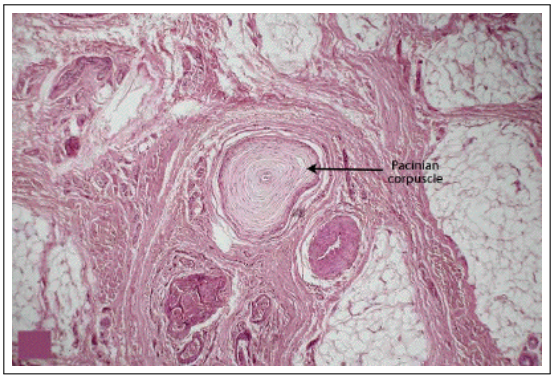


(b)

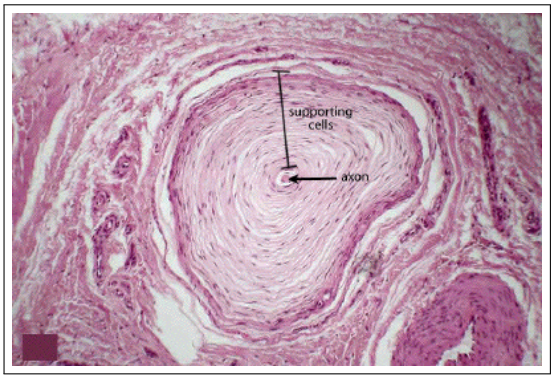


(c)

**Figure 1.5** a) The capsule is arranged like the layers of an onion consisting of 20-70 lamellae innervating a RA-2 fiber [9]. b) Histological sections of Pacinian corpuscles found in the glabrous skin. c) Histological section of Pacinian corpuscles (zoomed) found in the glabrous skin showing the supporting cells and axon. Histological slides were adopted from [27].

and response properties are different than Meissner's corpuscles. The Pacinian corpuscles are shaped like an onion in which they are surrounded with collagen fibers between lamellar cells [24,28,29] (Figure 1.5(a)). Usually, one mechanoreceptive fiber innervate the center of onion-shape corpuscles as shown in Figure 1.5(a). The capsule around the Pacinian corpuscles serves as a filter mediating transient responses at high frequencies such as 250-350 Hz. Adaptation pattern is usually more rapid and Pacinian corpuscles have lower threshold compared to Meissner's corpuscles. as shown in Figure 1.2. Thus, Pacinian corpuscles have higher sensitivity to discriminate fine surface textures or to detect high-frequency vibrations [10, 24].

Lastly, Ruffini's corpuscles are very similar to other cutaneous receptors yet their role is not well understood since they are sparsely located in the hand [30]. They are usually found in the dermis and parallel to the skin (Figure 1.1(b)) but they are also located in the ligaments and tendons. Although they are found in the hairy skin of the mammals, they are found in the glabrous skin of non-human primates along with their associative afferents (SA-2) [30]. Ruffini's corpuscles form about 20% of the cutenous receptors and due to their position in the skin they are particularly sensitive to skin stretch. Afferent associated with Ruffini's endings (SA-2) has greater RFs and respond to sustained stimuli in a more regular pattern than SA-1 fibers [11] (Figure 1.2).

### 1.2.3 Processing of Tactile Stimuli in the CNS

Tactile information is gathered through mechanoreceptors described earlier. These mechanoreceptors are connected to unique pseudo-unipolar nerve cells which consist of an axon extend to periphery reaching to the brain and a soma located at dorsal root ganglion of sensory cranial nerves. The nerve fibers carrying information from the different somatosensory submodalities are bundled together when they enter the dorsal root ganglia which are also called first order neurons [10,31]. However, when the fibers exit the dorsal root ganglia, they are seperated into medial and lateral divisions depending on type of the fibers [11]. The lateral division includes small-diameter fibers (thinly myelinated (A$\delta$)or unmyenilated fibers (C)) whereas medial division in-

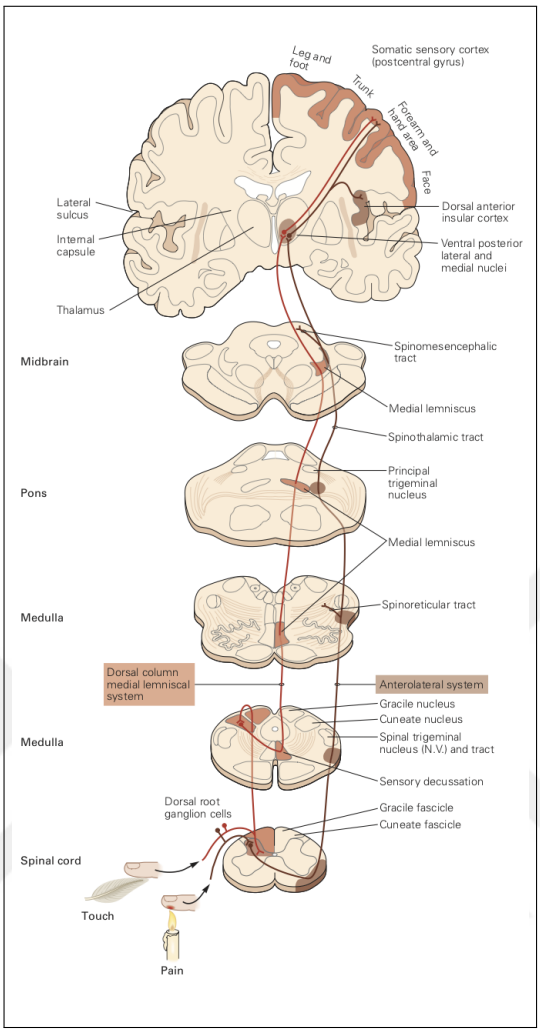


**Figure 1.6** Somatosensory Pathway. Somatosensory information is carried through two ascending pathways: dorsal column-medial lemniscal system and spinothalamic tract. Schematic illustration of information flow from the tactile and proprioception signals by large-diameter myelinated fibers and information related with pain, itch, temperature by small-diameter fibers. First, information is carried from receptors to spinal cord and then medulla. Second, they make synapses in the in thalamus through the pons and midbrain. The information reaches the somatic sensory cortex and make synapses there. Adopted from Figure 22-11 of Gardner and Johnson, 2012 [11].

cludes large and myelinated fibers such as A$\alpha$ and A$\beta$. These divisions are also called as ascending pathways: the dorsal column pathways and the spinothalamic tract. The *dorsal column-medial lemniscal system* carries the tactile and proprioceptive information whereas *spinothalamic system* carries the noxious, thermal and visceral information 1.6. Touch, pressure, vibration follows dorsal column-medial lemniscal pathyway as shown in Figure 1.6 as the nerve fibers are located in the medial aspect of the dorsal root entering the spinal cord. Some of sensory nerve fibers terminate at the spinal cord involved in the reflex responses leading to inhibition of pain transmission. The first

order neurons in the dorsal column tract ascend through medulla where they synapse in gracile nucleus and cuneate nucleus within the dorsal part of the caudal medulla. The axons of second order neurons decussate and reach medial lemniscus. The medial lemniscus tract connects the dorsal column nuclei with ventral posterolateral nucleus of the thalamus (VPL). The third order neuron within VPL make synapses in the primary somatosensory cortex in a topographic manner (cortical areas Area 1,2,3a,3b) (Figure 1.7(b)).

### 1.2.4 Somatosensory Cortex

Tactile information from mechanoreceptors is conveyed by afferent pathways through the spinal cord, the medulla, and the thalamus into the primary somatosensory cortex (SI) where information processing primarily occurs. SI is located in the anterior part of posterior parietal lobe in the brain (Figure 1.7(b)). It recieves input from VPL and ventral posteromedial nucleus (VPM) of the thalamus to areas 3a, 3b, 1 and 2 (Figure 1.7(a)). The four regions of the SI process different type of somatosensory information. For example, neurons located on area 3a receive input from muscle spindles and other deep receptors whereas neurons in area 3b process information from the touch receptors in the skin. Both area 3a and 3b have lateral connections to the areas 1 and 2 where neurons receive input mostly from multiple types of somatosensory receptors innervating the same body part. These areas are highly interconnected and send/receive sensory information to higher cortical areas in the parietal cortex such as secondary somatosensory cortex (SII) and area 5 (Figure 1.7(a)). They receive more input from primary areas and less input thalamic nuclei. The information becomes more abstract as it is processed in the higher cortical regions. For example, when SI respond to sensory stimuli discriminating the type and intensity of the stimuli, SII responds to them bilaterally and with higher sensorimotor integration or the information from the attention, learning, memory and sensory discrimination but less precision compared to SI [10, 11, 32, 33]. In addition, Broadmann's area 5 and 7 (the somatosensory association cortex) are located in the superior parietal lobe of the brain. They receive sensory inputs from one's hand as well as visual input during active hand movements [11, 34].

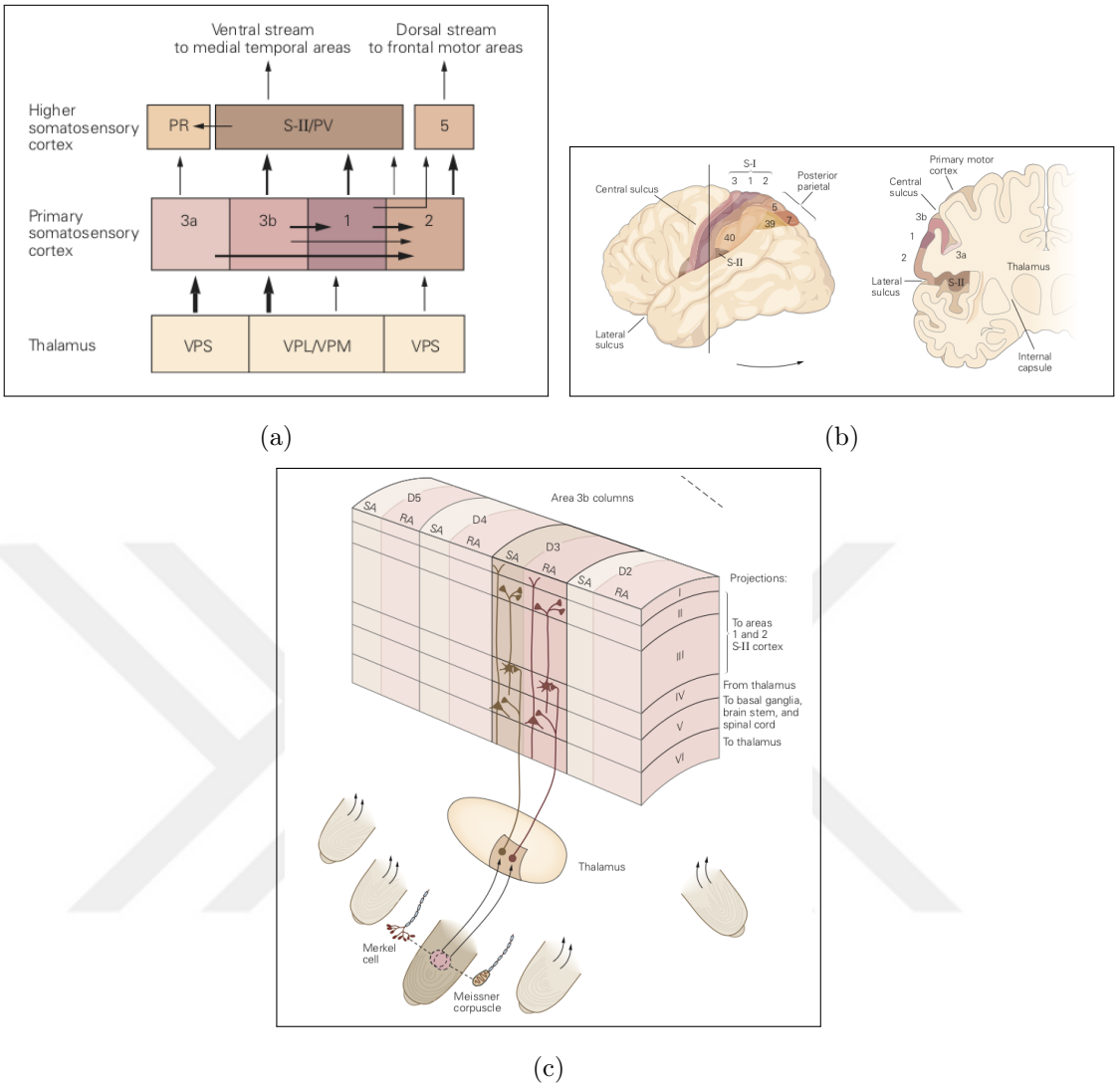


**Figure 1.7** The somatosensory areas of the cerebral cortex. a) Tactile information flow through afferent neurons. Primary somotasensory cortex is consisting of four regions (3a, 3b, 1, 2). They recieve input from different ventral posterior nuclei of the thalamus (VPL, ventral posterior lateral nuclei; VPM, ventral posterior medial nuclei; VPS, ventral posterior superior nuclei; PR, parietal rostroventral cortex; PV, parietal ventral cortex;). Adopted from figure 23-11 of Gardner and Johnson, 2012 [11]. b) Schematic representation of the somatosensory areas of the cerebral cortex. Adopted from figure 23-11 of Gardner and Johnson, 2012 [11]. c) Detailed columnar organization of the somatosensory cortex. Schematic representation of an information flow from mechanoreceptor to SI. Adopted from figure 23-13 of Gardner and Johnson, 2012 [11].

Each of these areas has a distinct representation of the body surface and its cytoarchitecture has somatotopic organization in the brain.

It has been known that the primary sensory cortices process the sensory information in columns organizing the relevant input depending on the location and modality [35–39] (Figure 1.7(c)). Cells located in different layers of each column receive the inputs from same receptor area and respond to same classes of receptors as

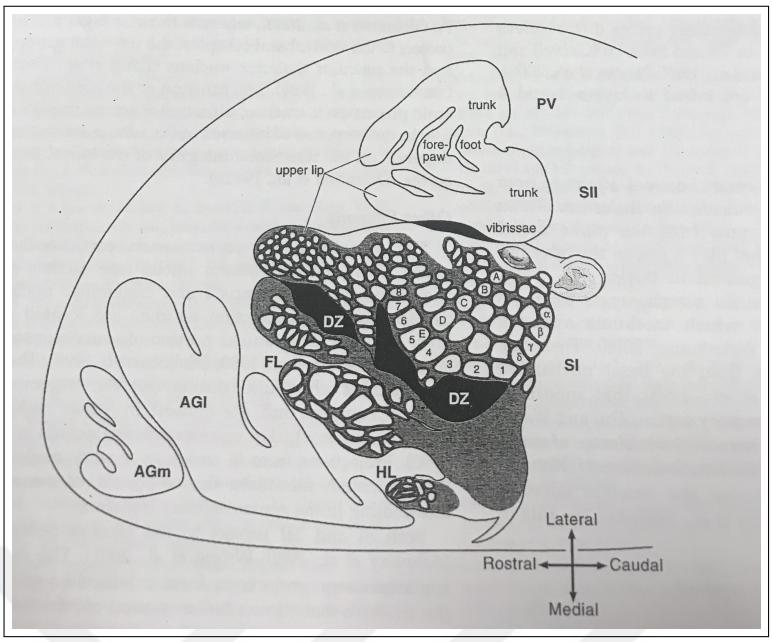


**Figure 1.8** Barrel shaped granular zones represents the mystacial vibrissae. They are arrenged in rows classified as A-E corresponding to rows of vibrissae. Barrels surrounded by perigranular cortex representing head and paws. Abbreviations: AGl: lateral agranular cortex, AGm: medial agranular cortex, FL: forelimb, HL: hindlimb. Adopted from Figure 4 of Tracey 2004 [46].

shown in Figure 1.7(c). In each column, thalamocortical inputs make synapse first in layer IV where the signal projects to upper layers of the cortex (layer II/III). Lastly, these signals pass to layer V and VI where the signal is transmitted to other areas of the brain or back to thalamus and periphery [40–43].

On the other hand, contrary to humans and primates, rats have one large representation of the body surface covering their face and whiskers as shown in Figure 1.8. Whisker representation in the rodents are the most devoted area in SI similar to hand representation for humans and primates [44]. In mouse, it covers approximately 69% of SI and 13% of the entire cortex [45]. Similar to primates and humans, rats have also somatotopic organization especially for their whiskers. Each vibrissa is represented in a special column called *barrels* (Figure 1.8 [44, 46]. In rodents, submodalities of the somatic sensation are usually overlapping including hindlimb, forelimb as well as motor area [47]. Rodent SI cortex are discussed in detail in Chapter 2.

### 1.2.5 Attention and cholinergic system

Attention can be defined as one of the complex cognitive processes which direct the mind/brain to the "relevant" object or event in the presence of distraction. In this context, this behavior can be triggered by an internal (goal-driven, attentional control) and/or external input. Internal input is a slower process and driven by a person's will voluntarily or involuntarily during execution of attention. On the other hand, external input is usually in a form of sensory stimulus and deployed very rapidly. For example, touching the body immediately switches a person's attention to that location as well as the conscious sensations coming from the receptors in that location, while ignoring other stimuli. Accordingly, two interacting modes of attention plays a major role in a way that how the sensory inputs are processed and perceived. Current understanding of attentional mechanisms is raising questions about which cortical regions are essential for attention, and it lacks considerable knowledge within the tactile modality. Attentional modulation of neural activity varies across cortical neurons and attention can lead to increases or decreases in average firing rates. Whether these variations in solely depend on sensory physiology and/or neuronal position within the local cortical architecture remains unknown.

There is substantial evidence that cholinergic system is one of the most significant neurotransmitter systems in the brain and essential for cognitive functions such as attention, cortical plasticity, learning and memory [48–50]. There are numerous behavioral, electrophysiological, psychophysical and imaging studies investigating the relationship between attentional processing and cholinergic systems. These studies support the hypothesis that cholinergic system contributes to attention by enhancing sensory input processing [51–56].

According to proposed model by Sarter et al. [49], attention is influenced by the cholinergic system through two distinct but overlapping/interacting neural mechanisms. One (bottom-up) is 'signal-driven modulation of detection' which is only mediated by external input signal via sensory systems whereas the other mechanism (top-down) is mediated by practice or knowledge based on changes in signal detection via prefrontal modulation of cholinergic inputs (Figure 1.9).

The main component of cholinergic system, acetylcholine (ACh) receptors, con-

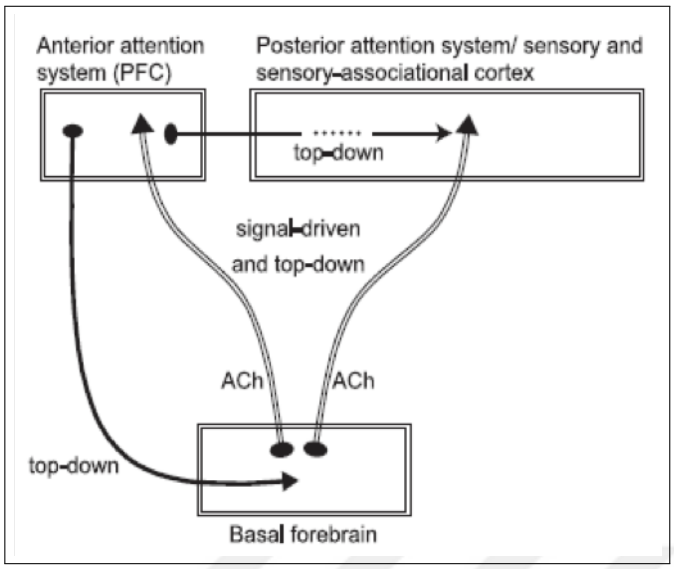


**Figure 1.9** Schematic illustration of bottom-up and top-down cholinergic modulation of attention with associated brain regions. Modified from Sarter et al. [49].

tribute to sensory-cognitive functions as shown in numerous behavioral studies with rats [52, 53, 57, 58] and primates [59–63]. This contribution is more likely through sensory system (auditory [64], visual [65,66], somatic [67–71], and other cognitive functions such as learning, memory [53, 72], conscious awareness or attention [48, 50], cortical plasticity [73]. In addition, studies showed that the abilities requiring the attentional demands such as responding to cues, signals, or targets were affected when cholinergic input to the associated cortex were blocked [74–76].

Depending on the source of input (either top-down modulation or bottom-up) mediating attention, the specific action of ACh differs in certain regions of the brain, even within the associated cortex [57, 77]. For example, in somatosensory cortex, excitatory and/or inhibitory inputs from cortico-cortical connections are suppressed or facilitated by ACh receptors while excitatory thalamocortical inputs (afferent fibers) are not affected. These specific actions of ACh are more likely due to characteristics of transmembrane receptors. They are usually classified according to pharmacology (i.e. relative affinities and sensitivities to different molecules). Thus, it leads to the hypothesis that ACh somehow regulates the sensory input processing in attentional performance through the activity of cholinergic receptors, i.e. nicotinic and muscarinic acetylcholine receptors, heterogeneously located within the cortex.

Based on the previous studies, it may be concluded that regulation of excita-

tory/inhibitory intrinsic connections (top-down) are via muscarinic receptors whereas the regulation of sensory input processing (bottom-up) are via nicotinic receptors [49]. These observations indicate that the somatosensory cortex has the ability to be reorganized under some conditions, and questions the ability of single neurons to alter their excitability to selected afferent signal. Cortical cholinergic activity reflects the complex interactions between these two modes (bottom-up and top-down) and mediates, enhancement of input processing (i.e. unmasking of previously subthreshold input) at the cellular level, and attentional performance at the behavioral level.

### 1.2.6 The distribution and contribution of the nicotinic and muscarinic receptors in the central nervous system

Nicotinic acetylcholine receptors (nAChRs) are proteins composed of different combinations of five type of subunits ($\alpha$, $\beta$, $\gamma$, $\delta$ and $\epsilon$) assembled as pentamer. nAChRs are widely distributed in central nervous system and can be found on soma and dendrites. According to our knowledge, 12 distinct subunits have identified: $\alpha$2-$\alpha$10, $\beta$2-$\beta$4 [78]. nAChRs are mostly found in the layer I, III and IV and upper layer VI in the rat cerebral cortex [79–81]. They mediate postsynaptic effects of ACh and are also found presynaptically on thalamacortical fibers [82, 83]. Moreover, nAChRs enhance the synaptic transmission at both thalamocortical synapses and intracortical synapses [80, 83–86]. The diversity in functional properties of nAChRs is probably due to the subunit composition [87]. There are functionally important two main subunits of nAChRs: high affinity nicotinic heteromic acetylcholine receptors (subunits containing $\alpha$4 and $\beta$2) and low affinity nicotinic receptors (subunits containing $\alpha$7) in the rat brain. Both are known to be mediate excitation of Layer I interneurons in somatosensory cortex [57] and appear to be critical for memory, learning and attention [58, 88].

Muscarinic acetylcholine receptors (mAChRs) are G-protein coupled complexes. Hammer et al. [89] found two distinguished 2 mAChRs subtypes by using the relative sensitivity of muscarinic receptor antagonist pirenzepine. Molecular and biological studies showed that there are five different genes expressed in rat [90]. However, 4 of mAChRs are pharmacologically distinguished which are denoted as M1-M2-M3-M4 in

rat [91]. It is has been known that differential effects of these receptor are present in different cortical layers and cell types [88], but the role of the these subtypes are unknown; and some of these subtypes seem to be ineffective pharmacologically (e.g.M4) in the somatosensory cortex [83]. Additionally, in human and rat cortices, it has been suggested that the M1 subtype is located in the post-synaptic membrane to facilitate cellular excitation while the M2 subtype is in the pre-synaptic membrane to regulate the release of ACh.

The action of ACh is mediated by nicotinic and muscarinic receptors which have been studied widely at neuroanatomical level [92]. The morphology of the nicotinic and muscarinic receptors are relatively well understood although the distinct roles of these receptors on the regulation of neuronal signals are not very clear. These receptors are likely involved in mediating in vivo responses to local release of ACh upon cue detection during attention tasks, as observed in sensory cortices [57, 77, 93]. Their potentially distinct contribution to responses questions the effect of these receptors at presynaptic sites [83,84,94,95]. Impact of combined muscarinic and nicotinic receptor blockade appeared to be stronger than each receptor type blockade alone; however, the underlying mechanism of these finding is still poorly understood [92, 96, 97].

### 1.2.7 The source and functional role of cortical ACh in the primary somatosensory cortex

It has been known that the primary somatic sensory cortex receives a cholinergic input from nucleus basalis magnocellularis in the basal forebrain and might have additional cholinergic innervation from intrinsic sources [81, 98–100].

Although studies, especially in the rat, have shown the presence of cholinergic neurons in the cortex, it seems that most ACh comes from extrinsic sources. Following combined histochemical techniques to determine the probable source of ACh in the somatosensory cortex, cells were found primarily in the ventral globus pallidus (GP) and substantia innominate (SI) which were the two major component of basal forebrain (BF). They were also found in the nucleus of the diagonal band, entopeduncular nucleus, ventral putamen and lateral hypothalamus. Specifically, many of the labeled

neurons corresponded to the regions described above is known as the nucleus basalis of Meynert (NB).

The locations and projection patterns of the cholinergic neurons in NB were reported previously in a study of 40 rhesus monkeys [98]. Based on projection patterns, four groups of cholinergic cells were defined and designated as Ch1 through Ch4. In particular, Ch4 was shown to innervate the brain regions containing the somatosensory cortex. The somatosensory cortex in the rat receives afferents from neurons in the ventral and medial GP and adjacent SI. These fibers follow different trajectories between NB and the cerebral cortex. They enter the cortex and initially run within layer VI to terminate mainly in layers V and I. The targets of the cholinergic fibers could be the apical dendrites of pyramidal and bipolar cells from layer II to V that extend terminal tufts up to layer I [101](Figure 1.10).

These neurons are the primary source of ACh for the neocortex. They receive

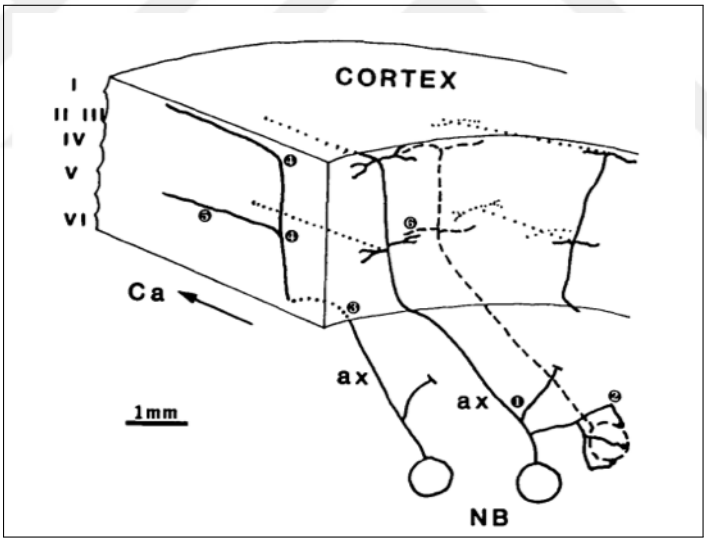


**Figure 1.10** Nucleus basalis (NB) projections to somatosensory cortex with proposed axonal branching patterns. 1,2) proximal branches of axon outside and within the NB respectively 3) Initial entrance to cortex in layer V/VI. 4) axons branching layer I and V. 5) Extended travel of axons through layer I and V. 6) intracortical branching of fibers. NB: nucleus basalis, Ca:caudal, ax:axon, Adopted from Kristt et al. [101].

inputs from predominantly limbic and paralimbic areas, including the amgdaloid complex, prepyriform, orbitofrontal and entorhinal cortices and the hypothalamus, midline thalamus and brainstem reticular formation [102, 103]. These areas have been implicated in motivation, attention and arousal. NB neurons do not receive input from the

ascending sensory pathways or the majority of cortical areas, including the primary sensory and motor cortices. Many electrophysiological data show that BF neurons do not respond to cutaneous mechanical stimulation, but in behaving monkeys they do respond to presence of food in a manner reflecting the animal's state of hunger. Thus, a mechanism exists by which only novel or significant afferent inputs influence cortical neurons and increase ACh levels indirectly. Obviously, this mechanism is not restricted only to the attention-related events, but also cholinergic effects on learning and memory. Similarly, the loss of cholinergic basal forebrain neurons is a major feature of Alzheimer's disease and the severity of the accompanying dementia has been correlated to the extent of the cholinergic deficit. Many symptoms of Alzheimer's disease may be attributed to the disruption of mechanism outlined here.

### 1.2.8 The mechanism of action of ACh in the sensory cortices: intracellular studies and sensory processing

The following literature describes studies with intracellular studies first in which the mechanisms of action of nicotinic and muscarinic receptors were investigated; the electrophysiological effects on the spontaneous activity or on activity induced by application of ACh before and after pharmacological manipulations. Subsequently, the effects of ACh on the responses of cortical neurons to natural stimulation and intracortical microstimulation (ICMS) were summarized.

Tian et al. [94] studied the cholinergic excitation of layer VI neurons in mouse primary motor cortex (M1), primary somatosensory cortex (SI) and medial prefrontal cortex (mPFC) since the main cholinergic innervation is through layer VI. There is a great diversity of responses to ACh especially in the SI cortex. Even though the responses to ACh in M1 and SI are weaker compared to medial prefrontal cortex, cholinergic responses are region and layer-specific based on the activity of nicotinic and muscarinic receptors. In other words, pharmacological manipulations of the cholinergic responses showed that how the balance between nicotinic and muscarinic receptors shape the activity within the different cortices. SI layer VI neurons showed the weakest average response to cholinergic stimulation and these responses were not homogenous.

The contribution of nicotinic-receptor mediated and muscarinic-receptor-mediated responses are 63% and 37%, respectively. On the other hand, the contribution of muscarinic receptors in mPFC is only 9% whereas in the primary motor cortex, it is 17%. These results indicate that the muscarinic receptors have a greater role in sensorimotor component of attention, since the cholinergic system triggered by peripheral stimuli is linked to the shifting of attentional focus [77]. In addition, contribution of nicotinic receptors in mPFC is 91%, so it might be concluded that nAChRs are more likely to involve in top-down modulation of attentional behavior. Overall, these findings show that layer VI neurons respond to cholinergic stimulation within in primary and associative cortices, which show their contribution to attentional performance. Levy et al. [83] studied the presence and the role of niconitic/muscarinic receptors in NMDA-receptor mediated synaptic activity in layer V somatosensory cortex neurons. Both nicotinic and muscarinic receptor agonists reduced the excitatory postsynaptic potentials (EPSPs) in the somatosensory cortex. However, the effects of nicotinic and muscarinic receptors were exerted through two routes. Nicotine induced reduction in EPSPs were through NMDA-receptor activation whereas the effect of muscarinic receptors did not depend on solely the activation of NMDA-receptors. Moreover, Christophe et al. [84] studied the sensitivity of layer I interneurons in response to specific and non-specific nicotinic receptor agonists. Although the morphology of the different neurons did not differ in response properties, pharmacologically subtype-specific nicotinic agonist has different effects. Taken together, although these responses were not elicited by natural stimulation, it shows the importance of specific receptor (nicotinic vs. muscarinic) and subtype ($\alpha 7$ vs. non-$\alpha 7$) on the particular neuron type and their interaction within the local circuitry.

The following literature summarizes the electrophysiological studies with different sensory systems which created the basis for our study. Responses to natural stimuli are recorded from the anesthesized animals. In cat visual cortex, Sillito and Kemp [65] investigated the effects of ACh by presenting optimally oriented bars of light. Results showed a large variation in the responses of neurons to iontophoretic application of ACh, including even opposite effects among different neurons in layers II-VI. Inhibition of both spontaneous and evoked responses by peripheral stimuli was seen in layers III and IV whereas the excitatory effects were mostly seen in layer V

and VI. In this study, it was not clear whether nicotinic or muscarinic receptors were activated and have specific role in these responses. The laminar distribution of cells affected by ACh was also described in detail. It appeared that cells were inhibited by ACh were found in layer III and IV, while those with enhanced responses were found in all cortical layers. In addition, a similar study by Sato et al [66] in which the effect of ACh in response to visual stimuli was investigated showed that 76% of the responses were increased and 14% of the responses were diminished. The inhibition were primarily observed in the superficial layers. These effects could be blocked by atropine (muscarinic antagonist), but not hexamethonium (nicotinic antagonist) in 93% of the 56 cells tested, which indicates that effects of ACh were mostly mediated through muscarinic receptors. However, they reported that ACh enhanced not only visual responses to optimal stimuli, as was shown by Silloto and Kemp [65], but also to non-optimal stimuli. A study showed that increase in the signal-to-noise ratio (number of spikes in the optimal visual response/total spikes) in 44% of the 81 cells tested while it did not change in 36% of the cases and it was reduced in 20% of the neurons.

In the primary somatosensory cortex, Donoghue and Carroll [69] observed an increase (both amplitude and duration) in discharges elicited by whisker stimulation in 76% of the 54 neurons tested during ACh application. This effect was antagonized by atropine in all cases. Whisker stimulation activated 11 out of these 54 neurons only during ACh administration. These cells had low background activity although they did not respond to air puffs or mechanical stimulation of any whiskers in the absence of ACh. This type of effect was not reported in the visual cortex since all neurons recorded respond in the presence of specific light stimulus. In the contradiction with the studies in the visual cortex, not only the evoked response increased but the background discharge rate also increased during ACh administration. This was observed in 85% of SI neurons (46 of 54 cells). Metherate et al. [68] investigated the cholinergic modulation of sensory responses to ICMS in cat ventoposterior lateral (VPL) nucleus of thalamus and natural stimuli applied on the forelimb. They studied these effects in terms of change in spike rate as well as the change in receptive field size. They showed that ACh increased the firing rate of 39% of the sample tested (203 neurons) and the receptive-field size was increased in 16% of the neurons. 10% of neurons had contradictory effects (i.e. both increasing and decreasing). Change in discharge pat-

terns were also seen indicating that ACh acts as excititatory or inhibitory according to unit. It is difficult to interpret this activity according to the generic characteristic of the drug. The responsiveness to only somatic stimuli of 29% were modulated and 7% were both modulated and driven. They also showed the muscarinic nature of ACh effects throughout the cortex. However, only 10% of the sample were tested with atropine. Next, same group Tremblay et al. [70, 71] investigated the effects of basal forebrain (BF) stimulation on the excitability of somatosensory cortical neurons in cats, since the major projection of cholinergic neurons to somatosensory cortex is from BF. SI neurons were excited with either glutamate or mechanical stimulation of forelimb paired with BF stimulation and atropine administration. They showed that 50% of the neurons excited with glutamate (7 of 16 neurons) was enhanced after BF stimulation, half of this enhancement (4 of 7 neurons) was blocked by atropine indicating the muscarinic receptors were mediating the responses. When neurons were activated by natural stimulation, the enhancement after BF stimulation was 60% (18 of 30 neurons). Total of 19 cells were also treated with atropine while BF stimulus was paired with a cutaneous stimulus. 58% of cells (11 of 19 neurons) showed no enhancement although other 8 cells showed very little enhancement(5%) compared to 112% enhancement without atropine administration paired with BF stimulation. Moreover, BF stimulation had similar effects as iontrophoretically administered ACh, but the effects of BF stimulation occurred more frequently.

Although there are some discrepancies between studies mentioned above, the overall evidence suggests that there is a broad distributed action of the cortical cholinergic system. These studies are important in terms of general mechanism of ACh throughout the different brain regions but needs more in-depth view for elaboration of sensory information processing. Thus, these findings eventually can be extrapolated to role of ACh in attentional processing.

## 1.3 Hypothesis and novelty

I presented the general introduction for the sense of touch in periphery and cortex in this section. These information about the tactile processing in the rat SI

are required to study how cortical neurons in each layer respond to suprathreshold mechanical stimulation. Furthermore, in the view of these studies investigating the synaptic connection within the primary somatosensory cortex, there is strong evidence that GABA is an important inhibitory neurotransmitter which controls both spatial and temporal properties of somatosensory cortical neurons. However, transient response observed in the cortex to high-frequency vibrotactile stimuli unlike the 1:1 firing in periphery does not depend on solely to GABAergic inhibition in the cortex but the contribution of NMDA and non-NMDA receptors. However, the balance between excitation and inhibition is changing very rapidly. In the case of any disruption of excitation and inhibition balance lead to a transient response to high-frequency vibrotactile stimuli. The imbalance between excitation and inhibition might occur due to antagonizing effect of the anesthetic agent, ketamine, on the NMDA receptors. Although ketamine antagonizes the NMDA receptors, the onset responses are observed during high-frequency stimulation due to activation of non-NMDA receptors. Due to excitation of inhibitory neurons by activation of non-NMDA receptors and lack of NMDA receptor activation on the excitatory neurons, the sustained responses to high-frequency vibrotactile stimuli are diminished. To further test the hypothesis, we observed the effects of GABA antagonist, bicuculline, and NMDA on the onset and sustained responses to vibrotactile stimuli on cortical neurons from the hindpaw representation in rat S1 cortex under the influence of anesthetic agent, ketamine. Moreover, there is no study investigated how the shift in the excitation-balance modulates these responses in the hindpaw representation of the primary somatosensory cortex. To understand the effects of excitation-inhibition balance in the SI and to generate a computational model from the experiment work, we recorded single-unit spikes evoked by sinusoidal stimulation of the glabrous skin in the presence of microinjected chemicals. We showed the frequency dependence of the drug effects highlighting the role of local cortical dynamics in the hindpaw area. Subsequently, we used the experimental data to construct the computational model showing how excitatory and inhibitory neurons in each layer responds the different vibrotactile stimulation and how these neurons were modulated by changing their corresponding input.

On the other hand, it remains unclear how cholinergic effects are mediated on the level of local microcircuits, which form the basic unit of information processing in

the neocortex. Here, we explore the actions of cholinergic synaptic activation on distinct cell types of SI cortex, its effects on overall network activity in the cortical column, and investigate the contributions of distinct cholinergic receptor subtypes in different layers and on different timescales. Our study aimed to take the current knowledge one step forward by showing how the differential cholinergic inputs into SI cortex effect the responses of different neurons and local circuitry. In addition, a computational model can be constructed for better understanding two working modes of attention.

One of the significance of this PhD work is to differentiate and to correlate the neural responses to attentional network, we have to be able to separate two interacting mechanism (bottom-up vs. top-down). Bottom-up mechanism can be activated by peripheral stimulation. In this study, hindlimbs of the rats were used for mechanical stimulation. This gave us and advantage of immobilization of the specific body part and application of controllable vibrotactile stimulus, thus generating novel stimulation of bottom-up processing. Previously, one study by Tremblay et al. [71] used a 1.2 second long trapezoidal indentation of the skin with varying amplitudes on different units. In the current study, we will 0.5 second long 5- , 40-, 250- Hz sinusoidal vibration with same amplitudes for each frequency and same parameters for each unit. We previously observed that cortical responses are dependent on the frequency of stimuli. Therefore, this allowed us to investigate the differential effects of drugs on tactile neurons stimulated with different frequencies of stimuli and give us better understanding of responses at receptor level.

On the other hand, it is difficult to activate "top-down" mechanism in an anesthetized animal. Top-down mechanism is thought to influence the overall brain and set the cortex in a specific mode according to dynamically updated behavioral status [104, 105]. In our study, we observed the effect of extrinsic ACh in the cortex as mimicking top-down mechanism activated and influencing the cortex. To activate cholinergic innervation to the neocortex, we electrically stimulated the basal forebrain (BF).

Lastly, in the previous studies, iontophoresis technique was chosen for the microinjection of drugs into the cortex. The advantage of this technique is that drug microinjection can be applied in small volumes into surrounding area of the recording electrode. This could also be achieved by pneumatic microinjection pump which we

used for our experiments. On the other hand, there are disadvantages of iontophoresis technique. With this technique, the experimenter do not know the amount of drug injected and the extent which drug spreads in the tissue. It is important to know the amount of drug injected in experimental paradigm since the certain drugs could cause hyperexcitation or conversely inhibition depending on the amount of drug injected. Moreover, the current passage in the iontophoresis technique could also change the neuron's excitability if the recording electrode is close to cell membrane. Another disadvantage is that not all the compounds are ionized so poorly ionized compounds cannot be injected into the cortex with using same parameters. We overcame these issues by using pneumatic microinjection pump since we can calibrate the amount of drug injected and there is only one factor (drug) effecting the neuron's excitability.

In the further studies after this PhD work, electrophysiological data can be integrated with behavioral studies in which rats are required to do attention task. Same vibrotactile parameters can be used in the custom-made operant chamber which will allow us to compare the differences between anesthetized and behaving animal with chronic implantation of recording electrode. Investigation of the drug effects in behaving animal might also be possible with chronic implantation where drugs are injected into the associated area. Such combination of electrophysiological and behavioral studies will make a groundwork for role of attention in the tactile modality. As a result, we will make significant contributions to existing literature of sensory processing involving cholinergic system. In addition, ultimately these findings would be useful for neuropsychiatric populations in which attention is disrupted, such as Alzheimer's disease, attention-deficit disorder and schizophrenia. It is a hope that this knowledge will help development of new drugs for treatment of cognitive disorders.

## 1.4 Outline

In this section, the motivation, the objectives of this thesis and the general introduction are presented. Chapter 2, 3 and 4 are main chapters and each chapter includes Introduction, Aim, Materials and Methods, Results, Discussion and Conclusion sections. Chapter 2 presents how the tactile processing in the central nervous system

(CNS) works and how it is modulated by the changing the excitation-inhibition balance in the primary somatosensory (SI) cortex. In Chapter 3, the differential effects of cholinergic inputs to SI on the cortical neurons are discuessed. Chapter 4 presents the computational model for tactile processing in the SI generated from the experimental work presented in Chapter 2. Chapter 5 of this thesis presents the general conclusions and the future work and possible outcomes of this thesis.

# 2. EXCITATION AND INHIBITION BALANCE IN THE PRIMARY SOMATOSENSORY CORTEX

This work has been published in;

Vardar, B. and Güçlü B., Non-NMDA receptor mediated vibrotactile responses of neurons from the hindpaw representation in the rat SI cortex. *Somatosensory and Motor Research* 34:3 189-203, 2017.

## 2.1 Introduction

Primates mostly depend on the four types of mechanoreceptors in the glabrous skin for exploratory touch: Meissner corpuscles, Pacinian corpuscles, Merkel cells and Ruffini endings [11, 106–110]. Although all mammals have these mechanoreceptors, some species (e.g. rodents such as mouse, rat, and hamster) predominantly use their whiskers, i.e. mystacial vibrissae, for tactile exploration by actively moving them. In those species, the major part of the primary somatosensory (SI) cortex is dedicated to process information originating from the mechanoreceptors associated with the vibrissae, and is called the barrel cortex (for a detailed review see [44]; [111]). Extensive studies on the barrel cortex at all levels of analyses, from molecules to behavior, resulted in useful models for cortical processing with parallels to other brain areas. The present work was motivated by this rich literature, but focuses on an area that has been much less studied in the rat SI cortex, i.e. the hindpaw representation which gets inputs largely from mechanoreceptors in the glabrous skin [40, 47, 67, 112, 113]. Our long-term goal is to understand the similarities and differences between this area and the barrel cortex. In addition, since humans do not have homologues for whiskers, but have the same set of afferents as in the rat glabrous skin [114–116], human psychophysical performance may also be contrasted with neural processing in the rat fore- and hindpaw areas, which contain simpler networks than those in primates [117]. Previously, we predicted psychophysical responses in humans by using computational models based

on spike data from cats and monkeys [118–123]

SI cortex in the rat has almost the same cell packing density as the primary visual cortex, and even higher myelination indicating dense connectivity [124]. Based on cytoarchitecture, SI cortex has been divided into granular (GZ), perigranular (PGZ), and dysgranular zones (DZ) within a single body map [125]. GZs are identified with granule cell-rich layer IV and are surrounded by less granular DZs. PGZs are transitionally dysgranular zones between GZs and DZs. Barrels conventionally refer to the GZs associated with the vibrissae [126], but it is also customary to group all barrel-like structures (center-spare barrels and granular aggregates) under GZs which include the hindpaw area as well. Barrel-like structures are historically the first cytoarchitecturally defined examples of cortical columns [35–39]. Single- and multi-unit mapping studies showed that neurons in GZs have discrete cutaneous receptive fields (RFs), as opposed to large, diffuse RFs of PGZs [47,127]. In the awake state, the RFs are generally larger and more volatile, but with center locations similar to those in the anesthetized state. Nevertheless, the hindpaw representation has a substantial RF variability within and across cortical layers even in anesthetized rats [40, 113, 128, 129].

The pattern of connectivity in GZs is different as compared to PGZs and DZs. The main thalamocortical input to GZs originates from the ventroposterior (VP) nucleus of thalamus (also called ventrobasal in nonprimates), and its lateral division (VPL) is associated with mechanoreception in the hindpaw glabrous skin [130]. The ascending axons are somatotopically bundled according to their target GZ and terminated mainly in cortical layer IV, with less dense terminations in layers I-III. On the other hand, PGZs and DZs mostly receive input from posterior (Po) nucleus of thalamus. Within GZs, there is a generally strong flow of information from layer IV to II/III, and from layer III to V. GZs only make short-range corticocortical connections, including those with PGZs and DZs which are considered to be higher-order areas for sensorimotor integration because they receive convergent inputs from cutaneous receptors and proprioceptors [47]. There is a reciprocal excitatory corticothalamic projection from layer VI to VPL [131]. Other corticofugal projections, e.g. to brainstem and telencephalic regions, originate from layer V [132]. The layer IV neurons in GZs are spiny stellate cells (excitatory), star pyramids (excitatory), and aspiny inhibitory cells receiving mostly (90%) excitatory synapses; and synapses from thalamocortical af-

ferents (18%) are all excitatory [133]. Moreover, thalamocortical afferents can synapse with apical dendrites of pyramidal cells in layers V and VI [134]. Based on intrinsic properties, pyramidal cells, e.g. those in layer V, can be classified as regular spiking (RS) or intrinsically bursting (IB) [135]. IB cells do not receive thalamic inputs, and they have relatively less inhibitory inputs than RS cells [136]. Inhibitory cells, e.g. aspiny cells in layer IV, are fast spiking (FS) or low-threshold spiking (LTS). In contrast to most LTS cells, FS cells can receive thalamic synapses, which have depressing short-term dynamics similar to RS cells [137]. Overall, inhibitory cells are more sensitive to thalamic inputs than excitatory cells, and limit excitation directed to layers II/III [138].

In the rat SI cortex, excitation is mainly mediated by ionotropic glutamate receptors and fast inhibition is mediated by ionotropic $\gamma$-aminobutyric acid type A ($GABA_A$) receptors [139, 140]. Layers II-IV have the highest glutamate and $GABA_A$ receptor densities [124]. There are at least three pharmacologically distinct glutamate receptors: N-methyl-D-aspartate (NMDA), $\alpha$-amino-3-hydroxy-5-methyl-4- isoxazoleproprionate (AMPA), and kainate receptor [141–143]. The strong thalamocortical feed-forward inhibition to layer IV affects the time course of excitation and can last up to 100 ms [144, 145]. The initial excitatory input is largely mediated by AMPA receptors [146], because the slower NMDA-receptor component coincides with the development of inhibitory inputs [147]. The excitation-inhibition balance is also kept by negative feedback of FS cells at low frequencies, and by LTS cells at high frequencies, because the synapses that LTS cells receive have facilitating dynamics. The ubiquity of inhibitory interactions result in mostly rapidly-adapting-type (RA-type) responses instead of slowly- adapting-type (SA-type) responses [44,112,125]. Furthermore, $GABA_A$ inhibition seems to be not dependent on NMDA receptors [148], which implies that inhibitory neurons mostly receive non-NMDA-type synapses.

Bicuculline, a $GABA_A$ receptor antagonist, has frequently been used in cortical microinjection and iontophoresis studies to understand local connectivity between excitatory and inhibitory neurons. In those studies, cutaneous RFs typically expand due to reduced inhibition especially for RA-type units [149–151], but bicuculline also uncovers new RFs even more than glutamate [67]. GABAergic in-field inhibition was shown to be stronger than surround inhibition [152]. Similarly, RFs of neurons in the

barrel cortex change according to a layer-specific pattern with bicuculline application. Onset/offset response magnitudes and durations increase, but latencies are not affected [153, 154]. Activity changes seem to depend on pre-drug activity levels; RS unit activity increased almost three times more compared to FS units when the activity was low before bicuculline application. Experiments on the barrel cortex show that NMDA receptors are essential for generating spikes at latencies 10-100 ms evoked by a brief (3 ms) whisker deflection [146] and as suggested by the reduction of tonic response in knockout animals because of impaired synaptic temporal summation [155]. However, in an earlier study, Salt [156] had argued that non-NMDA component in the thalamic neurons becomes less effective to repetitive (20 Hz) electrical stimulation due to inhibitory networks. More recently, Vahle-Hinz et al. [157] recorded spike activity from thalamic neurons responding to whisker vibration (>20 Hz) in rats anesthetized with low and high concentrations of isoflurane. High isoflurane concentrations produced only onset responses to vibratory stimuli, but the periodic spike activity, i.e. 1:1 firing, was recovered by iontophoretic application of either NMDA, AMPA, or bicuculline. Therefore, they stated that the high- frequency vibratory signals were available in the thalamus.

In the current study, we adopted an approach similar to that of Vahle-Hinz et al. [157]. We first blocked most of the NMDA receptors by ketamine anesthesia, and then tested the effects of bicuculline, NMDA, and AMPA microinjection. Ketamine typically reduces RF size, and neural activity [158, 159], and is sometimes utilized to avoid response variability due to NMDA receptor-mediated local and corticocortical interactions [160]. Since NMDA receptors are generally considered to be necessary for tonic responses, one may expect that only phasic responses would remain with ketamine. However, most of the previous studies supporting this were done with mechanical ramp-and-hold stimuli or electrical pulses, and their results do not easily apply to vibrotactile stimuli (e.g. [146, 156, 161]). Our preliminary work showed that cortical neurons in the hindpaw area mostly responded at the onset, i.e. initial cycles, of the vibrotactile stimulus at high frequencies (40 Hz and 250 Hz), but entrainment to all stimulus cycles could be observed at 5 Hz [123, 162–164]. This is unlikely to be entirely due to reduced NMDA receptor-mediated transmission, because similar reponses were measured previously in awake rats and under various anesthetics [125, 165].

Onset responses to ramp-and-hold and vibratory stimuli are also prominent in first-order afferents [166] and cortical neurons [167–172] of the vibrissal pathway. Excitation is frequently followed by inhibition, which signifies the contribution of local network dynamics to sensory transmission. However, the rapid adaptation to high-frequency stimuli may also be due to depressing thalamocortical synapses [137], given that the thalamic neurons can transmit these signals in appropriate conditions [157].

We specifically investigated the effects of vibrotactile stimulus frequency and excitation-inhibition balance on the primarily AMPA receptor-mediated fast responses in the hindpaw representation of rat SI cortex. We also focused on the differences in RS and FS cells because of their complementary roles in local dynamics. The data were analyzed based on average firing rate (AFR) calculated over two temporal windows (initial 100-ms and late 400-ms of stimulus duration) and vector strength (VS) of spike phases referenced to stimulus cycles. We hypothetize that shifts in the excitation-inhibition balance would modulate vibrotactile responses differently based on layer-specific cell type and stimulus frequency. In other words, the recovery (or the absence) of spikes would be indicative for the dynamical properties of excitation/inhibition at various stages of cortical processing related to the suprathreshold mechanoreceptive input from the glabrous skin. For example, if the AFR increases with bicuculline microinjection for an RS neuron in layer IV only in the initial stimulus period, this would imply a dominant role for thalamocortical feed-forward inhibition. If the increase described as such occurs later within the stimulus duration, longer-latency inhibitory connections would be indicated. On the other hand, VS is a general measure for the fidelity of vibrotactile information transmission through a chain of synapses. If VS never increases and there is no significant entrainment, this may suggest a corticothalamic or an entirely subcortical contribution. As such, strong vibrotactile signals would not reach layer IV. Generally, smaller differential effects of stimulus frequency with the application of bicuculline, NMDA, or AMPA would highlight more local cortical dynamics in our experiment. For example, microinjection of AMPA may compensate for the reduced response of depressing synapses, if VS is found to increase only at high frequencies. We also analyzed changes in the spontaneous activity due to drug application. In summary, our study aims to offer a wide framework for subsequent experiments and modeling related to mechanoreceptive inputs from the rat glabrous skin.

## 2.2 Materials and Methods

### 2.2.1 Animals and Surgery

Nineteen adult Wistar albino rats (10 female, 9 male, 3-8 months old, weight: 168-387 g) were used in the study. All experiments were approved by the Boğaziçi University Institutional Ethics Committee for the Local Use of Animals in Experiments. Each rat was initially anesthetized by ketamine (65 mg/kg) and xylazine (10 mg/kg) intraperitoneally (IP). The rectal temperature was monitored and kept at 37 °C by a heating pad (TCAT-2LV; Physitemp Instruments, Clifton, NJ, USA). The state of anesthesia was periodically checked by palpebral and pedal reflexes. If necessary, additional injections of anesthesia were administered at one third of the induction dose. Atropine (0.05 mg/kg) was injected IP before surgery to decrease bronchial secretions and to reduce bradycardia during the experiment. For long experiments, Ringer's lactate solution (40 mL/kg/24h, IP) was given to maintain normal physiological conditions. Additionally, to prevent brain edema and to decrease incranial pressure, furosemide (2 mg/kg) and mannitol (0.2 g/kg) were administered IP before the experiment. At the end of the experiment, the animal was euthanized either by an overdose of thiopental (200 mg/kg, IP) or perfused transcardially for subsequent histological examination of SI cortex. After the induction of surgical anesthesia, the animal's head was fixed to a digital stereotaxic frame (model 940; David Kopf Instruments, Tujunga, CA, USA) and a craniotomy was performed based on standard anatomical landmarks [47, 173] either over the left or right hemisphere in a random, counterbalanced order for each animal. A plastic recording chamber was fixed to the skull by using dental acrylic and it was filled with mineral oil to damp out brain pulsations.

### 2.2.2 Single-unit recording and vibrotactile stimulation

Extracellular action potentials (spikes) were recorded by using a carbon fiber (diameter: $\sim 7\ \mu$m) in a multi-barrel combination electrode shown in Figure 3.2(a) (Carbostar-6; Kation Scientific, Minneapolis, MN, USA). The combination electrode

was mounted on a hydraulic microdrive (MHW-4; Narishige International, London, UK). Spikes were amplified (x1000) and filtered (200 Hz - 10 kHz) by a custom-made microelectrode amplifier. Single units were selected by an amplitude window discriminator (model 121; World Precision Instruments). The RFs of the units were mapped by von Frey hairs. Only units responding to tactile stimulation of the glabrous skin in the hindpaw and those with sufficiently high signal-to-noise ratio (>3) were studied in each penetration. Both raw voltage data and discriminated spikes were saved on a personal computer by using the analog inputs of a data-acquisition card (USB-6251; National Instruments, Austin, TX, USA). The instrumentation system for the experiment was controlled by a custom-made program running in MATLAB Version R2008a (The MathWorks, Natick, MA, USA).

The waveforms for the vibrotactile stimulation were prepared in the MATLAB program and output by an analog output channel of the USB-6251 card. The stimulation signal was filtered by a custom-made 1-kHz low-pass filter and its level was adjusted during the experiment by a digital attenuator (model V2.0C; ISR Instruments, Syracuse, NY, USA) controlled by the same card. The vibrotactile stimuli were given with electrodynamical shaker (V101; Ling Dynamic Systems, Royston, Herts., UK) and applied at the RF center of each single unit by using a plastic cylindrical contactor (diameter: 1.8 mm) without a surround.

### 2.2.3 Drugs and microinjection

Combination electrodes for extracellular recording and application of drugs or dyes have been frequently used in the literature (for iontophoresis see Haidarliu et al. 1995, 1999 [174, 175]; for pressure microinjection see Akaoka et al. 1992 and Hupé et al. 1999 [176, 177]). For the sham condition, artificial cerebrospinal fluid (aCSF) was prepared with the following concentrations [178] in mM: NaCl 124, KCl 4.0, CaCl22.5, MgCl2 1.0, KH2PO4 1.0, NaHCO3 26, D-glucose 10 (pH 7.3-7.4, bubbled with 95% O2 + 5% CO2). Bicuculline (Sigma-Aldrich: 14340) was used at 200 $\mu$M. The concentrations of NMDA (Sigma: M3262) and AMPA (Sigma: A6816) were both 10 $\mu$M. During the experiment, each drug barrel was manually selected by a three-way valve

on a tubing manifold. The microinjection was performed by a pneumatic picopump (PV820; World Precision Instruments) at a pressure of 4-8 psi. The pump was digitally triggered by the USB-6251 card and controlled by the MATLAB instrumentation software mentioned above. Each microinjection pulse had a duration of 20 ms and the pressure was calibrated in the above range to yield a release of approximately 8 nL solution. Additionally, the microinjections were monitored during the experiment by a custom-made electronic counter.

### 2.2.4 Experimental Procedure

The stimulation parameters, i.e. amplitude and frequency, were selected to ensure that there was no decoupling of the contactor from the skin [179]. After RF mapping, the stimulation protocol was run (Figure 2.1). Subsequently, three sinusoidal frequencies (5, 40, and 250 Hz) were tested in random counterbalanced blocks for each single unit. The sequence of blocks in Figure 2.1 represents one protocol run at a given frequency. Each block includes 10 trials at the condition depicted with letters. For each frequency block, the vibrotactile stimuli were first applied without any microinjection to check the responsiveness of each isolated unit (mechanical-only condition). The stimuli were bursts sinusoidal mechanical displacements (amplitude: 100 $\mu$m peak-to-peak) superimposed on a static indentation of 0.5 mm. They started and ended as cosine-squared ramps with 50-ms rise/fall times, and duration of 0.5 s, as measured between half-power points (see upper traces in Figures 2.3,2.4,2.5 for stimulus waveforms). There were 10 trials; and each trial lasted 2 s (inter-trial interval: 3 s). Next, the vibrotactile stimulation was repeated with aCSF microinjection (sham condition). There were 5 microinjection pulses with 100-ms intervals applied before the vibrotactile stimulus (black dots above the stimulus traces in Figures 2.3,2.4,2.5). Then, the first drug condition was tested with bicuculline. After completing the drug condition, 5 minutes were allowed for recovery. The second drug condition was for AMPA and was preceded with another sham condition. The drug order was deliberately not randomized to compare baseline AFRs across the sequential sham conditions for verifying recovery from drug effects. Furthermore, the baseline AFRs across sham

conditions from different frequency runs (ordered in time) showed that neural activity was stable over time (see Results). We also applied NMDA in all experiments and confirmed that its effects did not depend on the vibrotactile frequency.

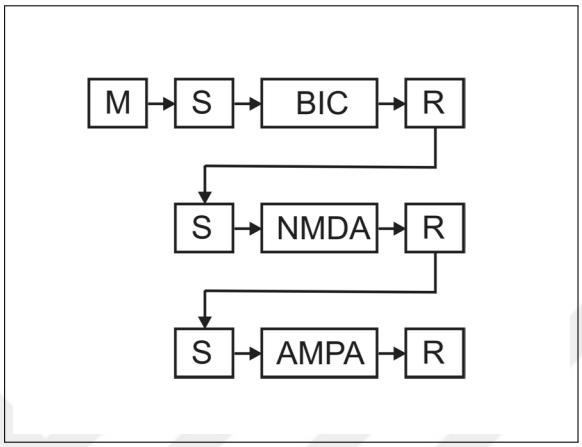


**Figure 2.1** Stimulation protocol. For each vibrotactile frequency, the sequence of blocks shown in the figure was completed. Each block included 10 trials at the condition depicted with the letters:M: mechanical-only, S: aCSF (sham), BIC: bicuculline, NMDA, and AMPA blocks. Vibrotactile stimulus was presented just after the microinjection pulses (see Figures 2.3, 2.4, 2.5). R: recovery block (5 minutes).

### 2.2.5 Analyses

The RF maps were categorized in Figure (2.2) according to a flowchart (for details, see Güçlü 2013 [180]). The main criterion was the inclusion of digits in the RFs and nine letter categories were determined: (A) single digit, (B) multiple digits, (C) only pad(s), (D) digit(s) and pad(s), (E) upper paw without digits, (F) lower paw, (G) digit(s), pad(s), and neighboring sole, (H) entire paw without digits, (I) entire paw. Additionally, the von Frey threshold of each unit was found. The units were classified into RS, FS, and intrinsically bursting (IB) neurons according to the spike shapes and the firing pattern [135, 167, 181]. The cortical layer was estimated based on the recording depth and it was occasionally verified by histological track tracing. According to previous reports [40, 112], the boundaries were on average at 165 $\mu$m, 293 $\mu$m, 577 $\mu$m, 879 $\mu$m, 1351 $\mu$m between the cortical layers I-VI. The sampled

neurons were found only in layers III-V, probably because of our high signal-to-noise ratio requirement during extracellular recording (see above).

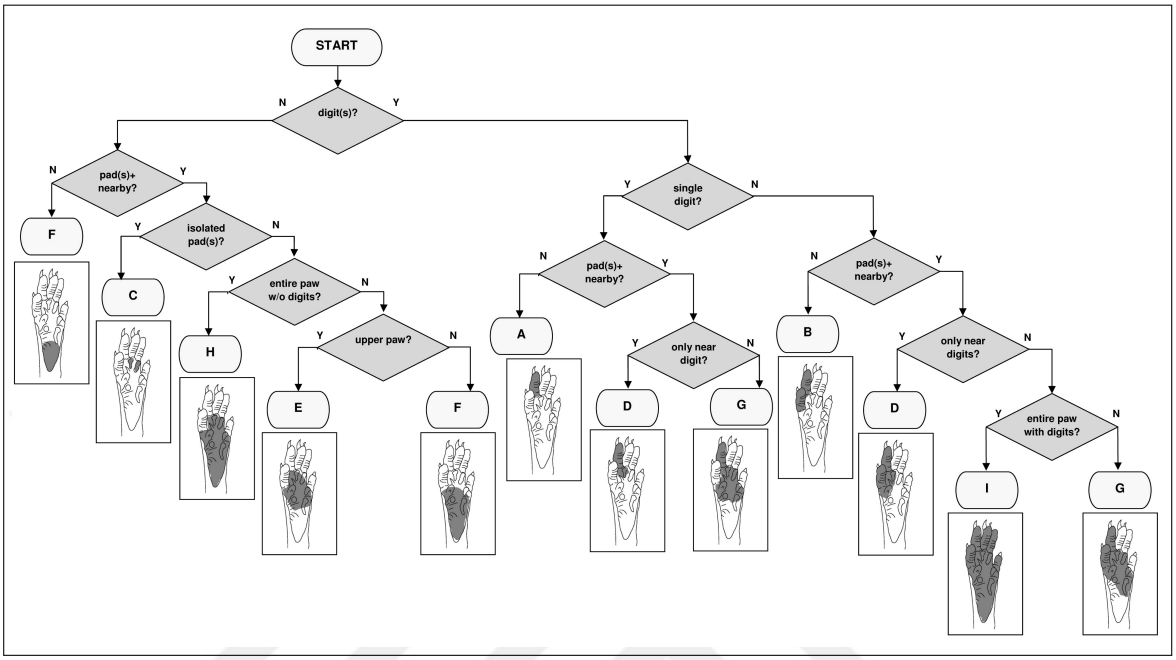


**Figure 2.2** Flowchart to group the receptive fields into 9 letter categories: (A) single digit, (B) multiple digits, (C) only pad(s), (D) digit(s) and pad(s), (E) upper paw without digits, (F) lower paw, (G) digit(s), pad(s), and neighboring sole, (H) entire paw without digits, (I) entire paw.

Spike times of each classified neuron were initially pooled across 10 trials in every frequency condition, and were used to construct peristimulus time histograms (PSTHs, bin size: 50 ms) and spike-phase (SP) histograms (bin size: 0.5° which is equivalent to $\pi/360$). AFR was calculated for the period (0-0.5 s) before the vibrotactile stimulus ($R_b$), during the initial 100-ms period of the stimulus ($R_o$), and during the remaining 400-ms period of the stimulus ($R_d*$). To quantify the entrainment in neural activity, i.e. periodicity with respect to the stimulus cycles, vector strength (VS) was calculated for each condition by using the pooled spikes [182–184]. Given the spike times $\{t_1,t_2,...,t_n\}$, the VS is defined as

$$\frac{1}{n}\sum_{j=1}^{n} = e^{i2\pi ftj} \tag{2.1}$$

where f is the vibrotactile frequency and i is the imaginary number. In this formula, the spikes are represented as unit vectors with phase on the complex plane and the vectors

are summated. VS is the modulus of the resultant vector normalized with the number of spikes and can vary in [0,1]. If the spikes occur regularly with the same period as the vibrotactile stimulus, VS approaches unity. The AFRs and VS values were statistically analyzed by repeated measures ANOVA in SPSS Ver. 22 (IBM Corp., Armonk, NY, USA). The vibrotactile frequency and drug vs. sham conditions were within-subject factors. Cortical layer and neuron type were between-subject factors. Only RS and FS neurons were included in the statistical tests, because the remaining sample of neurons was relatively small. Rayleigh test was applied to assess the significance of entrainment by using a MATLAB toolbox developed for circular statistics [185].

## 2.3 Results

### 2.3.1 Classification of vibrotactile neurons

Sixty-seven neurons were sampled from the hindpaw representation in the SI cortex of 19 rats: 23 from layer III, 26 from layer IV, and 18 from layer V (Table 2.1). The receptive-field types varied substantially within each cortical layer. All receptive fields were large, as typical of cortical neurons, except one which covered only a single pad on the upper paw (Type C). In layer III, Type B and Type D were most commonly found (6 and 7 of 23 neurons, respectively). Both of these types have digits involved, but Type D may consist of only one digit in addition to single/multiple pads. The neurons sampled from layer IV had receptive fields mostly of Type D and Type E (6 and 8 of 26 neurons, respectively), which both cover areas at upper paw. In layer V, Type E receptive field was observed more frequently (5 of 18 neurons). Single-digit (Type A) receptive fields were observed for only 9 neurons in the entire sample (13%).

The neurons which had medium spike thresholds (von Frey: 0.25-2.5 g) were more uniformly distributed across the cortical layers (17 neuron each in layers III-V). Those with low spike thresholds (von Frey: $<$0.25 g) were mostly found in layer IV (9 of 16 neurons). There were no neurons with high spike thresholds (von Frey: $>$2.5 g). Receptive fields of medium-threshold neurons were mostly of Type D and Type E (14 and 12 of 51 neurons, respectively). On the other hand, Type B receptive field was

**Table 2.1**
Classification of 67 vibrotactile neurons in the hindpaw representation of SI cortex. The receptive-field (RF) categories refer to the letters defined in Figure 2.2. Low von Frey threshold: <0.25 g; Medium von Frey threshold: 0.25-2.5 g. Numbers are the neuron counts. Percentages and bold numbers refer to a particular neuron group counted in rows (based on von Frey threshold, neuron type, or cortical layer) and columns (based on cortical layer or RF category).

| | *Cortical Layer* | | | *Receptive Field* | | | | | | | | | |
|---|---|---|---|---|---|---|---|---|---|---|---|---|---|
| | III | IV | V | A | B | C | D | E | F | G | H | I | Total | |
| Low Threshold | 6 | 9 | 1 | 1 | 5 | 0 | 2 | 3 | 4 | 1 | 0 | 0 | 16 | 24% |
| Medium Threshold | 17 | 17 | 17 | 8 | 5 | 1 | 14 | 12 | 5 | 2 | 1 | 3 | 51 | 76% |
| Regular-Spiking (RS) | 12 | 9 | 10 | 7 | 7 | 1 | 5 | 4 | 4 | 1 | 0 | 2 | 31 | 46% |
| Fast-Spiking (FS) | 9 | 8 | 7 | 2 | 2 | 0 | 7 | 7 | 4 | 2 | 0 | 0 | 24 | 36% |
| Intrinsically Bursting (IB) | 2 | 9 | 1 | 0 | 1 | 0 | 4 | 4 | 1 | 0 | 1 | 1 | 12 | 18% |
| Layer III | - | - | - | 3 | 6 | 0 | 7 | 2 | 3 | 2 | 0 | 0 | 23 | 34% |
| Layer IV | - | - | - | 3 | 4 | 1 | 6 | 8 | 2 | 0 | 1 | 1 | 26 | 39% |
| Layer V | - | - | - | 3 | 6 | 0 | 7 | 2 | 3 | 2 | 0 | 0 | 23 | 27% |
| Total | 23 | 26 | 18 | 9 | 10 | 1 | 16 | 15 | 9 | 3 | 1 | 3 | 67 | - |

found the most (5 of 16 neurons) for low-threshold neurons.

The neurons were also classified as RS (46%), FS (36%), and IB (18%) based on the spike shape. Within each class, the neurons were usually distributed uniformly across layers, except IB neurons which were primarily found in layer IV (9 of 12 neurons). The receptive fields of RS neurons were commonly of Type A and B (both 7 out of 31 neurons), i.e. covering the digits. For FS and IB neurons, the receptive fields were mostly of Type D and E (FS: both 7 out of 24 neurons; IB: both 4 out of 12 neurons); therefore, they were usually at the upper paw.

### 2.3.2 Response to mechanical stimulation of the skin

The spike activity of neurons in response to mechanical stimulation was first analyzed by PSTHs and SP histograms (Figures 2.3, 2.4, 2.5). The displacement waveforms (amplitude: 100 $\mu$m peak-to-peak) applied to the skin are shown above the

PSTHs and share the same time axes in the figures. The black bars in the PSTH plots and black lines in SP histograms were obtained for the sham (aCSF) condition, and show the general response to mechanical stimulation at 5-, 40- and 250-Hz frequency without any drug effects. Consistent with the previous studies, spikes were mostly generated at the initial 100-ms duration of the sinusoidal stimulus for all neurons tested at 40 and 250 Hz, but many more spikes could be generated later during the 5-Hz stimulus. Entrainment (1:1 firing) was almost always found at 5 Hz, but not as much at 40 and 250 Hz. This was observed by the periodic occurrence of spikes in the PSTHs, and by the accumulation of lines in a small angular range in the SP histograms. Rayleigh test showed that all RS neurons and 92% of FS neurons had significant VS values at 5 Hz. However, at 40 Hz, 48% of RS neurons and 29% of FS neurons had significant entrainment. Similarly, 42% of RS neurons and 33% of FS neurons were significantly entrained at 250 Hz. Since the stimulus level was quite high, and well above physiological threshold, some neurons could also generate two spikes for each cycle of the stimulus (2:1 firing) at 5 Hz. This was observed by doubled bars in the PSTHs and the axial accumulation pattern in the SP histograms (e.g. see 5-Hz plots for the RS neuron in Figures 2.3, and 2.4). Additionally, some neurons seemed to be inhibited between excitation bouts (e.g. see 40-Hz plots in Figures 2.3,2.4,2.5). The trial-by-trial variability of stimulus-evoked responses was not high in both sham and drug conditions (not shown); therefore, PSTHs and AFR measures were adequate to characterize the responses across time.

To assess the change in spike activity due to vibrotactile stimulation, the background AFR ($R_b$) was subtracted from the AFR during the initial 100-ms period of the stimulus ($R_o$) and from the AFR during the remaining portion of the stimulus ($R_d*$) for each neuron. As such, $R_o$-$R_b$, $R_d*$-$R_b$, and entrainment, measured by the VS of spike phases, were analyzed by ANOVA only for the sham conditions with stimulus frequency as a within-subject factor, and cortical layer and neuron type (RS and FS) as between-subject factors. Stimulus frequency had a significant main effect on both firing-rate measures and entrainment ($R_o$-$R_b$: $F(2,98)=5.36$, $p=0.006$; $R_d*$-$R_b$: $F(1,48)=17.96$, $p<0.001$; VS: $F(1,48)=114.0$, $p<0.001$). Post-hoc analyses showed that the AFR change during the initial 100-ms period of the stimulus ($R_o$-$R_b$) was higher at 40 Hz (22.7±1.6 spikes/s) compared to 5 Hz (18.3±2.1 spikes/s) and 250 Hz (18.1±1.6

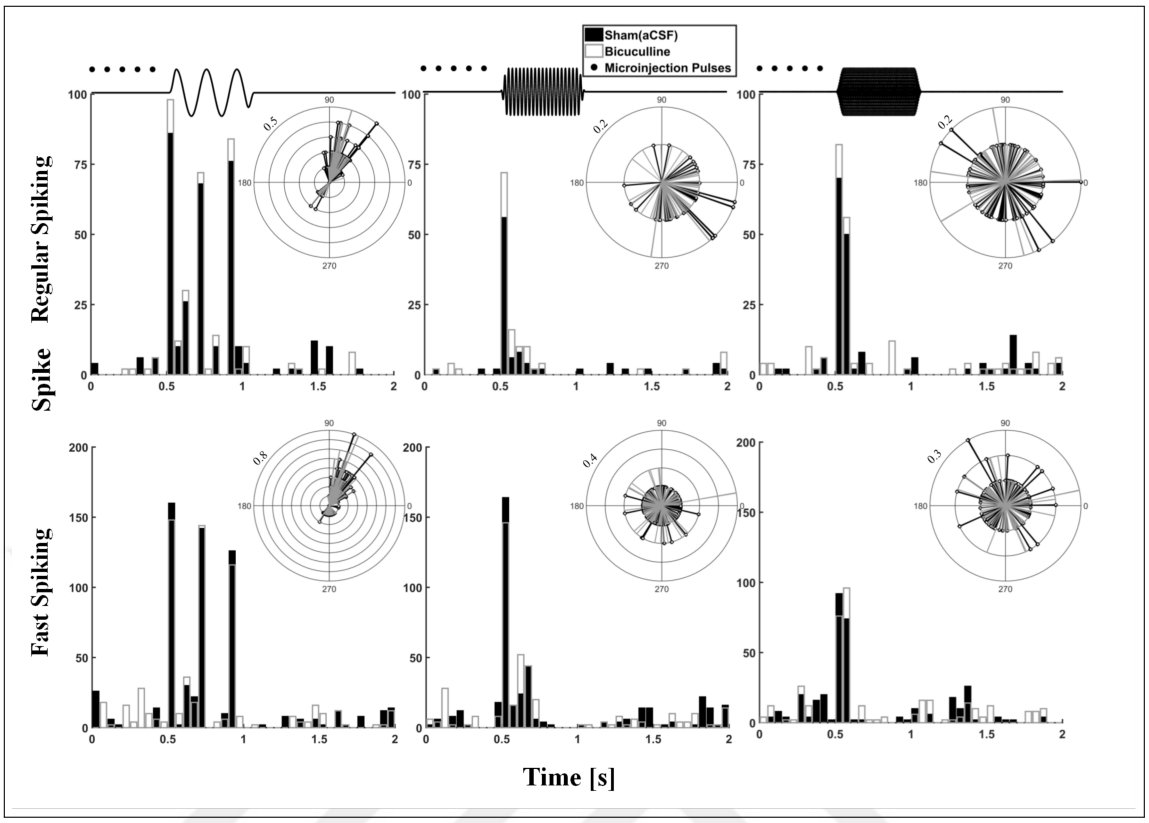


**Figure 2.3** Peristimulus time histograms (PSTHs) and spike-phase (SP) histograms of a regular spiking and a fast spiking neuron. The vibrotactile displacement waveforms are given above the PSTHs and share the same time axes (left: 5 Hz, middle: 40 Hz, right: 250 Hz). Black dots above the waveforms are microinjection pulses. Black bars in the PSTHs (bin size: 50 ms) and black lines in the SP histograms (bin size: 0.5°) are for the sham (aCSF) condition. Empty bars with gray outlines in PSTHs and gray lines in SP histograms are for the bicuculline application. The angular axis in the SP histograms is given in degrees, and the radial axis shows the number of spikes per trial in each bin (tick label printed near the outer circle).

spikes/s)(Figure 2.6(a)). On the other hand, for the remaining portion, the change due to the vibrotactile stimulus ($R_d$*-$R_b$) was highest at 5 Hz (7.3±1.2 spikes/s) and significantly different than those at 40 Hz (1.3±0.6 spikes/s) and 250 Hz (2.3±0.5 spikes/s) (Figure 2.6(b)). As expected from the histogram plots, the VS was significantly higher at 5 Hz (0.55±0.03), compared to 40 Hz (0.21±0.02) and 250 Hz (0.15±0.01). Furthermore, the VS for 40 Hz was significantly higher than the VS for 250 Hz (Figure 2.6(c)).

Main effects due to cortical layer and neuron type could not be found for the calculated spike-rate measures. On the other hand, VS was significantly influenced by layer ($F(2,48)=6.26$, $p=0.004$) (Figure 2.6(c)). The average VS in layer III (0.37±0.02) was significantly higher than VS in layer IV (0.27±0.02) and VS in layer

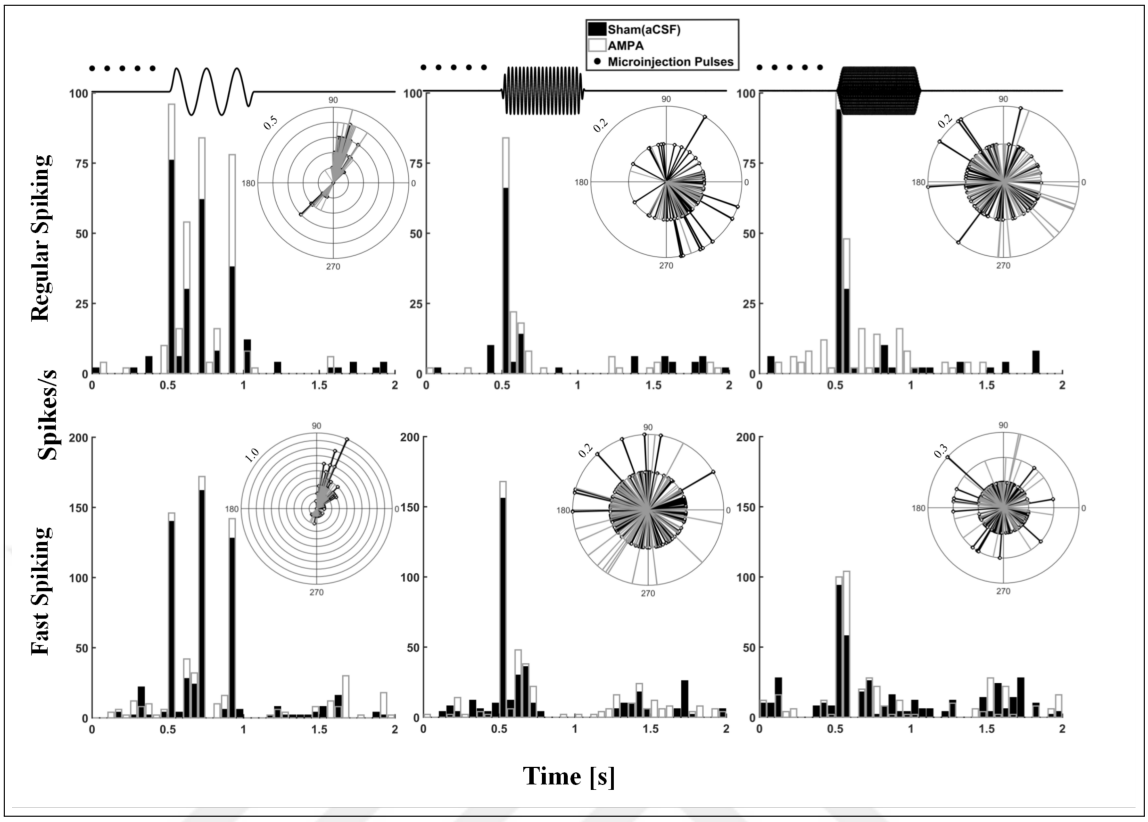


**Figure 2.4** Peristimulus time and spike-phase histograms of the same regular spiking and the same fast spiking neuron as in Figure 2.3 (see caption for details). The histograms show data from the block with AMPA microinjection and the sham condition before that.

V (0.27±0.02). Additionally, there was a marginal main effect of neuron type on entrainment ($F(1,48)=3.99$, $p=0.051$). RS neurons had higher (0.33±0.02) VS compared to FS neurons (0.28±0.02) (Figure 2.6(c)).

There was also an interaction between frequency and cortical layer for entrainment ($F(2,48)=3.66$, $p=0.033$). It was observed that for both 40 and 250 Hz, there was a slightly decreasing trend in VS towards deeper layers (Figure 2.6(c)). However, the VS in layer V was found higher than the VS in layer IV at 5 Hz. No other interaction effects were found.

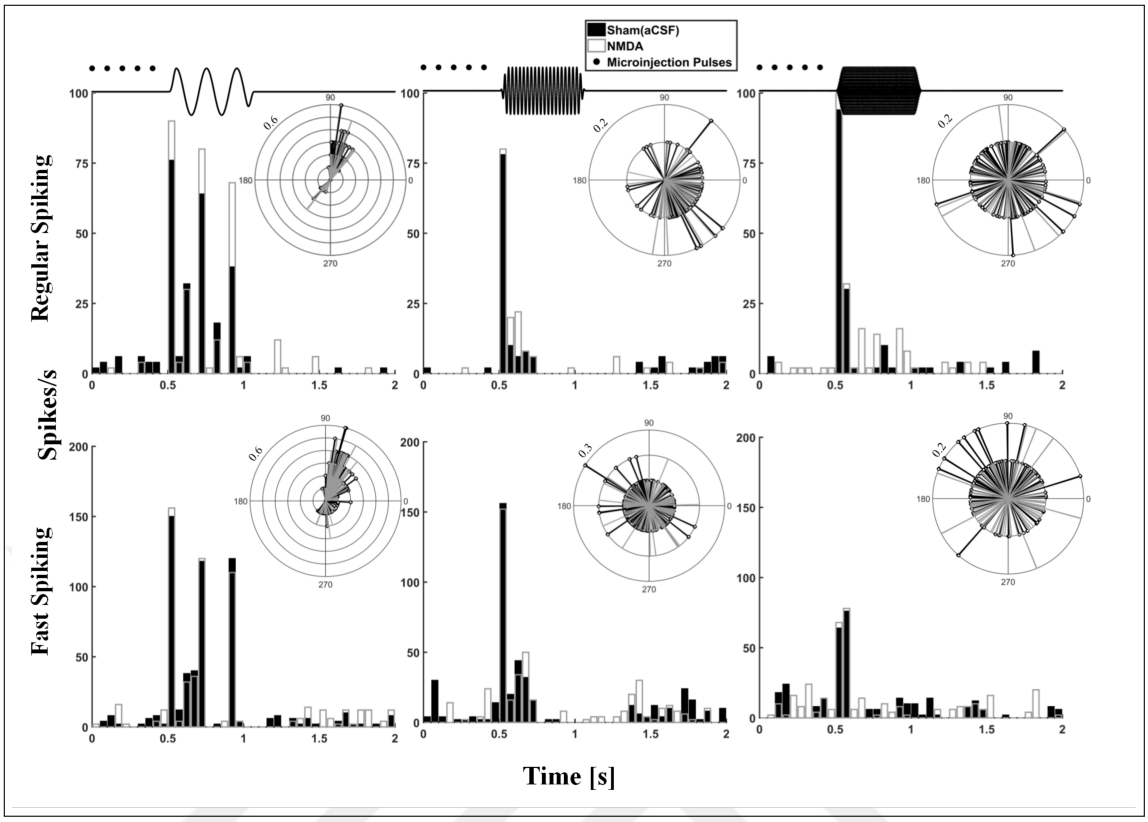


**Figure 2.5** Peristimulus time and spike-phase histograms of the same regular spiking and the same fast spiking neuron as in Figure 2.3 (see caption for details). The histograms show data from the block with AMPA microinjection and the sham condition before that.

### 2.3.3 Main effects of applied drugs and other factors

Among 67 neurons which were treated with bicuculline and NMDA, 37 were also treated with AMPA. It was verified that the activity of neurons returned to baseline AFR ($R_b$) between each drug administration. This was tested by using ANOVA with particular sham condition of each drug and consecutive test blocks for the stimulus frequency as two within-subject factors. The cortical layer and neuron type were between-subject factors. There were no significant main effects due to either particular sham condition ($F(2,96)=0.38$, $p=0.685$) or time represented as consecutive test blocks for frequency ($F(2,96)=0.04$, $p=0.964$). There was no significant main effect due to neuron type, but $R_b$ changed due to cortical layer ($F(2,48)=5.74$, $p=0.006$). The baseline activity gradually increased at deeper layers. Specifically, $R_b$ was significantly higher in layer V (8.5±1.0 spikes/s) compared to $R_b$ in layer III (4.2±0.9 spikes/s). There were no statistically significant differences between $R_b$ in layer IV (5.3±0.9 spikes/s)

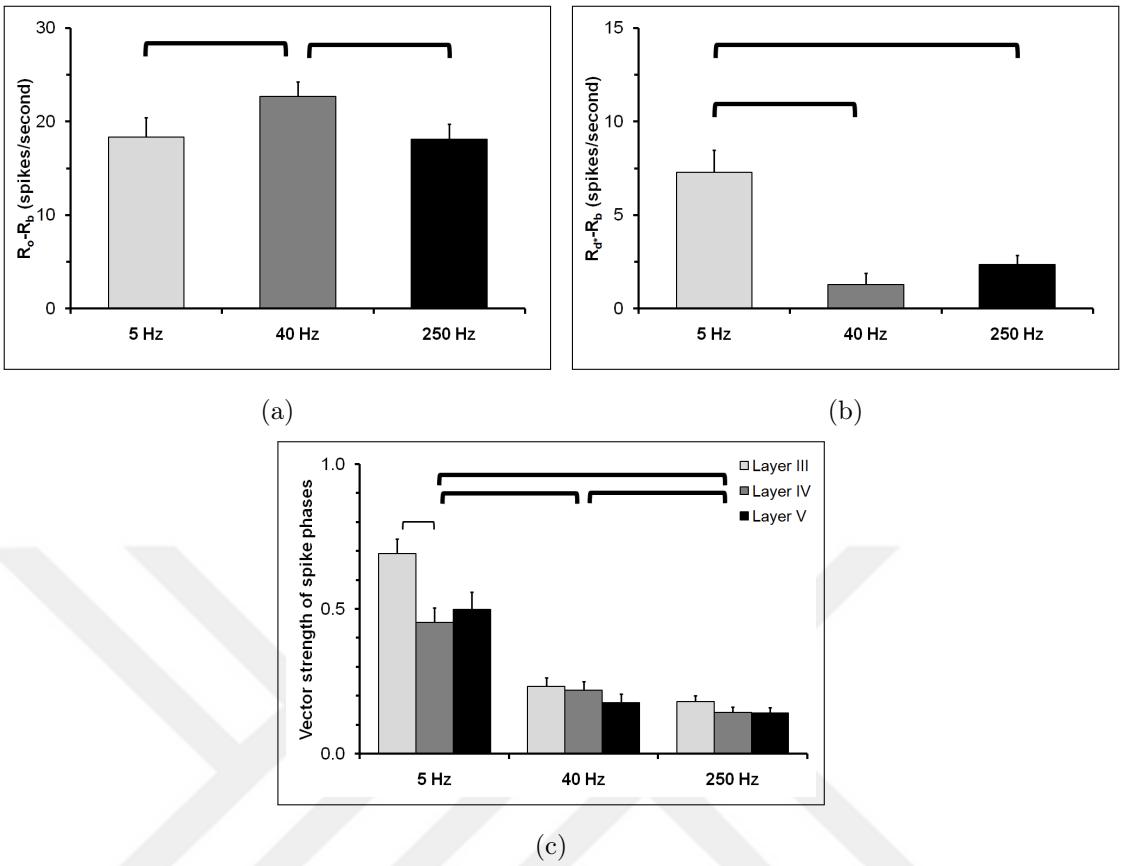


**Figure 2.6** Average firing rates (AFRs) and vector strength (VS) values for the mechanical-only (M)condition. Error bars are the standard errors. Main effect of vibrotactile frequency was significant for all response measures (thick lines for post hoc comparisons).Thin lines show post-hoc comparisons only within a condition indicated by the grouped bars. All comparison lines: $p<0.05$. (a) Change of AFR during the initial 100-ms period of the stimulus with respect to background ($R_o$-$R_b$).(b) Change of AFR during the remaining 400-ms period of the stimulus with respect to background ($R_d$*-$R_b$). (c) VS of spike phases from the entire stimulus duration (0.5s). There were other significant effects on VS (cortical layer, vibrotactile frequency x cortical layer).

and $R_b$'s in the other layers. There were also no interactions between the experimental factors regarding their effects on the baseline activity.

It is interesting to note that drug injection itself did not change $R_b$, but changed the responses of neurons during vibrotactile stimulation of the skin. As such, different ANOVAs showed that there were no drug vs. sham effects in $R_b$, although the microinjection pulses were applied during the time window in which the baseline AFR was calculated (bicuculline: $F(1,48)=2.66$, $p=0.109$; NMDA: $F(1,48)=0.375$, $p=0.543$; AMPA: $F(1,24)=3.16$, $p=0.088$). The below analyses for the remaining part of this subsection consist of repeated measures ANOVA with frequency and drug vs. sham condition as two within-subject factors, and cortical layer and neuron type as two

between-subject factors. Since stimulus frequency had main effects similar to those mentioned above in response to mechanical stimulation, it will not be included in further discussion unless necessary (see interaction effects below).

i) *Bicuculline*: The main effects due to bicuculline was evident in all activity measures. It increased AFRs significantly in the vibrotactile responses ($R_o$-$R_b$: $F(1,48)=12.01$, $p=0.001$; $R_d*$-$R_b$: $F(1,48)=18.93$, $p<0.001$) (Figure 2.7). This can also be seen in the PSTHs in Figure 2.3 especially for RS neurons. Bicuculline also significantly increased VS ($F(1,48)=11.32$, $p=0.002$) (Figure 2.7(c)). There was a main effect of cortical layer on VS similar to that one explained for the response to mechanical stimulation above ($F(2,48)=3.76$, $p=0.030$).

ii) *NMDA*: The results for the NMDA application were quite similar to those obtained with bicuculline. Significant AFR increases were found both for the initial and the remaining portion of the stimulus ($R_o$-$R_b$: $F(1,48)=14.74$, $p<0.001$; $R_d*$-$R_b$: $F(1,48)=13.88$, $p=0.001$) (Figure A.4(A,B)). NMDA caused an increase in the VS ($F(1,48)=45.55$, $p<0.001$) (Figure A.4(C)). Within this experiment, layer differences in VS were more prominent ($F(2,48)=7.63$, $p=0.001$) compared to bicuculline application, and similar to the general results as explained for the response to mechanical stimulation above. Additionally, the same main effect due to neuron type was found, i.e. RS neurons with higher VS values ($F(1,48)=10.45$, $p=0.002$). Some of these findings can also be observed in the exemplar histograms of Figure 2.5.

iii) *AMPA*: Similar to the results described above, AMPA microinjection caused a clear drug effect (Figure 2.8). It increased the calculated AFR measures ($R_o$-$R_b$: $F(1,24)=75.24$, $p<0.001$; $R_d*$-$R_b$: $F(1,24)=25.81$, $p<0.001$) and the VS ($F(1,24)=77.69$, $p<0.001$).

### 2.3.4 Differential effects of drugs based on the vibrotactile frequency

It was shown above that stimulus frequency had robust, but dissimilar effects on both entrainment and the AFR measures. Additionally, we found significant interaction effects between frequency and some of the drug vs. sham conditions. This implies that

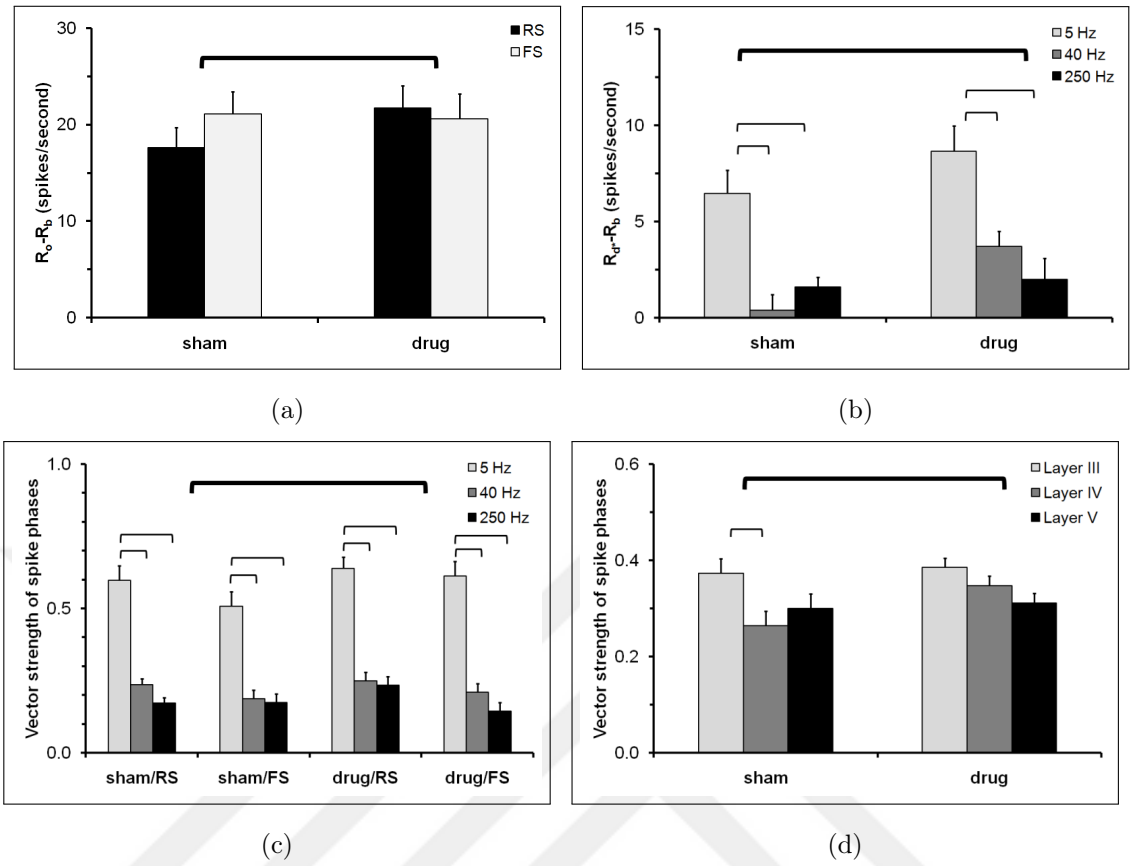


**Figure 2.7** Average firing rates (AFRs) and vector strength (VS) values for the bicuculline (BIC) condition. Error bars are the standard errors. Main effects of vibrotactile frequency and cortical layer were significant and similar to those in Figure 2.6 for all response measures. Thin lines show post-hoc comparisons only within a condition indicated by the grouped bars. All comparison lines: $p<0.05$. (a) Change of AFR during the initial 100-ms period of the stimulus with respect to background ($R_o$-$R_b$). There were significant main (thick line: drug vs. sham condition) and interaction effects (drug vs. sham x neuron type). (b) Change of AFR during the remaining 400-ms period of the stimulus with respect to background ($R_d$*-$R_b$). There were significant main (thick line: drug vs. sham condition) and interaction effects (drug vs. sham x vibrotactile frequency). (c) VS of spike phases from the entire stimulus duration (0.5 s). There were significant main (thick line: drug vs. sham condition) and interaction effects (drug vs. sham x vibrotactile frequency x neuron type). (d) VS values are re-plotted to show another significant interaction (drug vs. sham x cortical layer).

the related drugs modified the responses based on the dynamical time course of vibrotactile stimulation. Specifically, bicuculline had different effects on $R_d$*-$R_b$ at different frequencies ($F(2,96)=3.57$, $p=0.032$). The greatest increase in $R_d$*-$R_b$ was observed at 40 Hz (Figure 2.7(b)), and there was only a slight change on average at 250 Hz. However, this interaction effect itself was not dependent on cortical layer or neuron type. On the other hand, $R_d$*-$R_b$ was influenced by a triple interaction with AMPA: drug vs. sham condition x frequency x neuron type ($F(2,48)=6.33$, $p=0.004$)(Figure 2.8(b)). This is because that, at 40 Hz, AMPA did not increase $R_d$*-$R_b$ in RS neurons, but it

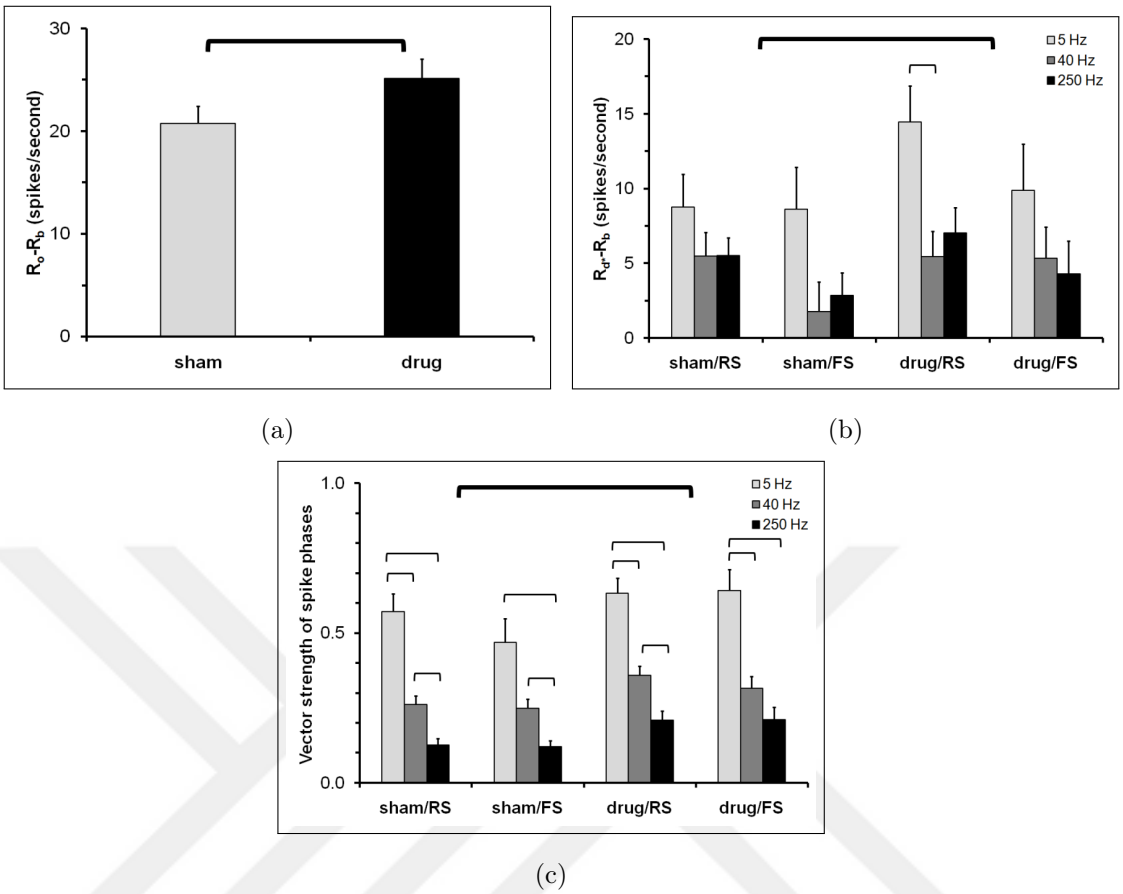


**Figure 2.8** Average firing rates (AFRs) and vector strength (VS) values for the AMPA condition. Error bars are the standard errors. Main effect of vibrotactile frequency was significant and similar to that in Figure 2.6. Thin lines show post-hoc comparisons only within a condition indicated by the grouped bars. All comparison lines: $p<0.05$. (a) Change of AFR during the initial 100-ms period of the stimulus with respect to background ($R_o$-$R_b$). Main effect of drug vs. sham condition was significant (thick line). (b) Change of AFR during the remaining 400-ms period of the stimulus with respect to background ($R_d*$-$R_b$). There were significant main (thick line: drug vs. sham condition) and interaction effects (drug vs. sham x vibrotactile frequency x neuron type). (c) VS of spike phases from the entire stimulus duration (0.5 s). There were significant main (thick line: drug vs. sham condition) and interaction effects (drug vs. sham x vibrotactile frequency x neuron type).

did increase $R_d*$-$R_b$ for FS neurons. On the opposite side, the activity in RS neurons was affected much more than FS neurons at 5 Hz. Such interaction effects related to frequency were not found for the AFRs during the initial portion of the stimulus, i.e. $R_o$-$R_b$, for AMPA. Moreover, the effects of NMDA were not influenced by frequency in any of the AFRs (Figure A.4).

There were interactions between frequency and drug vs. sham condition which affected the VS measure; moreover, these also interacted with neuron type. In particular, bicuculline application had differential effects on neuron type, which also depended

on the stimulus frequency ($F(2,96)=3.87$, $p=0.024$). On average, VS increased at all frequencies. However, when the data from different neuron types were studied, it was found that the VS actually decreased at 250 Hz for FS neurons due to bicuculline. Additionally, the increase in the VS of FS neurons due to bicuculline was higher than that in RS neurons at 5 Hz. The same type of interaction was found marginally for AMPA application ($F(1,24)=4.37$, $p=0.047$). Again, the VS of FS neurons increased much higher at 5 Hz. However, due to axial spike phases in some RS neurons, their entrainment and any increase as such were actually underestimated at 5 Hz (see Discussion). VS increased at all other conditions with a more or less similar value. No significant drug vs. sham condition x frequency interaction could be found in entrainment due to NMDA.

### 2.3.5 Differential effects of drugs on the neuron types

Besides some of the interactions with stimulus frequency mentioned above, there were also pure drug vs. sham condition x neuron type interactions. In other words, regardless of stimulus frequency, some drugs had differential effects on RS and FS neurons. Specifically, the AFR somewhat decreased on average in the initial 100-ms period with bicuculline application to neurons, although it increased in RS neurons ($R_o$-$R_b$: $F(1,48)=20.48$, $p<0.001$). No effects were found for the remaining portion of the stimulus duration related to neuron types. The results from initial period were similar for NMDA application ($R_o$-$R_b$: $F(1,48)=6.50$, $p=0.014$), except the AFR increased for both neuron types on average, but with a smaller change in FS neurons. Again, no effects were found for the remaining portion of the stimulus with NMDA. Pure interactions between drug vs. sham condition and neuron type were not found for any tested drug in the VS values.

### 2.3.6 Differential effects of drugs on the cortical layers

Differential effects on neurons sampled from different cortical layers were found only in one condition (Figure 2.8). The AFR changes due to bicuculline were not influenced by layer, but there was indeed a significant interaction effect in the VS values ($F(2,48)=5.13$, $p=0.010$). At each layer, there was an average increase in the VS, but in layer IV, this was much higher. This is because, bicuculline somewhat decreased entrainment in layers III and V at 250 Hz, and also in layer V at 40 Hz. However, the triple interaction itself, i.e. drug vs. sham condition x frequency x cortical layer, was not significant ($F(4,96)=1.06$, $p=0.380$)

## 2.4 Discussion

In this article, we investigated the effects of bicuculline, NMDA and AMPA on the vibrotactile responses of RS and FS neurons in the hindpaw representation of rat SI cortex. These drugs shifted the excitation-inhibition balance and caused differential changes in the AFRs and VS values, which specifically depended on the vibrotactile frequency. The results have important implications regarding local processing in this cortical area. Unlike the whisker-to-barrel pathway, which does not exist in humans, the sensory information in the hindpaw area originates from the mechanoreceptors in the glabrous skin and these mechanoreceptors are very similar to those in humans [114–116]. Consistent with the literature on the barrel cortex, the neurons in the hindpaw area generated spikes entrained more to the stimulus cycles at the lowest frequency tested in this experiment (5 Hz), and these spikes could also occur during the late period of the stimulus. At 40 and 250 Hz, however, the spikes were mostly generated during the initial 100-ms period of the vibrotactile stimulus. Since the stimulus was not purely a static indentation, it is not appropriate to call this a 'phasic' response. Nevertheless, the response profile emphasizes the importance of inhibitory synaptic interactions. It is important to note that, at the suprathreshold amplitude level (i.e. 100 $\mu$m peak-to-peak) tested here, many rapidly-adapting first-order afferents innervating the glabrous skin would produce periodic spikes through the entire stimulus duration even at high

frequencies, but they would respond phasically to a static indentation, hence the name 'rapidly-adapting' [107, 116, 121]. The drugs changed the responsivity of neurons to the vibrotactile inputs. In other words, the background activity was not altered with microinjection, and changes were only observed during the stimulus period. This is probably due to the small volumes applied (∼40 nL at each trial), and shows the high selectivity of the experimental protocol. However, this amount of microinjection released picomoles of molecules and could in theory still produce secondary effects, i.e. excitation/inhibition of neighboring neurons with synapses on the particular neuron studied. For simplicity, we focused on the neuron we recorded from in the following discussion. Additionally, the drug effects were adequately removed between the protocol steps (see Figure 2.1). Recovery was statistically confirmed for the tested sample of neurons, and there was also no significant change of activity over time.

### 2.4.1 General conclusions

All three drugs increased the AFRs in both the initial (100 ms) and late (400 ms) periods of the stimulus duration. They also significantly increased entrainment to stimulus cycles. That is to say, the drugs shifted the synaptic balance to excitation and facilitated more spikes to be generated. Moreover, the spikes became more synchronized with the afferent inputs. These results imply that periodic vibrotactile signals were already present subcortically at all tested frequencies, which is similar to the conclusion given by Vahle-Hinz et al. [157]. As a matter of fact, the VS increase in the neurons sampled from layer IV was significantly higher compared to the other tested layers. In addition to thalamocortical feed-forward inhibition in layer IV, other inhibitory influences may contribute to the suppression of the vibrotactile responses after ∼100 ms as explained below.

The increase in AFR activity significantly depended on the frequency of the vibrotactile stimulus; the interaction was different for each drug. This is a rather remarkable result, probably revealed as most of the NMDA receptors were blocked by anesthesia. It shows that the local networks were modulated by the specific drug dynamically during the time course of stimulation. Bicuculline was particularly ef-

fective at the late time period with 40-Hz stimulation. This means that, in addition to the dominant feed-forward inhibition, bicuculline might have reduced the effect of longer-latency inhibitory connections tuned to mid-frequency, i.e. 40 Hz. AMPA also facilitated the late response, but with different tuning in RS and FS neurons. FS neurons were more sensitive to AMPA at 40 Hz, which is consistent with the fact that they are expected to be part of a similar tuned inhibitory network. On the other hand, RS neurons were more sensitive at 5 Hz; and AMPA was not sufficient to recover late response much at higher frequencies. As a corollary, the excitatory flow of information seems to be restricted to low frequencies at later periods. An interesting finding was that NMDA did not modify the frequency dependence of AFRs and VS values. This cannot be explained entirely by the blockade of NMDA receptors by ketamine anesthesia, because NMDA did indeed increase AFR and VS. The lack of interaction suggests that NMDA is not as important as AMPA in the local processing of fast-changing vibrotactile information (e.g. see Ling and Benardo 1995 [148]).

Based on the presented results, a conceptual model is proposed in Figure 2.9 for a hypothetical neuron. The neuron type, i.e. RS or FS, cortical layer, and specific synaptic connections are not specified for simplicity, but details related to these factors are discussed below. The neuron (filled circle) is considered to operate within a network of unidentified neurons (unfilled circles in Figure 2.9). The thalamocortical inputs to the network are excitatory and carry information about the frequency of the vibrotactile stimulus. Three inhibitory factors shape the spike response of the neuron: (1) synaptic depression which operate at each input cycle and hinder high-frequency transmission, (2) feed-forward inhibition which lasts up to 100 ms after each excitatory cycle, (3) longer-latency inhibition which can suppress response after 100 ms and be re-triggered with each excitatory cycle. Since the period of a low-frequency input is long (e.g. 200 ms for 5 Hz), first two inhibitory factors are not effective, and a single cycle is not adequate to build up longer-latency inhibition. Therefore, the output mimics the periodicity of the input for the entire stimulus duration with high entrainment. At mid-frequency input, initial excitatory cycles are effective to compensate for the feed-forward inhibition during the stimulus onset to a certain extent, but the longer-latency inhibition grows large enough to suppress the response afterwards. The entrainment is quite low even for the spikes generated during the initial cycles. A high-frequency

input, on the other hand, is mainly suppressed by synaptic depression and feed-forward inhibition. The probability of a spike per cycle decreases considerably, and only initial spikes are transmitted with still low entrainment.

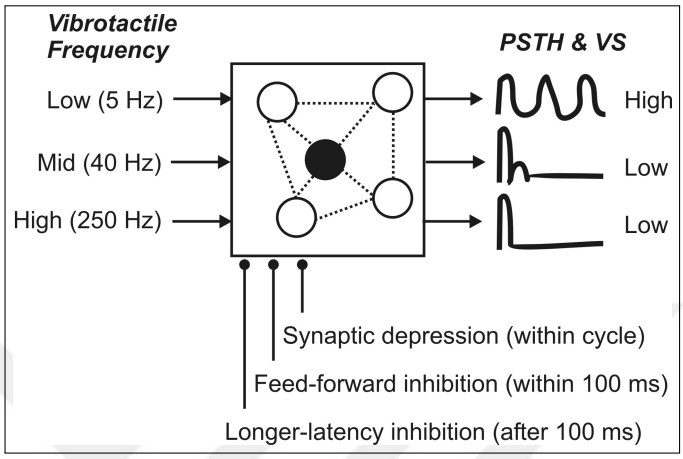


**Figure 2.9** Conceptual model for a hypothetical cortical neuron in the hindpaw area. PSTH profiles and VS levels are given for different vibrotactile frequencies. Three inhibitory influences were proposed (see text).

### 2.4.2 Comparison of the vibrotactile responses with previous literature

Most of the previous rat studies focused on the barrel field of the rat SI cortex. Therefore, it is useful to refer to work done on the regions of SI cortex which receive inputs from the glabrous skin in different animals as well. Studies in monkeys and cats [181, 186–188] have shown that SI neurons can be partially entrained to vibrotactile inputs with higher periodicity at low frequencies (<50 Hz). However, the entrainment at any frequency is always lower than that observed in first-order afferents. Moreover, the probability of a spike per stimulus cycle monotonically drops after the onset response at high frequencies. Although many studies related the periodicity levels of cortical neurons to their primary afferent inputs, e.g. RA-like, PC-like, Pei et al. [189] recently showed that there is considerable submodality convergence on the monkey SI neurons. The current evidence suggests that both amplitude and frequency information are encoded in neuronal populations, but not efficiently in single neu-

rons [190]. The general response profiles of our results obtained in the mechanical-only and sham conditions are consistent with the monkey and cat studies in the literature.

Chapin et al. [165] studied the cutaneous response properties in awake and halothane-anesthetized rats. They observed that, in the awake animals, the cortical neurons habituated very rapidly, and they responded not only to tactile inputs, but also to a variety of arousing or distractive stimuli, such as loud sounds. Punctate stimuli were applied on the forepaw glabrous skin at 1-6 Hz frequency, and there were prominent onset peaks in the PSTHs obtained from both the awake and the anesthetized animals. However, the neurons could not follow the stimulus repetitions fully even at 6 Hz. The authors could identify sequential short-latency excitatory components (E1a, E1b), a post-excitatory inhibitory phase (I1), and/or an long latency excitatory component (E2) in the PSTHs. The E1b and E2 were largely related to non-specific responses, which were depressed by anesthesia. The entrainment we observed at 5 Hz was much higher than reported in their study, but we also observed excitation-inhibition bouts in the PSTHs (e.g. see 40-Hz response of the FS neuron in Figures 2.3, 2.4, 2.5). A subsequent study by Chapin and Lin [47] also confirmed their earlier results, this time also by using sinusoidal mechanical vibrations and electrocutaneous stimulation of the hindpaws. Although spikes are sparse and entrainment is not high in single cortical neurons associated with the glabrous skin, Foffani et al. [191] showed that the precision of the spike timing carries a significant amount of information, in their work regarding coding for stimulus location on the forepaw. The neurons receiving inputs from the forepaw skin usually display higher activities and shorter latencies (as expected from the shorter neural pathway) than hindpaw neurons [113]. It is interesting to note that in a comprehensive study of 534 neurons, only 25.8% were found to be activated by somatosensory stimuli and only 9.4% had cutaneous RFs [112]. Unresponsive neurons were found by iontophoretic glutamate application. This suggests that our neuron sample may be a smaller representative subset within the SI cortex, i.e. one which is associated with tactile inputs directly.

Similar to forepaw and hindpaw areas, neurons in the barrel cortex can be partially entrained to vibratory whisker deflections. In a seminal work, Simons [167] showed that in the unanesthetized paralyzed rats, RS neurons can be entrained up to 20 Hz, and FS neurons up to 40 Hz particularly in layer IV. They also adapted to the

vibratory stimulus, i.e. the activity was higher at the onset periods, but spikes could be generated through the entire stimulus duration somewhat more than those reported in our study. After decades of research, the cumulative evidence suggests that slow inhibitory influences and thalamocortical adaptation may cause a band-pass response (5-10 Hz) as measured by entrainment and spike rate, respectively [170]. This was also supported by the finding that there is little phase-locked activity over 19 Hz, but the product of stimulus amplitude and frequency, which is related to speed, can be encoded in the firing rate of neuronal ensembles [171]. Although a bit lower than the first-order afferents, is higher than the cortex [157]. Therefore, the findings by Hartings and Simons [192] and Diamond et al. [193] suggest that the major frequency effect in entrainment starts at the cortical level within the lemniscal pathway (however, see Ahissar et al. [194] about thalamocortical loops). Our results, as such, are consistent with the generous amount of studies in anesthetized, awake, and behaving rats demonstrating frequency adaptation as discussed here (Stüttgen and Schwarz [195]; for review of barrel cortex function, see Feldmeyer et al. [111]). However, it is still worthwhile to note that the neuronal responses may vary substantially according to the animal's behavioral state (e.g. see Fanselow and Nicolelis [196]), and even for anesthetized animals, on the nature of sensory information, e.g. as modulated by artificial whisking in rats [197].

### 2.4.3 General role of RS and FS neurons during low and high-frequency vibrotactile stimulation

The results related to only mechanical stimulation to the hindpaw is consistent with previous literature. Previous studies in monkeys [181, 198] and in rodents [196] showed that both thalamus and SI cortex has capacity for frequency following characteristic of tactile stimuli. However, somatosensory responses in both VPM thalamus and the SI cortex vary substantially according to the behavioral state during which an animal receives a tactile stimulus. For example, in anesthetized rat, although the first-order neurons do not show suppression to high-frequency sensory input, frequency-dependent inhibition is present in both the cortical and subcortical regions. Some

studies have shown that thalamocortical neurons can follow whisker stimulation up to 12 Hz [168, 192] while others confirmed frequency-dependent suppression above 5-Hz [199] or 2-Hz [194]. The discrepancies between studies are probably due to the use of different methods (e.g. types of anesthesia). In the present study, we have shown similar results that there is 1:1 firing rate at only 5-Hz, but not at 40- and 250-Hz. Moreover, we showed that onset activity is always present at all frequencies but significantly higher at 40-Hz. Onset activities among different layers were similar although they were slightly lower in layer IV. This might be due to that inhibitory neurons does not get direct thalamocortical input in layer III and layer V which is known to be stronger in layer IV although there was no interaction observed between cortical depth and neuron type. In addition, there were no statistical differences for the onset activity of RS and FS neurons in contrast to the remaining portion of stimulus which implies the contribution of these neuron in inhibition of high-frequency sensory inputs depends on the time course of vibrotactile stimuli as well as fast kinetics of thalamic input onto FS neurons. It is expected to have similar onset activity for RS and FS neurons since there is a short delay until inhibition reaches RS neurons due to slower kinetics of GABA channels.

For the remaining portion of mechanical stimulus ($R_d*$) spikes rates depended on neuron type and they were much lower compared to onset activity. This likely results from at least three reasons: first, fast dynamics of network within the cortex, i.e feedforward inhibition, powerful thalamic synapse onto GABAergic FS interneurons masking activity due to the repetitive stimulation; second, depressed thalamocortical synapses due to feedback inhibition or frequency-tuned inhibition; third, use of ketamine as anesthetic agent blocking NMDA receptors which are responsible for the sustained response during continuous activation of periphery whereas low-frequency synaptic transmission is mediated by AMPA receptors. We showed that repetitive stimulation cause suppression in the activity of RS neurons mainly due to feedforward inhibition during 40- and 250-Hz. On the other hand, this frequency-dependent inhibition is more present on FS neurons at 40- and 250-Hz (Figure A.1d) in terms of both entrainment and firing rate measure ($R_d*$) (Figure A.1f). This would imply the specific contribution of RS and FS neurons to fast network dynamics in sensory transmission. In other words, frequency information is still present on RS neurons (higher VS com-

pared to FS neurons) although it is highly suppressed at high frequencies depending the degree of feedforward inhibition. Moreover, with the increasing frequency the activity ($R_d*$) of FS gradually decrease. Except at 5-Hz, responses of FS neurons were close to background activity and shows little adaptation to high-frequency stimulation. RS neurons itself gets excitatory inputs with one another from corticocortical connections while inhibitory neurons gets indirect excitatory input except in layer IV [154]. This might account for the reduced response of FS neurons observed in the sham conditions This is contradicting with studies with barrel cortex in which whisker stimulation causes high responsiveness (almost three times larger) on FS neurons compared to RS neurons [145, 200, 201]. A large and fast response of FS neurons in barrel cortex would imply importance of feed-forward inhibition in temporal integration of somatosensory stimuli, although such behavior was not observed in the hindpaw representation of rat SI cortex.

### 2.4.4 Role of GABAergic inhibition in SI- frequency dependency and layer-specific pattern

GABA is the main inhibitory neurotransmitter in the somatosensory cortex. Except $GABA_C$ subtype, both $GABA_A$ and $GABA_B$ receptor subtypes are present in the cortex. Although the presence of $GABA_B$ is known and they have a role in controlling the receptive field size in the barrel cortex [140, 153, 202], $GABA_A$ receptors have a greater role in controlling the dynamic responses of neurons due to faster kinetics [203]. To understand the local connectivity between excitatory and inhibitory neuron, bicuculline, $GABA_A$ receptor antagonist, has been frequently used. The direct or indirect effects of bicuculline on the RF properties, response magnitudes and durations of neurons, as well as its role in the feedforward inhibition has been studied widely in the barrel cortex. In the present study, we showed that the responses of RS and FS neuron during bicuculline depend on time course and frequency of vibrotactile as well as cortical layer. This can be expected due to different inhibition mechanisms and heterogeneous receptor densities between layers. It is important to note that in contrast to previous studies, we have not observed any change in the spontaneous ac-

tivity followed by burst discharges although bicuculline was microinjected in the same time period when Rb was calculated.

Phasic inhibition is rather dispersed compared to tonic inhibition in which the responses are robust among different layers and neurons. Onset activities change with the bicuculline application depending on both frequency of the stimulation and cortical layer. Bicuculline increased the onset activity in layer III at all frequencies whereas phasic inhibition is reduced at only 250-Hz in layer IV and at only 40-Hz in layer V (Figure A.2(A)). When neurons are classified, it is clear that onset responses of FS units did not get affected by bicuculline injection whereas the onset responses of neurons increased at all frequencies. Unlike the onset activity, bicuculline significantly increased the responses of both RS and FS neurons with higher impact on RS neurons in all layers. This would support the hypothesis that RS neurons have almost always surround inhibition mediated by $GABA_A$ receptors which makes RS neuron more susceptible to bicuculline whereas not all FS neurons gets direct inhibitory input making them insensitive to bicuculline in some cases [154] due to their sparse connections mediated by multiple synapses between interneurons [204]. The number of synapses as well as the type of connections might be the reason why FS neurons affected less than RS neurons during bicuculline injection. In addition, we have not found any differences statistically in terms of effectiveness of bicuculline among different layers. Overall differences from sham conditions are similar for all frequencies in each layer.

Average VS increases after bicuculline injection are small but similar for both neurons in layer III and V. On the other hand, frequency-dependent excitation and increased entrainment of RS neurons are significantly different during antagonism of $GABA_A$ receptors in layer IV. This shows that feed-forward inhibition indeed exists in hindlimb representation and primarily mediated by $GABA_A$ receptors. However, increases in average spike rate for the remaining portion of mechanical stimuli are not close to onset activity and increases VS are statistically significant but small. This implies disinhibition due to bicuculline injection is not enough on its own to eliminate frequency-dependent suppression on RS neurons. This behavior can be explained by several arguments. First, inhibitory neurons make more synapses (approximately 15-30 synapses per target) than excitatory neurons do [204], it is possible that injected bicuculline is not enough to disinhibit all $GABA_A$ receptors. Second, it also possible

that suppression of activity during high-frequency stimulation can be also mediated by not only $GABA_A$ but $GABA_B$ receptors. Their contribution in widening RF size in barrel cortex was suggested in the previous studies [153]. Third, transient response does not depend on solely to GABAergic inhibition in the cortex but the contribution of NMDA and non-NMDA receptors. There is a delicate balance between excitation and inhibition. In the case of any disruption of excitation and inhibition balance lead to a transient response to high-frequency vibrotactile stimuli. The imbalance between excitation and inhibition might occur due to antagonizing effect of the anesthetic agent, ketamine, on the NMDA receptors. To provide further evidence, simultaneous disinhibition of $GABA_A$ receptors and excitation of depressed NMDA should be investigated.

### 2.4.5 Role of Glutamergic excitation in SI- frequency dependency and layer/neuron specific pattern

We investigated excitatory synaptic transmission in SI through two ionotropic glutamate receptors: NMDA and AMPA. Importance of NMDA and AMPA receptors in the cortical processing of sensory input as a component of excitatory and inhibitory balance has been previously mentioned [205]. Due to the faster kinetics of non-NMDA receptors, it is thought that NMDA receptors have a major role in plasticity and a minor role in neural transmission since timing and magnitude on the activation of NMDA receptors are secondary [206]. However, the importance of NMDA receptors has been shown in many studies [207–209]. First, it has been shown that both non-NMDA and NMDA receptors are responsible for cortical responses to peripheral stimulation in the ventrobasal thalamic complex [156, 210]. They showed that excitation in thalamus are mediated by two separate components suggesting that NMDA receptors are responsible for the sustained response during continuous activation of periphery whereas low-frequency synaptic transmission is mediated by AMPA receptors. Consistent with previous studies, we have shown that their significant contribution depend time course of vibrotactile stimulus and neuron type located in specific layer. Unlike bicuculline, frequency of the mechanical stimulation do not cause dispersed onset responses after injection of NMDA and AMPA. At all frequencies, onset responses of neurons did not

get affected by NMDA injection in layer IV while increases in the activity are present at layer III and V. This is probably due to strong thalamocortical input to layer IV creating an inhibitory postsynaptic potential (IPSP) which outruns the NMDA component due to its sensitivity to hyperpolarization caused by IPSP [146,211]. Moreover, neurons located in layer II and III have mixture of NMDA and non-NMDA component and have highest density of NMDA receptors which would account for the increase in the activity in layer III [212, 213]. Layer Va neurons has second highest density for NMDA receptors [214]. Although similar responses observed with AMPA microinjection in layer III and V, in contrast to NMDA, AMPA significantly increased the onset activity in layer IV. Accordingly, IPSP produced by strong thalamocortical input to layer IV have slower kinetics than AMPA component of EPSP which explains layer-specific increase in the onset activity for both type of neurons. It is also important to note that NMDA injection did not have an effect for the onset activity on FS neurons while AMPA increased the onset responses of both neuron type at all frequencies which is consistent with previous studies [146, 148]. For the remaining portion of the mechanical stimuli, AMPA had layer-dependent increases whereas NMDA had both layer-dependent and frequency-dependent increases in the activity of both neuron types. AMPA recovered the suppressed activity in layer IV and V but not in layer III. NMDA had similar effects in layer IV and V but this behavior was not present at 40-Hz stimulation. Conversely, NMDA recovered the sustained responses at only 40-Hz in layer III. Although there is substantial evidence that frequency is an important factor depending on the injected drug, for firing-rate measures, no differences were observed in terms of entrainment. In other words, both NMDA and AMPA significantly increased the VS at all frequencies in each layer observed in both type of neurons. We can conclude that glutamergic excitation of FS and RS neurons both depended on NMDA and AMPA receptors. Layer-dependent responses highlight the importance of local circuitry in the corresponding layer. It was also interesting to see that late responses cannot be recovered by NMDA or AMPA in layer III. This may show the differences in the local circuitry of cortical subregions (i.e. SI barrel cortex vs. SI hindlimb) and species (rat vs. cat).

### 2.4.6 Ketamine anesthesia

The rats were mostly in intermediate and deep anesthesia during single-unit recording in the experiments presented here. We observed an ongoing background pattern of spike bursts as reported by Duncan et al. [158] for subanesthetic doses of ketamine in monkeys, and by Erchova et al. [215] for urethane anesthesia in the rat barrel cortex. This is not to be confused by intrinsic bursting of neurons, but is a characteristic of population activity and a result of increased synchronization in networks. Typically, RF sizes decrease and neuronal representations become more segregated with anesthesia (for multi-unit RFs, however, see Stryker et al. [216]). Ketamine is a non-competitive NMDA receptor antagonist, but its neuropharmacology is very complex, and it is associated with many other receptors [217]. Whitsel et al. [160] studied the effects of intravenous administration of ketamine in monkeys under halothane/nitrous oxide anesthesia. Brushing stimuli were applied on the skin to evoke spike responses in SI neurons. They reported that, although the average firing rates sometimes increased with ketamine, there was always a reduction in the coefficient of variation in spike rates. In other words, intertrial response variation decreased. The authors attributed this to the suppression of corticocortical connections which are mainly mediated by NMDA receptors. Despite the unnatural state caused by ketamine anesthesia, it was suitable for our experiments which focused on the faster and less variable AMPA receptor-mediated transmission, which is also not influenced as much by synaptic plasticity. On the other hand, awake experiments would be difficult for our work due to the non-specific spike responses mentioned in the previous subsection and the requirement of fine stimulus control having micrometer precision on the glabrous skin (for head-fixed procedure, see Schwarz et al. [218]).

### 2.4.7 Release from GABAergic inhibition

Bicuculline was frequently used in earlier studies on various animals (i.e. rat, cat, monkey) to antagonize $GABA_A$ receptors [67, 150–152]. RF sizes generally increase with bicuculline, and distinct cutaneous RFs appear for previously unresponsive

neurons. Interestingly, bicuculline blocked the poststimulus inhibitory period during repetitive thalamocortical inputs [150]. Although we did not re-test RFs after drug application, our results support the previous findings about repetitive inputs, that the activity increases in the late period after the initial cycles of the vibrotactile stimulus. Similar to the results of Kyriazi et al. [153], we found differential effects of bicuculline on RS and FS neurons during the initial period of the stimulus. The activity of RS neurons increased appreciably, but the change in FS neurons was not much, and actually negative on average. This may imply that RS neurons receive greater surround inhibition, which makes them more susceptible to bicuculline. Not all FS neurons get direct inhibitory inputs due to their sparse connections mediated by multiple synapses between interneurons [204]. Kyriazi et al. [154] showed that bicuculline mostly affected layer IV neurons in the barrel cortex regarding defocusing of the RFs. That is to say, the relative spike activity caused by the stimulation of an adjacent whisker increased much more in layer IV, compared to the stimulation of a principal whisker. In our data, changes in spike activity, i.e. AFR, due to bicuculline were similar across the layers, but entrainment indeed increased more in layer IV of the hindpaw area, which implies that the thalamocortical feed-forward and other inhibitory connections mainly involve $GABA_A$ receptors in that layer. Although $GABA_B$ receptors are also present in the barrel cortex and have some contributions to RF size [140, 153, 202], $GABA_A$ receptors play the dominant role in controlling the dynamic responses of neurons due to their faster kinetics [203]. It is important to note that, in contrast to some of the studies, we did not observe any variation in the spontaneous activity, e.g. in terms of burst discharges. However, this may be due to the short time period (0.5 s) for which $R_b$ was calculated before the stimulus onset.

An important contribution of the current study is the finding regarding the frequency dependence of bicuculline effects during the late period of the stimulus. This was discussed above based on the change in the AFRs. Additionally, bicuculline had different effects on entrainment depending on frequency. Regardless of neuron type, bicuculline decreased entrainment at layers III and V at high frequency. Since layers III and V are higher in computational hierarchy, they are subject to more variable synaptic influences. Release from inhibition in those layers would increase excitatory influences, which are likely to be less synchronized within a network due to additional

synapses in the flow of sensory information. Apparently, since entrainment in layer IV starts lower at 250 Hz compared to 5 Hz (see Figure 2.6(c)), the divergence of this information causes much larger desynchronization within target neural populations. However, such a desynchronization seems to be not enough to decrease entrainment at 5 Hz. We could not classify data for LTS neurons; therefore, we do not know whether their synaptic facilitating circuits contributed to our results at high frequency [137]. The conceptual model in Figure 2.9 may be revised in that respect.

### 2.4.8 AMPA vs. NMDA receptor-mediated transmission

It has been well established that thalamic neurons in VPM are excited by both NMDA and non-NMDA receptors [156,157], and similarly, both receptors are utilized at thalamocortical synapses [161] and within the barrel cortex [146]. As a matter of fact, if repetitive stimuli with frequency >20 Hz is used with NMDA-receptor antagonist, the late period of the thalamic response is reduced [156]. On the other hand, NMDA application can bring back the response which was reduced by isoflurane anesthesia [157]. At first, one can attribute the lowered late-period response (the interval of 100-500 ms) in our mechanical-only and sham conditions to the antagonism of ketamine. However, it is important to note that this phenomenon was only observed at 40 and 250 Hz as consistent with previous literature, but not at 5 Hz in our data. Since AMPA-mediated transmission was not hindered by ketamine, it is not clear why the late cycles can be signaled at 5 Hz, but not at higher frequencies. Therefore, the reduction of the late response (after 100 ms) cannot be entirely due to ketamine. Armstrong-James et al. [146] showed that the shortest latency response to single whisker deflection was mainly due to non-NMDA receptors, and NMDA receptors were mostly responsible for the late response in the latency range of 10-100 ms.

The most parsimonious explanation for our findings (see Figure 2.9) in light of previous studies can be founded on two pieces of evidence: (1) AMPA-mediated transmission cannot be perfectly re-triggered in the initial 100 ms with multiple cycles of a high-frequency stimulus, (2) AMPA-mediated transmission is largely suppressed by inhibitory networks in the interval of 100-500 ms, but not for 5 Hz inputs. We

re-analyzed entrainment only for spikes generated in the onset period for the 250-Hz stimulus and the average VS values were 0.26 and 0.23, respectively for RS and FS neurons. These values are slightly higher than those reported in Figure 2.6(c), but still much lower than the results at 5 Hz. This verifies the first statement above, and the inability of generating repetitive phase-locked responses with high frequency may be due to AMPA receptor desensitization [219], in addition to feed-forward inhibition. The second statement is supported by the drug effects presented in this study. By cyclic re-triggering of the feed-forward inhibition and/or activating longer-latency inhibitory influences, the response during the interval of 100-500 ms is reduced in a frequency-dependent manner. It is interesting to note that most of the FS neurons in our data also increased their AFRs with NMDA application, but with a smaller change relative to RS neurons. These small changes may be because of the secondary effects of drugs on neighboring neurons, because fast inhibition is typically not NMDA dependent [148]. To understand the contribution of NMDA receptors to the vibrotactile information transmission, bicuculline and NMDA can be applied concurrently in future work.

### 2.4.9 Limitations and other issues

Since we did not perform a dose-response study, the drug concentrations used here are not directly comparable. Therefore, statistical comparisons were not applied on data obtained from different drugs. However, it is theoretically possible to investigate the multi-drug interactions parametrically in the pressure microinjection approach, and perhaps more easily than iontophoresis. An unexpected result was that both bicuculline and AMPA increased VS values of FS neurons more than those of RS neurons at 5 Hz. The main reason for that was the spike phases in some neurons were slightly axial, i.e. some spikes also occurred during the retraction phase of each mechanical cycle due to the high level of the stimulus. Almost half of the RS neurons and one third of FS neurons had some axial spikes. VS as calculated in Equation 2.1 is not the best measure for axial data and periodicity is underestimated (see Materials and Methods). However, we did not prefer to introduce another measure which would only be relevant for RS neurons at 5 Hz in the analyses. RS neurons still had higher VS

values than FS neurons, but as more spikes were generated due to drug microinjection, SP histogram became more axial, and it seemed that the increase in VS was smaller for the RS neurons. This difference was statistically marginal, and the SP histograms (Figures 2.3, 2.4, 2.5) suggest that increase in periodicity was actually similar for both neuron types.

It is technically difficult to place the vibrotactile stimulator and the compound (recording & microinjection) electrodes very close to each other; therefore, we could not work on the forepaw area [191, 220], and chose the hindpaw area instead. It is interesting to note that, under light pentobarbital anesthesia, there seems to be considerable integration of information from both sides, and from forepaws and hindpaws in the infragranular neurons [113]. In other words, due to corticocortical and cortico-subcortical integration in layers V and VI, neurons in the hindpaw area may also respond to ipsilateral inputs, and also those applied on the forepaw. We never observed such complex RFs in our layer V neurons, probably due to the depth of anesthesia and the fact that most NMDA receptors were blocked. In fact, this approach enabled us to distinguish the small changes due to drug effects and vibrotactile frequency.

Another limitation of the study was that we do not know the fine location of each neuron regarding GZ, DZ, or PGZ. This would require a detailed mapping work which was out of scope for our purpose. We did not observe proprioceptive RFs in our neuron sample, but our unit classification did not systematically search for them in the entire limb and trunk, except for some basic checks (see Materials and Methods). It is well known that there is submodality convergence in the limb representations [221], especially in the PGZs and DZs [47]. As a matter of fact, the neighboring parts of SI and the primary motor cortex seem to overlap with each other, creating a functionally sensorimotor area [222, 223]. This makes sense from developmental and ecological views, because movement requires the simultaneous processing of sensory and motor signals. Our work here focused on passive sensation, because stimulus control would be very difficult with limb movement. Most of the results presented in the current article would be muddled with the confounding factor of skin-contactor coupling in awake behaving rats. Despite the limitations of the study, the ubiquity of the response profiles supports the conceptual model, based on vibrotactile frequency, of Figure 2.9, as a testable hypothesis for future work. As such, we have started to incorporate the

current findings in a computational network model to guide subsequent experiments (see Chapter 4).

## 2.5 Conclusion

In the present work, we quantitatively investigated the effects of bicuculline, NMDA and AMPA on RS and FS neurons at different depths in response to 5-, 40- and 250-Hz mechanical stimulation in the hindpaw representation of rat SI. We presented the results in terms of direct action on the neuron recorded, rather than secondary effects resulting from any effect on neighboring neurons. It is important to note that drugs were microinjected at nanoliter volumes near recording area and it was presumed that drugs injected have high probability of convergence onto cortical neurons neglecting influence on other inputs from neighboring neurons. In addition, electrode penetration was in a controlled manner by using micro-drive with 1$\mu$m resolution. Layer-specific findings in this study were robust and not critical for the neurons recorded near boundaries of layers. All findings outlined above are based on specific changes in responsivity of different mechanical stimuli depending on drug injection, neuron type, and cortical layer.

The main conclusions of this study presented in this chapter are: 1) Regardless of any drug application, frequency of vibrotactile stimulus change the responses of different neurons depending on time course of vibrotactile stimulation. This reveals the role of RS and FS neurons in cortical processing of inputs and differences of local connectivity in cortical layers. 2) Although the effect of bicuculline was prominent at each layer for all firing-rate measures on both types of neurons at all frequencies, the most significant effect was observed in terms of entrainment which increased in only RS neurons at layer IV. This imply dynamical properties of excitation and inhibition at various stages of cortical processing, i.e. feedforward inhibition. 3) NMDA did not affect the onset activity of FS neurons but significantly increased firing rate and vector strength the activity during remaining portion of stimulus, especially at 40-Hz and 250-Hz, i.e. reversal the effects of ketamine. 4) Compared to bicuculline and NMDA, AMPA had larger impact on firing rates and vector strength at all layers which were

similar for RS and FS neurons, i.e. similar receptor characteristics on different neurons, faster kinetics of AMPA receptors. 5) Differential drug effects on the frequency dependence.

# 3. DIFFERENTIAL EFFECTS OF CHOLINERGIC INPUTS ON SOMATOSENSORY CORTICAL NEURONS

## 3.1 Introduction

Sensory processing in the cortex is modulated by central dynamics of cortical network [224–226]. These intrinsic dynamics include neuromodulatory circuits (i.e. cholinergic system) which are essential for regulating the behavioral state of an animal. The main component of cholinergic system, acetylcholine (ACh) receptors, contribute to sensory-cognitive functions as shown in numerous behavioral studies with rats [52, 53, 57, 58] and primates [59–63]. This contribution is more likely through sensory systems (auditory [64] visual [65, 66], somatic [67–71, 112], and other cognitive functions such as learning, memory [53, 72], conscious awareness or attention [48, 50], cortical plasticity [73]. In addition, studies showed that the abilities requiring the attentional demands such as responding to cues, signals, or targets were affected when cholinergic input to the associated cortex were blocked [74–76]. In particular, the basal forebrain cholinergic system originating from nucleus basalis projects diffusely throughout the neocortex, and it has been implicated in vital brain functions such as arousal, attention [49,227,228] and experience-dependent cortical plasticity [229,230]. However, the current understanding of attentional mechanisms is raising questions about which cortical regions are essential for attention, and it lacks considerable knowledge within the tactile modality. The effects of tactile attention on behavior are assumed to be mediated by the enhancement of neuronal activity (i.e. increase in firing rates of a subset of cells) and/or synchronized spiking activity [61, 62]. On the other hand, the neural mechanisms (i.e. cortical cholinergic input) maintaining the control of attention in the related cortex are less well understood. According to proposed model by Sarter et al. [49], attention is influenced by cholinergic system through two-distinct but overlapping/interacting neural mechanisms. One (bottom-up) is "signal-driven modulation of detecetion" whichis only mediated by external signal via sensory systems whereas the other mechanism (top-down) is mediated by practice or knowledge based

on changes in signal detecetion via prefrontal modulation of cholinergic inputs. Since both mechanisms require activation of basal forebrain circuit, nucleus basalis activation may be important in the dynamic modulation of sensory processing. However, it is not known yet why and how nucleus basalis activation enhances the sensory processing.

Although considerable anatomical and pharmacological evidence exist suggesting that ACh is a neuromodulatory neurotransmitter in primary sensory cortices, its role in sensory processing remains unknown. For example, studies on the somatosensory cortex of both rats [67, 69] and cats [68, 231] have shown that ACh can modify the response to sensory inputs. It was consistently found in these studies that pairing ACh with a somatosensory input results in an increased response to the somatosensory input; this usually occurred without an increase in the baseline activity of the neuron. A variety of changes in the response to sensory input were noted in different cells, for example an increase in the receptive field size, a decrease in threshold and/or a stronger response to a constant stimuli. However, since none of these studies analyzed the response properties of the cortical neurons in the same detail as for visual cortex, the concept of improved signal-to-noise ratio have not been analyzed.

On the other hand, apart from the studies investigating the immediate effects, ACh has also long-lasting facilitatory effect on the responses of cortical neurons. This behaviour has been described in a variety of studies with different species (cat, rat, and racoon) and cortical areas (somatosensory, auditory, and visual) in both in vivo and in vitro experiments [67,68,70,71,231–233]. These experiment have differed in the type of cholinergic input to produce this enhancement in the way that ACh have been applied (iontophoretically, by electrical stimulation of basal forebrain), and in the type of response being measured (single unit activity or population responses).

There are numerous studies about peripheral sensory mechanisms involved in transducing the tactile stimuli [64, 106, 115, 116, 118, 234–238]. However, the neural mechanisms involved in processing of tactile sensation in S1 are not well understood, other than whiskers area [112, 167, 191, 220, 239–241].Tactile information from mechanoreceptors is conveyed by afferent pathways through the spinal cord, the medulla, and the thalamus into the primary somatosensory cortex (SI) where information processing primarily occurs. It has been known that the primary sensory cortices (auditory, visual and tactile) process the sensory information in columns organizing

the relevant input depending on the location and modality [35–39]. Cells located in different layers of each column receive the inputs from same receptor area and respond to same classes of receptors. In each column, thalamocortical inputs make synapse first in layer IV where the signal projects to upper layers of the cortex (layer II/III). Lastly, these signals pass to layer V and VI where the signal is transmitted to other areas of the brain or back to thalamus and periphery [40–43]. The cortex also receives cholinergic innervations, mainly from neurons located at the nucleus basalis magnocellularis in the basal forebrain (BF) [98, 242]. Microiontophoresis of ACh and stimulation of nucleus basalis magnocellularis induced long-lasting modifications of neuronal responses that were also present during wakefulness [57, 68, 70, 71, 73, 243]. In this content, to investigate the differential effects of cholinergic inputs on the vibrotactile responses of cortical neurons in the rat SI cortex regarding the hindlimb, we previously studied the effects of local application of ACh and atropine [244]. We found that the responses to mechanical vibrations depend on muscarinic receptors in deeper layers while the spontaneous activity was increased by ACh application more in supragranular layers. To have better understanding of these local changes and how synaptically ACh influences the rat SI cortex in general, we have electrically stimulated the BF, the source of cholinergic projections to the cortex, and investigated both short-term and long-lasting effects while recording single-unit activity from cortical neurons in the hindpaw representation of rat SI cortex. Here, we explore the evoked cholinergic input on distinct cell types of SI cortex in different layers and on different timescales. We previously reported that cortical responses are dependent on the frequency of stimuli and cortical layer [245]. Thus, we specifically studied the effects of BF and the vibrotactile stimulus frequency on the differences in regular-spiking (RS) and fast-spiking (FS) neurons because of their role in local dynamics. Short-term and long-lasting effects of BF stimulation were analyzed on the average spike rate calculated for three periods; before mechanical stimulus, onset period (initial 100-ms of stimulus), and remaining portion (400-ms) of vibrotactile stimuli applied in different frequencies (5-, 40-, 250-Hz). On the other hand, another objective of this study to investigate the changes in vector strength for the analysis of vibrotactile information transmission. If cholinergic innervation from BF has an effect (i.e. better tuning to stimuli) on VS in particular frequency, it would help us understanding the role of cholinergic receptors on the spatial and temporal pa-

rameters of cortico-cortical and horizontal connections within the specific column since the cholinergic projections from BF are wide and diffuse, they can alter the global activity pattern in the brain.

## 3.2 Materials and Methods

### 3.2.1 Animals and Surgery

All experiments were approved by the Boğaziçi University Institutional Ethics Committee for the Local Use of Animals in Experiments and performed at the Institute of Biomedical Engineering, Boğaziçi University. Twenty-four adult Wistar albino rats (12 female, 12 male, 3-22 months old, weight: 183-470) were used in the study. Rats were maintained in the cages facilitated in a climate-controlled room on 12:12-h light-dark cycle. For surgery, rats were anesthetized with ketamine (65 mg/kg) and xylazine (10mg/kg) intraperitoneally (IP). Rectal temperature was checked and kept at 37 °C by a heating pad (TCAT-2LV; Physitemp Instruments, Clifton, NJ, USA). The general condition of the rat was checked periodically as well as the state of anesthesia by controlling eye and pedal reflexes. To maintain the appropriate level of anesthesia, additional 1/3 dose of injection of anesthesia was given. Moreover, to prevent brain edema and to decrease incranial pressure, furosemide (2mg/kg), and mannitol (0.2g/kg) were injected IP. Additionally, atropine (0.05mg/kg) was injected IP before surgery to decrease bronchial secretion. Lactate Ringer solution (40ml/kg/24h, IP) were given to maintain normal physiological condition for longer periods of operation. The head was fixed to a stereotaxic frame, and the craniotomy 3.1(a) was performed on the areas representing the hindlimb area of the primary somatosensory cortex (red circle Figure 3.1(c)) and nucleus basalis (NB) location (blue circle Figure 3.1(c)) [47, 173]. Bipolar stimulating electrodes were implanted in NB of the left or right hemisphere (Figure 3.1(b)) and fixed with recording chamber over SI using dental acrylic. After surgery, the rat was either euthanized with an appropriate dose of thiopental (200mg/kg, IP) or perfused transcardially for post-mortem histology.

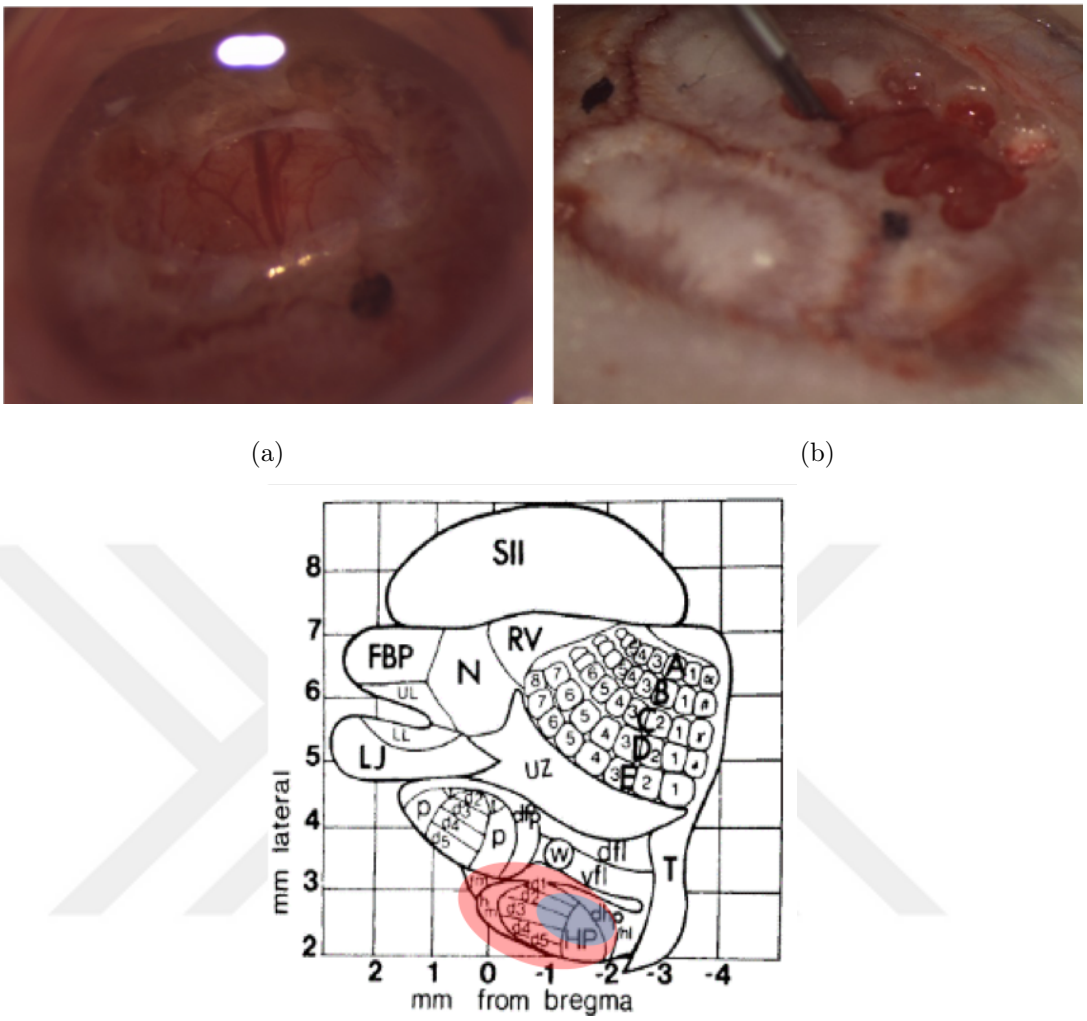


(c)

**Figure 3.1** a) Craniotomy over SI area, black dot represents the Bregma. b) Basal forebrain electrical stimulation electrode implanted with 20° angle, rostral black dot represents Bregma, caudal black dot represents Lambda. c) Stereotaxic coordinates reproduced from Chapin et al. [47], red circle shows the area representing the hindlimb area of SI cortex for recording whereas blue circle gives location of NB area for electrical stimulation of BF.

### 3.2.2 Single-unit recording and vibrotactile stimulation

Single-unit action potentials (spikes) were recorded through carbon fiber electrode assembled in multi-barrel glass pipette (Carbostar-6; Kation Scientific, Minneapolis, MN, USA) (Figure 3.2(a)). All recordings were done in a Faraday cage (1.58 x 1.05 x 1.20 m3). Once the regions representing glabrous skin of the rat hind limb was isolated, RF were searched and mapped by using Von Frey (VF) hairs manually. The recording electrode was positioned using hydraulic Microdrive (MHW-4; Narishige

International, London, UK). Spikes were amplified by a custom-made microelectrode amplifier (x1000). Single-units were discriminated with an amplitude window discriminator (121; World Precision Instruments, Sarasota, FL, USA), and neuronal activity was visualized and heard by an analog oscilloscope and a speaker, respectively. All data including raw voltage traces and discriminated spikes were collected in a PC through custom-made MATLAB software (The MathWorks, Natick, MA, USA).

Mechanical stimuli are generated by a digital-to-analog card (USB-6251; National Instruments, Austin, TX, USA) connected to a PC and amplified to drive an electrodynamical shaker (V201; Ling Dynamic Systems, Royston, Herts, UK). Vibrotactile stimulation were applied at RF area of each unit by using a plastic cylindrical contactor (diameter: 1.84 mm) connected to the shaker. The stimuli are presented as bursts of sinusoidal mechanical vibrations (amplitude: 50 $\mu$m peak-to-peak) upon 0.5-mm static indentation which are consisted with stimulus conditions used in the previous neurophysiological studies [116, 179]. The test stimulus frequencies are 5-, 250- and 40-Hz, which started and ended as cosine-squared ramps with 50-ms rise/fall times. Displacements on the skin were calibrated by using a Photonic sensor (MTI-2100; MTI Instruments, Albany, NY, USA) and stimulus amplitudes generated by the PC were adjusted by using a digital attenuator (V2.0C; ISR Instruments, Syracuse, NY, USA).

### 3.2.3 Electrical stimulation

We stimulated the nucleus basalis of anesthetized rats with a custom-made bipolar electrode Figure 3.2(b)) while recording from ipsilateral SI. Location for BF stimulation was determined according to rat brain atlas (ML: 2.4 mm; AP: -1.3mm; DV: 6.8 mm) [173]. Since the location of electrical stimulation was involve SI area, the stimulation electrode was implanted with an angle of 20° (ML: 3.78 mm; AP: 2.4mm; DV: 7.24mm) to have larger recording area. Electrical stimulation per trial consisted of 50 pulses (500 $\mu$s per pulse Figure 3.2(c)) at 100 Hz with amplitude of 50$\mu$A.

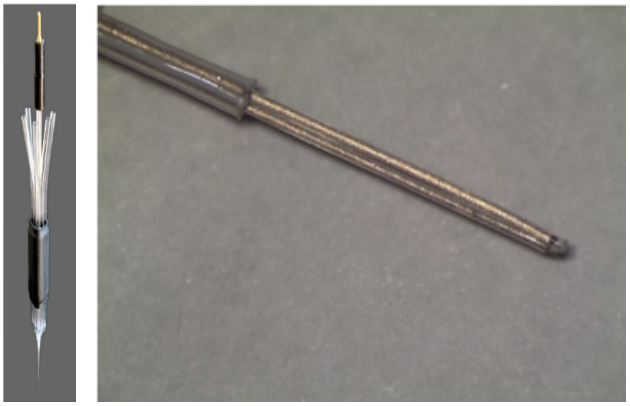

(a) (b)

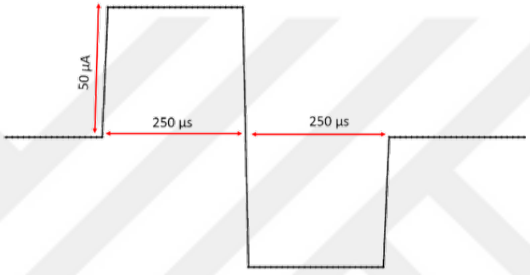


(c)

**Figure 3.2** a) Carbostar-6, a carbon fiber electrode assembled in multi-barrel(5) glass pipette. b) A custom-made bipolar electrode. c) A single pulse electrical stimulation.

### 3.2.4 Experimental procedure

After locating RF for each neuron, the stimulator (probe diameter:1.84 mm) was placed on the RF area for vibrotactile stimulation. Each unit recording from SI consisted of two blocks and each block consisted of three different vibrotactile stimuli under control (OFF) and BF conditions (ON) (Figure 3.3(a). Under control conditions, train of 10 trials (i.e. 3.3(b)) for each frequency was tested without BF stimulation. Under BF conditions, the same procedure as in control conditions were repeated, and BF stimulation was administered just before start of vibrotactile stimulation. Total duration of each trial is 2 seconds, and the inter-trial-interval is 3 seconds. Each vibrotactile stimulation last 500ms as well as BF stimulation. The remaining duration in each trial was also recorded for the analysis of background activity. Blocks were separated with 30-minute break to further study the long-lasting effects of BF stimula-

tion. To ensure that the effect of BF had diminished, 10-minute-break was given before the start of OFF conditions of each vibrotactile stimuli. The sequence of frequency of tactile stimuli was kept in order of 5-40-250 Hz to further analyze the effect of time on cortical responses regardless of BF stimulation.

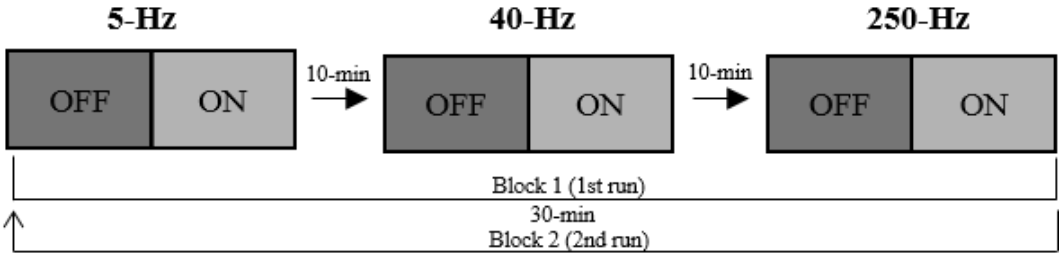


(a)

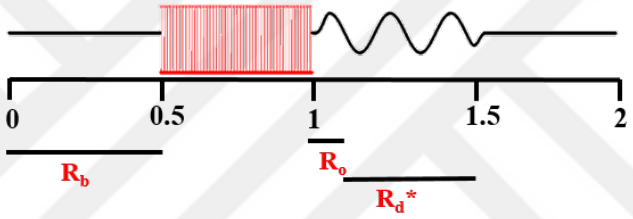


(b)

**Figure 3.3** a) Experimental procedure. Each condition (OFF and ON) is run for each frequency with the following order: 5-Hz, 40-Hz and 250-Hz. After each frequency block, there was 10-minute break. After all 3-frequency blocks are completed, 30-minute is given and whole protocol is run for $2^{nd}$ run. b) Figure shows a 2-s trial applied in each condition (OFF or ON). During, 0-0.5 second there were no mechanical stimuli or BF stimulation but only recording. During 0.5-1 second, BF stimulation is applied for only ON condition. During 1-1.5 second, mechanical stimuli is applied on the hindpaw of rat. During 1-5-2 second, there were no mechanical stimuli or BF stimulation but only recording. Each condition includes 10 trials (inter-trial interval=3-second). During OFF trials, no BF stimulation is applied, while ON conditions includes BF stimulation between 0.5-1s. $R_b$ denotes background average firing rate between 0-0.5s, $R_o$ denotes average firing rate during first 100-ms of mechanical stimulation applied on the hindpaw of rat whereas $R_d*$ represents average firing rate during last 400ms of mechanical stimuli.

### 3.2.5 Unit Classification and Data Analysis

Data were collected in a PC through MATLAB software including raw data and spikes times for each trial. Each neuron was classified according to RF mapping, VF

threshold, recording depth as well as spike shape. Receptive field and layer classification are shown in Table 3.1 (See details in (Figure 2.2, [180, 245]). Each letter categorized RF boundaries for each unit and average layer boundaries were determined according to previous literature [40, 112]. Additionally, units were classified according to their spike shape and firing pattern (i.e., Regular-spiking (RS), fast-spiking (FS), and intrinsically bursting (IB)) [135, 167, 181]. We classified units similarly, in which duration of the individual fast-spiking units were <0.5 ms whereas RS units have slower repolarization rate, and duration of RS units were > 0.5 ms, IB units are easily recognizable since the spikes are in a clustered pattern, the burst (See example for RS and FS in Figure 3.4).

**Table 3.1**
Classification of RF mapping and cortical layer.

| Receptive Field Mapping | |
|---|---|
| A | Single digit |
| B | Multiple digits without pad |
| C | Isolated pad (upper small |
| D | Digits + only near pad |
| E | Upper paw (only pads) |
| F | Lower paw |
| G | Multiple digit with entire pads |
| H | Entire paw without digits |
| I | Entire paw with digits |

| Layer | Cortical Depth($\mu$m ) |
|---|---|
| I | 0-165 |
| II | 165-292 |
| III | 292-577 |
| IV | 577-879 |
| V | 879-1351 |
| VI | 1351-2106 |

To visualize the rate and timing of neuronal spike discharges in response to a vibrotactile stimulus, peri-stimulus time histograms (PSTHs, bin size: 50ms) and spike-phase (SP) histograms (bin size: 0.5°) were constructed. For each frequency and condition (OFF and ON), data were pooled for 10 trials and analyzed for changes in average firing rate and vector strength (VS). Average firing rates (AFR) were calculated for different time periods: before stimulus ($R_b$), onset period ($R_o$) (first 100 ms of stimulus), and last 400 ms of vibrotactile stimulus ($R_d*$). To quantitatively compare the response of a neuron to mechanical stimulation, background activity ($R_b$) was

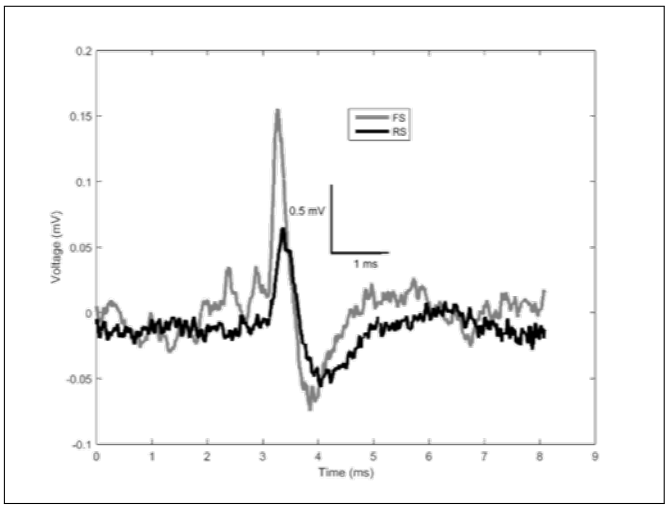


**Figure 3.4** An example of unit classification. Black line: RS neuron, Gray line: FS neuron.

subtracted from average firing rates during onset ($R_o$) and entire stimulus duration ($R_d*$) for each frequency. To quantify the synchronization of the responses with respect to 5-,40- and 250- Hz vibrotactile stimuli, vector strength (VS) was calculated. Each spike is considered as a vector with a phase angle ($\theta_i$) ranging from 0 to $2\pi$ (in each period of stimulus). $\theta_i = (2*\pi*t_i)/ T$ where $\theta_i$= phase angle of each spike i , $t_i$=timing of each spike (i), T=period of the vibrotactile stimulus. For a set of n unit vectors with angles ($\theta_1$,$\theta_2$ ...,n), rectangular coordinates (x,y) of the mean angle can be written as [183]:

$$(x, y) = (\sum_{i=1}^{n} x_i, \sum_{i=1}^{n} y_i) = (\sum_{i=1}^{n} cos\theta_i, \sum_{i=1}^{n} sin\theta_i) \tag{3.1}$$

The length of resultant vector r;

$$r = \sqrt{x^2 + y^2} = \sqrt{(\sum_{i=1}^{n} cos\theta_i)^2 + (\sum_{i=1}^{n} sin\theta_i)^2} \tag{3.2}$$

Vector strength defined as;

$$VS = \frac{1}{n}\sqrt{(\sum_{i=1}^{n} cos\theta_i)^2 + (\sum_{i=1}^{n} sin\theta_i)^2} \tag{3.3}$$

Vector strength is in between 0 and 1 where 1 implies that mean vector is unidirectional whereas it is 0 when all spike timings are randomly distributed in each period

of stimulus.

Data analysis were done among different frequencies, cortical layers, and spike shape. Statistics and graph analysis were performed in MATLAB 2018b (The MathWorks, Natick, MA, USA), and Excel (Microsoft Office 2013). Statistical analysis includes repeated measures ANOVA computed in SPSS Ver.23 (IBM Corp., Armonk, NY, USA) in which the vibrotactile frequency, OFF vs. ON conditions, and time-block were within-subject factors while cortical layer and neuron type were between-subject factors. IB neurons were not included in the statistical analyses as neuron type since the number of IB neurons were small.

## 3.3 Results

### 3.3.1 Classification of vibrotactile neurons

Total of eighty-seven neurons were recorded from 24 rats (12 female, 12 male) in the hindpaw representation of SI cortex. Neurons were sampled from layer III (n=10), IV (n=33), V (n=35) and VI (n=9) (Table 3.2). Neurons had primarily medium-VF thresholds (84%) and mostly found in layer IV (n=24) and V (n=31) while those who had low-thresholds (16%) were mostly found in layer IV (9 out of 14 neurons). There were no units recorded with high VF thresholds ($>$ 2.5 g). The receptive-fields were largely varied throughout the cortex and across neurons but most-common receptive-field was D (28%) for all layers which covers a single digit in addition to single/multiple pads on the paw. Type E (13%) and G (16%) which are covering upper paw and multiple digits were the second and the third most common RFs among all neurons.

Additionally, the neurons are classified as RS (n=42), FS (n=31), and IB (n=14) based on spike shape. Although the number of neurons recorded from layer III and VI are low, all type of neurons are uniformly distributed throughout the cortex. On the other hand, consistent with previous studies the receptive fields of RS neurons were commonly of Type A, B, and D (i.e. covering the digits). For FS and IB neurons, the receptive fields were mostly of Type D and E while they are usually covering the upper paw not including digits.

**Table 3.2**
Classification of 87 vibrotactile neurons in the hindpaw representation of SI cortex. The receptive-field (RF) categories refer to the letters defined in Figure 2.2. Low von Frey threshold: <0.25 g; Medium von Frey threshold: 0.25-2.5 g. Numbers are the neuron counts. Percentages and bold numbers refer to a particular neuron group counted in rows (based on von Frey threshold, neuron type, or cortical layer) and columns (based on cortical layer or RF category).

| | *Cortical Layer* | | | | *Receptive Field* | | | | | | | | | | |
|---|---|---|---|---|---|---|---|---|---|---|---|---|---|---|---|
| | III | IV | V | VI | A | B | C | D | E | F | G | H | I | Total | |
| Low Threshold | 1 | 9 | 4 | 0 | 0 | 2 | 0 | 5 | 1 | 1 | 3 | 0 | 2 | 14 | 16% |
| Medium Threshold | 9 | 24 | 31 | 9 | 6 | 7 | 3 | 19 | 10 | 7 | 11 | 5 | 5 | 73 | 84% |
| Regular-Spiking (RS) | 6 | 18 | 15 | 3 | 4 | 4 | 1 | 10 | 3 | 6 | 6 | 5 | 3 | 42 | 48% |
| Fast-Spiking (FS) | 2 | 10 | 15 | 4 | 1 | 5 | 2 | 10 | 4 | 2 | 6 | 0 | 1 | 31 | 36% |
| Intrinsically Bursting (IB) | 2 | 5 | 5 | 2 | 1 | 0 | 0 | 4 | 4 | 0 | 2 | 0 | 3 | 14 | 16% |
| Layer III | - | - | - | - | 1 | 0 | 0 | 3 | 0 | 1 | 2 | 2 | 1 | 10 | 11% |
| Layer IV | - | - | - | - | 4 | 3 | 2 | 8 | 3 | 4 | 5 | 1 | 3 | 33 | 38% |
| Layer V | - | - | - | - | 1 | 3 | 1 | 9 | 8 | 2 | 7 | 2 | 2 | 35 | 40% |
| Layer VI | - | - | - | - | 0 | 3 | 0 | 4 | 0 | 1 | 0 | 0 | 1 | 9 | 11% |
| Total | 10 | 33 | 35 | 9 | 6 | 9 | 3 | 24 | 11 | 8 | 14 | 5 | 7 | 87 | |

### 3.3.2 Nature of cortical neurons and responses to mechanical stimulation without BF stimulation

For qualitative comparisons, we constructed PSTHs which show the time histograms of spikes recorded before, during and after each mechanical stimulus for both OFF and ON conditions (Figure 3.5,3.6). The black bars in both PSTHs and SP histograms show OFF conditions in which there is no BF stimulation but only mechanical stimulation of the skin. These histograms were adequate to characterize the response patterns of each type of neuron in response to mechanical stimuli since the trial-by-trial variability is low. Activity of each unit during OFF conditions was recorded in response to 10 trials of sinusoidal stimulation at the three different frequencies (5-, 40-, and 250-Hz). Of 87 neurons, almost all showed that spikes were mostly generated at the onset (first 100-ms) of the 40- and 250-Hz sinusoidal vibrations, but could be entrained (1:1) at 5-Hz (see 5- Hz plots in Figure 3.5, 3.6). Entrainment can also be

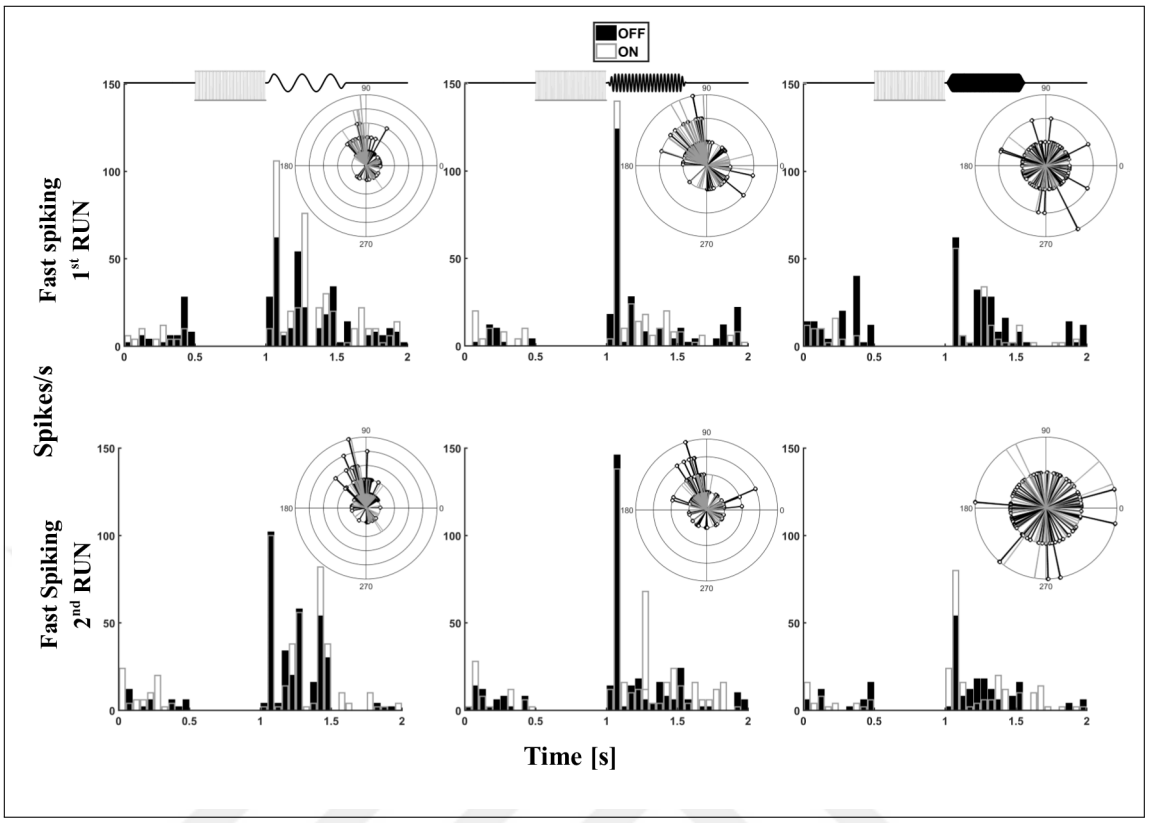


**Figure 3.5** Peristimulus time histograms (PSTHs) and spike-phase (SP) histograms of a fast spiking for 1st and 2nd run. The vibrotactile displacement waveforms are given above the PSTHs and share the same time axes (left: 5 Hz, middle: 40 Hz, right: 250 Hz). BF stimulation preceded the mechanical stimuli. Black bars in the PSTHs (bin size: 50 ms) and black lines in the SP histograms (bin size: 0.5°) are for OFF condition condition. Empty bars with gray outlines in PSTHs and gray lines in SP histograms are for the ON condition. The angular axis in the SP histograms is given in degrees, and the radial axis shows the number of spikes per trial in each bin (tick label printed near the outer circle).

seen in spike phase histograms. During 5-Hz stimulation, spikes were accumulated in certain angular range whereas at 40- and 250-Hz, lines were scattered. Consistent with conceptual model presented [245], even though the thalamacortical inputs are present, the spikes after initial 100-ms is hindered at high frequency stimulation due to synaptic depression and feed-forward inhibition. To statistically assess the spike activity across neurons due to only mechanical stimuli, the background average firing rate ($R_b$) was subtracted from the average firing rate during the initial 100-ms period of the stimulus ($R_o$) and from the average firing rate during the remaining portion of the stimulus ($R_d*$). Statistical tests for the measures and VS were done by ANOVA with stimulus frequency as within-subject factor, and cortical layer and neuron type (RS and FS) as between-subject factors. The overall ANOVA analysis showed that the frequency is a

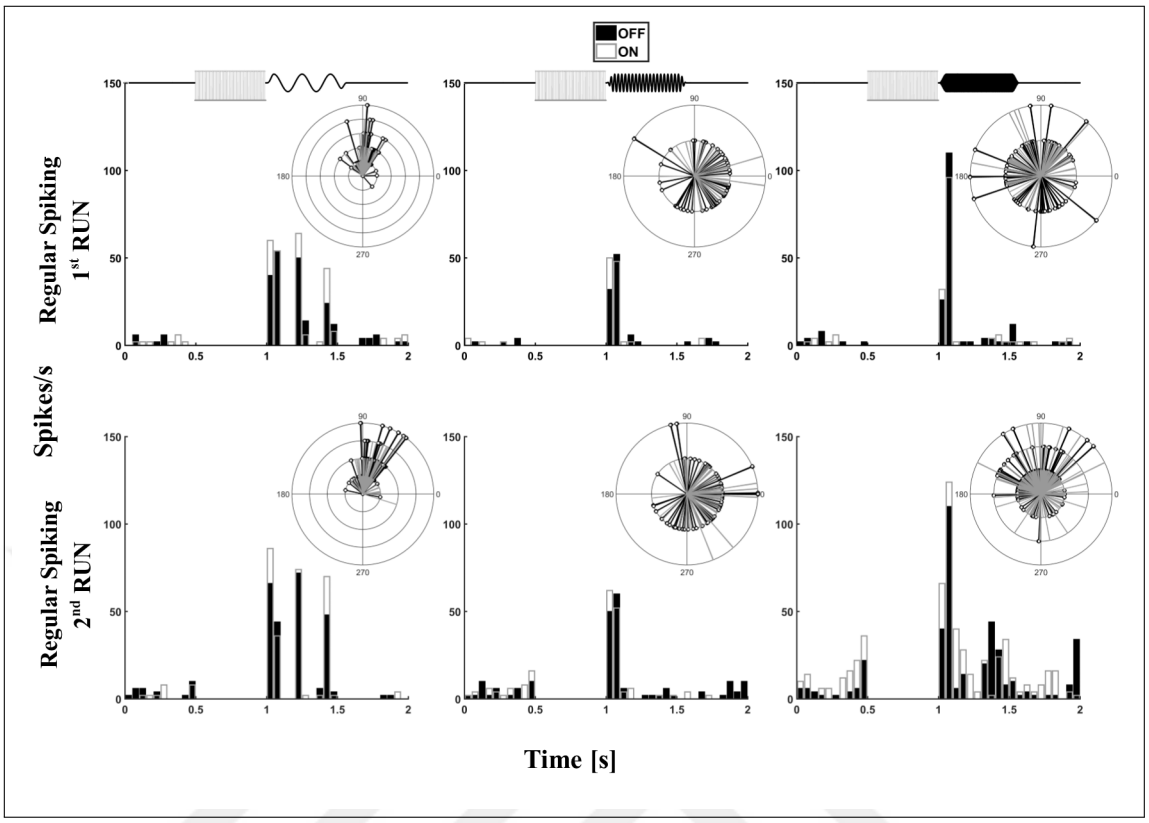


**Figure 3.6** Peristimulus time histograms (PSTHs) and spike-phase (SP) histograms of a regular spiking for 1st and 2nd run. The vibrotactile displacement waveforms are given above the PSTHs and share the same time axes (left: 5 Hz, middle: 40 Hz, right: 250 Hz). BF stimulation preceded the mechanical stimuli. Black bars in the PSTHs (bin size: 50 ms) and black lines in the SP histograms (bin size: 0.5°) are for OFF condition condition. Empty bars with gray outlines in PSTHs and gray lines in SP histograms are for the ON condition. The angular axis in the SP histograms is given in degrees, and the radial axis shows the number of spikes per trial in each bin (tick label printed near the outer circle).

main factor for AFR at $R_d$*-$R_b$ and VS (p=0.035 and p<0.001, respectively) but not for $R_o$-$R_b$ for all the conditions tested. As shown in Figure 5a, AFR at 5-Hz for $R_d$*-$R_b$ (7.96 ± 1.6 spikes/s) is significantly higher compared to 40-Hz (4.84 ± 1.1 spikes/s) and 250-Hz (4.76 ± 0.88 spikes/s) while the onset activity at 40-Hz is slightly different than of 5-Hz and 250-Hz. However, frequency was not a main factor on $R_o$-$R_b$. The mean spikes rates for 5-Hz, 40-Hz and 250-Hz are as follow: 17.78 ± 1.98 spikes/s, 18.06 ± 6.26 spikes/s and 16.40 ± 1.97 spikes/s, respectively. On the other hand, main effects of neuron was found on background activity (p=0.021) as well as the cortical layer and neuron interaction (p=0.018) (Figure 3.7(a)). AFR for background activity of FS neurons (10.71 ± 1.855 spikes/s) is significantly higher than of RS neurons (6.05 ± 1.12 spikes/s). This is due to high background activity due FS neurons located in

layer III. The baseline activity of FS neurons at layer III (15.4 ± 3.917 spikes/s) significantly higher than all other layers whereas Rb for RS neurons were similar throughout the cortex (Figure 3.7(b)). There was no other significant differences between FS and RS regarding $R_b$. As described detailed in Methods, entrainment of neurons were measured by VS of spikes phases. As shown in SP histograms, the VS was significantly higher at 5-Hz (0.55 ± 0.04) while 40-Hz (0.23 ± 0.02) and 250-Hz (0.20 ± 0.02) had much lower VS values (Figure 3.7(c)). Similar to spike-rate measures, main effects due to cortical layer and neuron type could not be found for VS values.

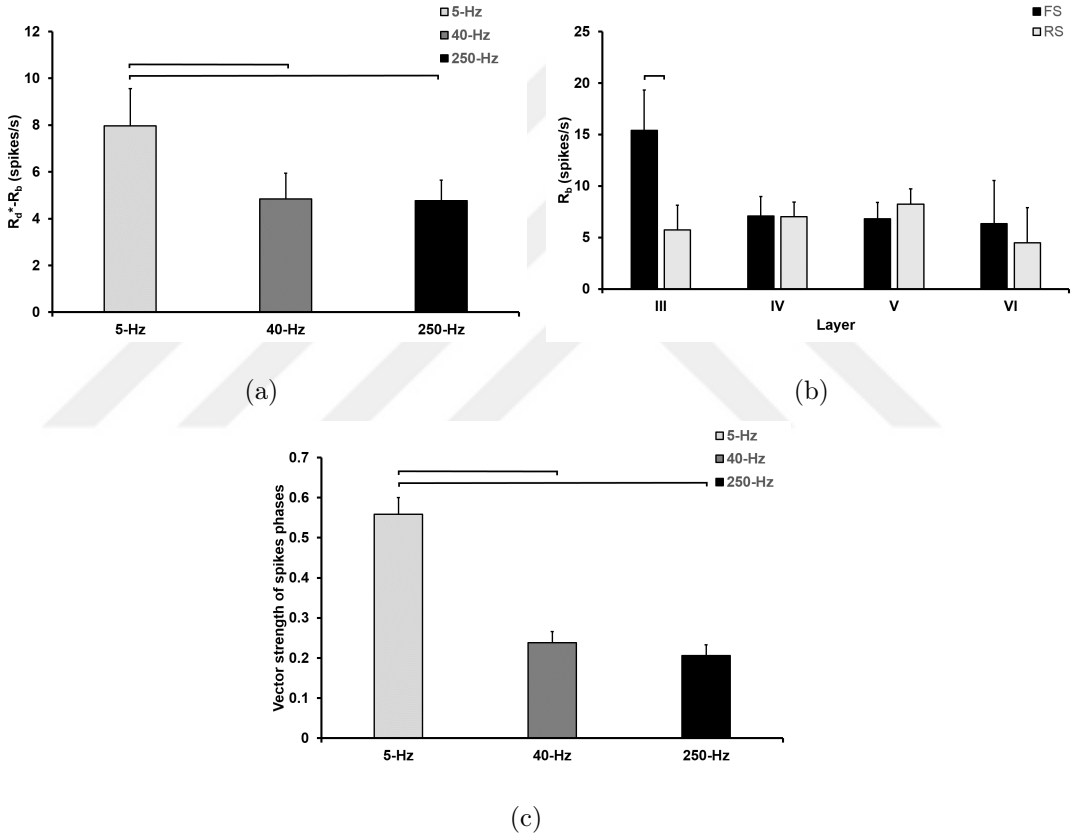


**Figure 3.7** Nature of cortical neurons and responses to mechanical stimulation. a) Spike rate ($R_d$*-$R_b$) during different frequencies of mechanical stimuli (5-, 40-, 250-Hz) without BF stimuli. b) Background activity ($R_b$) differences among different neurons (RS and FS) in different layers (Layer III, IV, V) during no BF stimulation. c) Vector strength values during different frequencies o mechanical stimuli without BF stimulation.

### 3.3.3 Short-term effects of BF stimulation

This section summarizes the immediate effects of BF stimulation. OFF and ON conditions during 1st run and 2nd run were compared. Firing rate measures ($R_b$, $R_o$, $R_d*$, $R_o$-$R_b$, $R_d*$-$R_b$) and entrainment (VS) were analyzed by ANOVA with stimulus frequency and OFF vs. ON conditions as within-subject factor, and cortical layer and neuron type (RS and FS) as between-subject factors. Since the number of IB units is low, neuron type comparisons were done among RS and FS neurons unless specified. BF ON trials preceeded the OFF trials for each frequeny tested. After all frequencies were tested for OFF and ON conditions (1st run), 30-min break was given to observe effects related with time and BF. Same protocol were repeated (2nd run) after this time-break to study differences between each run.

Although neuron type and cortical layer had significant effects on the background activity, we did not find any significant changes on Rb related with BF stimulation during 1st run or 2nd run ($p=0.22$ and $p=0.43$, respectively). Moreover, BF stimulation did not cause any significant changes for other spike-rate measures ($R_d$, $R_d$-$R_b$, $R_o$-$R_b$) during mechanical stimuli for both 1st and 2nd run. However, although BF did not have an effect on $R_o$ during 1st run, neuron was a main factor and there was significant frequency and BF stimulation interaction on this spike-rate measure during 2nd run. Post-hoc analyses showed that this facilitatory effect of BF was observed only during on 5-Hz mechanical stimulation (Figure 3.8(a)). Moreover, when the Rb background activity subtracted from the onset activity, marginal significant triple interaction between BF, layer, and neuron were observed (Figure 3.8(b)).

Frequency and BF stimulation were main factors for VS values during only 2nd run ($p<0.001$ and $p=0.002$, respectively) (Figure 3.8(c)). BF significantly increased the VS values but post hoc analyses showed that this increase was only observed for 5-Hz stimulation (Figure 3.8(c)). Although repeating the protocol after 30-min break did not increase the spike-rate in the particular condition, the vibrotactile responses were more tuned to frequency of stimuli especially for 5-Hz for both type of neurons. This effect has not been observed for 40- or 250-Hz.

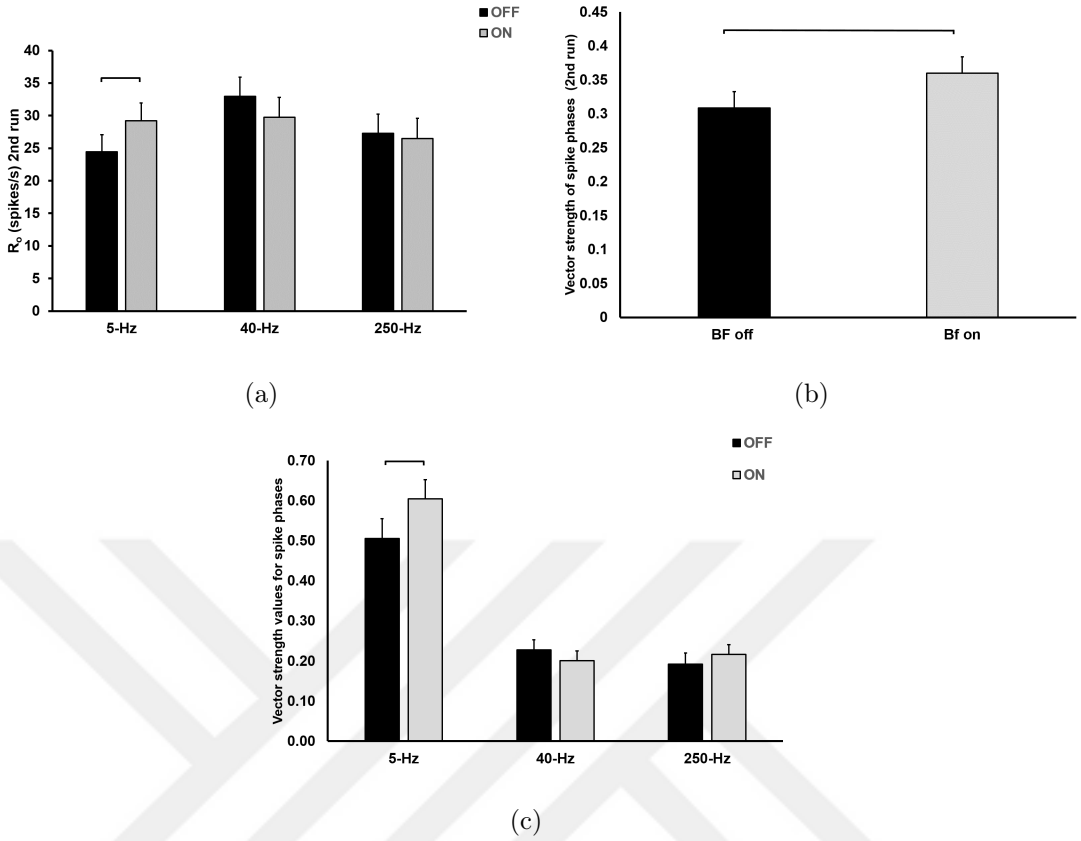


**Figure 3.8** Short-term effects of BF stimulation. ON trials preceded OFF trials. a) Onset activity ($R_o$) including background activity during different mechanical stimuli (5-, 40-, 250-Hz) for ON and OFF conditions. b) Vector strength values for frequencies pool conditions during ON and OFF conditions. c) Vector strength (VS) values for each different mechanical stimuli. Increase in VS were observed in only 5-Hz mechanical stimulation for the short-term effects of BF stimulation.

### 3.3.4 Long-lasting effects of BF stimulation

This subsection includes statistical analyses to compare the long-lasting effects of BF stimulation. We compared OFF conditions during 1st and 2nd run as well as the ON conditions during 1st and 2nd run. Thus, two different repeated measures ANOVA for each spike-rate measure ($R_b$, $R_d*$, $R_o$, $R_d$-$R_b$, $R_o$-$R_b$) and VS values were done with stimulus frequency and time block (30-min) as within subjects, and cortical layer and neuron type (RS and FS) as between-subject factors. Moreover, to quantify the effect size of BF stimulation, we have calculated VS differences during 1st run and 2nd run. Specifically, ON values were subtracted from OFF values in the corresponding run. These differences were analyzed by repeated measures ANOVA with stimulus frequency and effect of BF as within-subject factors, and cortical layer and neuron

type as between-subject factors.

BF had a significant effect VS change values (OFF-ON). The increase in VS of vibrotactile neurons much higher in the 2nd run, thus vibrotactile periodicity becomes more prominent (Figure 3.9(a)). Post-hoc analyses showed that there are significant interactions between BFxneuron and BFxlayer (p=0.05 and p=<0.001, respectively). Moreover, VS of both RS and FS neurons increased, albeit in different amounts, due to BF stimulation in the 2nd run. The increase in VS of RS neurons were higher than of FS neurons compared to 1st run (Figure 3.9(b)). Similar results were observed in different layers although the change behaviors were different among 1st and 2nd run. For example, overall change in VS of neurons in layer III was negative during 1st run while BF had increased the VS during the 2nd run (Figure 3.9(c)). On the other hand, opposite effects were seen in layer IV. Furthermore, the changes in VS were similar for both 1st and 2nd run in layer V whereas effect size of BF was much higher during 2nd run in layer VI.

On the other hand, the effects of BF activation on firing rate developed over time. Except the stimulus frequency, there was no significant main effect on spike-rate measure ($R_d*$-$R_b$, $R_o$-$R_b$) regarding the responsiveness of vibrotactile neurons to mechanical stimuli. However, triple interaction (TimeXlayerXneuron) was observed for only one spike-rate measure ($R_d*$-$R_b$) when ON conditions were compared (Figure 3.9(d)).

Long-lasting effects and repetitive activation of cholinergic input to SI were shown to be more effective and dependent on cell type and layer, probably due to projecting pattern from BF.

## 3.4 Discussion

Among its numerous characteristics in cognitive functions, the basal forebrain-cholinergic system has an effect on sensory processing. For example, ACh release in sensory cortices enhances stimulus-evoked responses, modifies selectivity and leads to long-lasting increase in cortical neuronal excitability in both somatosensory and auditory cortex. Although BF stimulation produced an enhancement of cutaneously

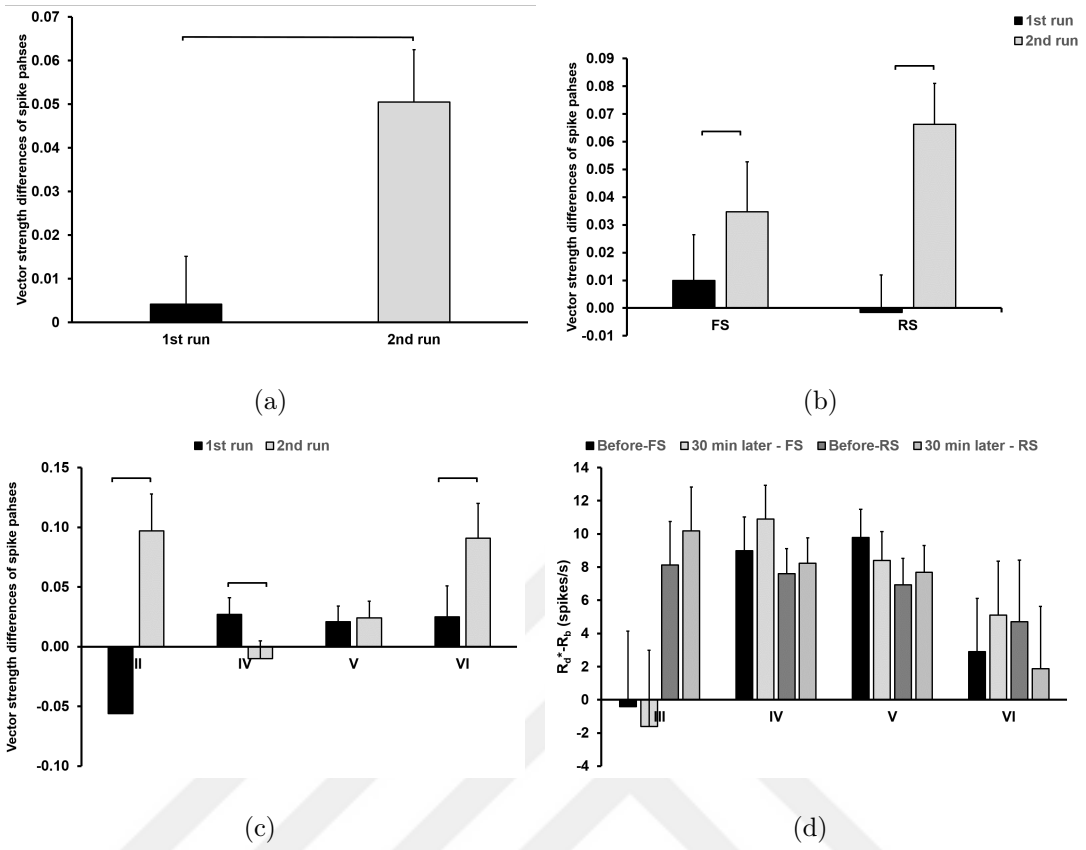


**Figure 3.9** Long-lasting effects of BF stimulation. Observed effects were compared after 30-min break. a) Differences in vector strength (VS) values during 1$^{st}$run and 2$^{nd}$run. b) Differences in VS values among different neurons (RS and FS) during 1$^{st}$run and 2$^{nd}$run. c) Differenes in VS values in different layers (Layer III, IV, V, VI) during 1$^{st}$run and 2$^{nd}$run. d) Triple interaction (Timexlayerxneuron) result among different neurons in different layers.

evoked somatosensory potential lasting up to 4h, and this long-lasting activation is dependent on muscarinic receptors at the level single cortical neurons, we particularly showed that BF stimulation modulates vibrotactile responses of rat SI neurons based on cell type, layer and in a time-dependent manner. The principal findings are: (i) that although average firing rates are not affected, BF stimulation had significant short-term effects on VS values during 2$^{nd}$ run. Long-term enhancement is dependent upon a second concomitant neural process not similar with learning mechanism related with long-term potentiation. Repeating the sensory event after BF stimulation strengths the cortical response and vibrotactile periodicity becomes more prominent; (ii) when 1$^{st}$ and 2$^{nd}$ runs were compared in terms of VS change in ON vs. OFF, significant interactions between BFxlayer and BFxneuron were found. Repetitive activation of cholinergic input to SI by stimulation of BF were shown to be more effective and

dependent on cell type and layer.

### 3.4.1 Short-term and long-lasting effects of BF stimulation

Short-term effect and long-lasting effects of BF were only observed with vector strength enhancement. This enhancement is only observed during 5-Hz stimulation. Inhibition mechanism proposed in the previous studies were present and this behavior was not affected by cholinergic activation. Overall effect of BF activation on different neurons were different. Opposite behavior among neurons were observed. Even though FS cells receive thalamic synapses depressing the short-term dynamics similar to RS, it seems FS has more impact on the average firing rates during vibrotactile stimulation and in terms of spontaneous activity. On the other hand, vibrotactile periodicity (only at 5-Hz) becomes more prominent for RS neurons over period of time. Cortical location and diversity of neurons within the corresponding layer determines the degree of periodicity and response patterns. The effects of BF activation on the firing rate developed over time. Previous studies showed that there was no change in firing rate due to time. Hypothesized mechanism would be similar to plasticity and/or LTP.

### 3.4.2 Relationship with previous studies

Long-lasting cholinergic enhancement was present in the previous studies investigating the somatosensory-evoked potential and at the level of single cortical neurons in cats [68, 70, 71, 73, 246].

Local application of ACh has an effect on firing rates and receptive field sizes (plasticity). These effects were blocked by muscarinic antagonists but not by nicotinic receptors, especially in deeper layers. Metherate et al [231] argued as others have, that neuronal activity was the critical process required to produces to long-term changes in the presence of ACh since they occurred preferentially when ACh was paired with glutamate administration or with tactile stimulation and very rarely when ACh was given alone. Similar to this, Sillito and Kemp [65] studied the effects in the visual cortex,

and they found a cumulative enhancement of visual responses when successive administrations of ACh were repeated before responsiveness to visual stimuli declined to the control value. BF was active and producing action potential continuously in the awake monkeys and it was reported that BF neurons showed phasic changes in the average firing rate at specific times during a behavioral task. Therefore, stimulating the BF in the present study might have changed weak tonic activation into a more robust effect leading possibly to persistent changes in the membrane resistance of cortical neurons.

### 3.4.3 Other effects of BF stimulation

NBM also sends GABAergic input to the cortex that may be involved in arousal/ attentional modulation. In addition, NBM may not solely act in isolation but also together with other known components of the attentional functions. Only 1/3 of the projections are known to be cholinergic thus it is difficult to separate the contributions of cholinergic and GABAergic nucleus basalis neurons. Although we did not observe any inhibitory effect of BF stimulation related to possible GABAergic projections, especially the activity of FS neurons has an impact on the spontaneous activity of neuron.

Here, we have presented the results of SI recording ipsilateral to BF stimulation. However, to assess the global activation of BF stimulation in the brain since there is also contralateral projection to other sensory cortices, we have recorded from SI in the contralateral hemisphere with or without the vibrotactile stimulation. In both cases, we did not observe any changes in firing rate or vector strength. Although the number of neurons compared to main experiments are low (n=12), we can conclude that these local changes in responses to vibrotactile stimulation were directly due to BF stimulation ipsilateral to SI.

### 3.4.4 Theoretical issues, limitations and future directions

BF seems to be capable of producing long-lasting effects and has several other implications for understanding nervous system processing. In other cortical areas, ACh has been implicated in learning and in the control of memory. Also, the deficit in higher cognitive functions including memory problems in Alzheimer's disease has been correlated to the loss of cholinergic BF neurons. If the BF is necessary for certain kinds of long-term changes related to learning and memory in the somatosensory cortex, then loss of BF neurons in Alzheimer's disease would prevent these processes and block long-term facilitation required for these aspects of learning and memory.

Under anesthesia, it is also difficult to assess the characteristics or possible mechanisms of bottom-up and top-down attention. BF/ nucleus basalis receives input from both sub-cortical regions and prefrontal cortex to process both bottom-up and top-down signals. Nevertheless, we tried to assess the effects of 'top-down' modulation of attention by applying the electrical stimulation of BF prior to secondary input (i.e. vibrotactile stimulation) and repeated the all experimental procedures to understand and to compare the effects for prospective chronic recording from rat SI cortex during a behavioral task.

We also did not assess that whether these changes due to BF stimulation are dependent on muscarinic or nicotinic receptor mediated. It has been known that the distribution of both muscarinic and nicotinic receptors are not homogenous throughout the cortex. This supports the hypothesis that responses are dependent on layer and cell type. The synaptic release of ACh from BF fibers projecting to SI can be inferred from the anatomy of the system since previous experiments showed that muscarinic receptors are required to express the effect from the BF in the cortical neuron. To elucidate mechanism of action, we need more information about the nature of BF projections to the cortex.

## 3.5 Conclusion and future work

Bottom-up and top-down attention are two separate but interacting cholinergic input to SI which targets diverse cell types in multiple cortical layers. We don't really know how these two processes work. When you look from behavioral point of view, you can divide these processes into two types of models and it is easier to understand the nature of bottom-up and top-down signals. You can test these possibilities with novel attentional tasks and find answers to whether they work as one entity with two branches, or separate entities in which both mechanisms strongly influence each other or separate entities working independently. However, it is not easy to identify brain structures and circuits or the pathways involved in attention. It is also not possible what kind of substrates involved. One of drawbacks previously mentioned studies is lack of investigation of specific nicotinic and muscarinic compounds. In order to see more detailed view of the influence of cholinergic modulation, it would be important to study using specific nicotinic and muscarinic antagonists by the help of microinjection. With the application of different compounds into the cortex, the functional properties of the specific neurons responding to each drug in each layer can be revealed. This would make contribution not only to the understanding of neural mechanisms of ACh but also reveal the effects of drugs on the spatial and temporal parameters of cortico-cortical and horizontal connections within specific column. It is possible to study contribution of cholinergic receptors on vibrotactile responses of cortical neurons in the rat primary somatosensory cortex (only bottom-up) by microinjection of ACh, atropine (muscarinic receptor antagonist), Methyllycaconitine (MLA) ($\alpha$7 subtype-specific nicotinic receptor antagonist), Dihydro-$\beta$-erythroidine hydrobromide (Dh$\beta$E) ($\alpha 4\beta 2$-subtype-specific nicotinic receptor antagonist). This would give us knowledge about role and distribution of receptor subtypes throughout the cortex. We also found that distribution of both muscarinic and nicotinic receptors are heteregenous and specific nicotinic receptor subtypes are modulated by BF stimulation [247, 248]. Therefore, a study investigating the effects of these drugs on the vibrotactile responses of cortical neurons similar to study in Chapter 2 can be performed.

# 4. A COMPUTATIONAL MODEL FOR TACTILE PROCESSING IN THE PRIMARY SOMATOSENSORY CORTEX

This work has been published in;

Vardar, B. and Güçlü B., Effects of Bicuculline and NMDA on the Excitatory and Inhibitory Neurons in the Rat Somatosensory Cortex: A Preliminary Model. *2016 20th National Biomedical Engineering Meeting (BIYOMUT)*, 2016.

## 4.1 Introduction

The sense of touch is mediated by the different type of cutaneous mechanoreceptors located in the various layers of the skin. There are four types of mechanoreceptors found in the mammalian glabrous skin: Meissner corpuscles, Pacinian corpuscles, Merkel cells and Ruffini endings [11,107,109,119]. In addition to these receptors, there are non-encapsulated hair-follicle receptors and C-mechanoreceptive fibers in the hairy skin [109,249–251]. Classification of these receptors depends on not only their morphology, innervation pattern, and depth in the skin but also adaptation and receptive fields. Each receptor as part of peripheral nervous system responds to particular mechanical stimuli. Tactile information from these receptors is conveyed by afferent pathways through the spinal cord, the medulla, and the thalamus into the primary somatosensory cortex where information processing primarily occurs. It has been known that the primary sensory cortices (auditory, visual and tactile) process the sensory information in columns organizing the relevant input depending on the location and modality [35–39]. Cells located in different layers of each column receive the inputs from same receptor area and respond to same classes of receptors. In each column, thalamocortical inputs make synapse first in layer IV where the signal projects to upper layers of the cortex (layer II/III). Lastly, these signals pass to layer V and VI where the signal is transmitted to other areas of the brain or back to thalamus and periphery [40–43,252]. However,

cortical responses to mechanical stimuli applied on the skin in the SI cortex are different than those of peripheral afferents [116, 180]. The reason why tactile information is modulated while conveyed to cortical area is the involvement of excitatory and inhibitory processing in the cortex. Thus, it is important to understand the relationship between the characteristic of mechanical stimuli and cortical responses. Sensory systems can be used to build a model system for cortex in general since the physiological activation of neural circuits using sensory stimuli is possible. To understand the signal processing within a cortical column, we need to determine the structure and function of individual synaptic connections among different neurons. A column involves two major classes of neurons: excitatory neurons that constitute 80-85% of neuron population and GABAergic inhibitory interneurons [203, 253]. The response of an individual neuron to sensory stimuli depends on the interaction of excitatory (glutamatergic) and inhibitory (GABAergic and glycinergic) synapses [254]. Specifically in primary somatosensory cortex, inhibitory interactions are mediated by $GABA_A$ receptors whereas excitation is mediated by ionotropic glutamate receptors [139, 140]. According to our knowledge, there are at least three pharmacologically distinct ionotropic receptors responsible for deriving excitatory and inhibitory balance in SI: NMDA, AMPA and kainite receptors [141–143].

Although main sensory input to cortex is obtained from the thalamus, significant processing occurs within the local cortical circuitry [240]. Thalamocortical afferents form synapses directly with both excitatory/regular-spiking(RS) and inhibitory neurons/fast-spiking (FS) [134, 145]. Moreover, FS neurons make strong synaptic connections with RS neurons in the same layer. We have recently characterized the vibrotactile responses of RS and FS neurons in the hindpaw representation of rat SI cortex after bicuculline, and NMDA microinjections [163, 245]. Consistent with the previous studies, spikes were mostly generated at the initial 100-ms duration of the sinusoidal stimulus for all neurons presented in this study. Entrainment (1:1 firing) was found at 5 Hz, but not at 40 and 250 Hz. At all tested frequencies, the tonic responses of RS (excitatory) neurons increased, but the phasic responses did not change. Both phasic and tonic responses of FS (inhibitory) neurons were not influenced by bicuculline and NMDA. Additionally, in the sham conditions, the phasic responses were always greater than tonic responses driven by vibrotactile stimulation. Following this logic,

we proposed a computational model to simulate the effects of bicuculline and NMDA on vibrotactile responses of excitatory and inhibitory neurons in SI cortex [244, 255].

The current computational model is based on a previous model for excitatory (E) and inhibitory neurons (I) in response to ramp-and-hold stimuli in whisker cortex. Pinto et al. [256] presented an analytic investigation of how thalamocortical response transformations occurs in rodent barrel cortex. In this study, we simulated E and I neurons subject to sinusoidal vibrotactile stimulation (5- and 40-Hz) applied on the hindpaw of rats before and after bicuculline and NMDA microinjection. Moreover, the populations of excitatory and inhibitory neurons were each reduced to a single non-linear differential equation (Figure 4.1, Equation 4.2,4.3). Inhibitory ($w_{ii}$, $w_{ie}$) and excitatory weights ($w_{ee}$, $w_{ei}$) on both excitatory and inhibitory neurons were probabilistically decreased or increased according to drug effects. In order to mimic the random variation among neurons, all weights were sampled from their particular probability distribution functions (Table 4.1). We simulated firing rates of 31 RS and 24 FS neurons to compare with our experimental data recorded from the SI cortex (n=55). Similar to existing literature and experimental data, E and I neurons mostly responded at the onset of 40-Hz, but could be entrained (1:1 firing) at 5-Hz (Figure 4.2a and 4.2b). Simulated E and I neurons shows similar response properties as observed in RS and FS neurons, respectively. For example, I neuron is more active (both stimulus evoked and background activity) while response of E neuron to mechanical stimuli temporally sharper during the same time period.

## 4.2 Materials and Methods

### 4.2.1 Animals and Experimental Data

To compare the output of the computational model, the previous experiments were used in which we recorded single-unit spike activity before and after drug microinjection from 67 tactile neurons in the hindpaw representation of 19 anesthetized Wistar albino rats (Chapter 2) (See details of experimental data in Chapter 2.2.1). Intracortical drug microinjections were given before the mechanical stimulus by using

pneumatic pump. The neurons (n=67) were classified as regular spiking (n=31) and fast-spiking (n=24) (IB=12 but they were not included in the computational model). For each neuron, average firing rates and percent changes from the sham condition were calculated for two time windows: onset ($R_o$) (first 100ms stimulus) and entire stimulus duration ($R_d$). The experimental data were published [245]. All experiments were approved by the Boğaziçi University Institutional Ethics Committee for the Local Use of Animals in Experiments.

### 4.2.2 Mechanical Stimuli

The details of the waveforms for the vibrotactile stimulation were explained in Chapter 2.2.2. The vibrotactile stimuli were given with electrodynamical shaker (V101; Ling Dynamic Systems, Royston, Herts., UK) and applied at the RF center of each single unit by using a plastic cylindrical contactor (diameter: 1.8 mm) without a surround. Apart from the experimental work, only two sinusoidal frequencies (5, and 40Hz) were tested in random counterbalanced blocks for each single unit. The stimuli were bursts sinusoidal mechanical displacements (amplitude: 100 $\mu$m peak-to-peak) superimposed on a static indentation of 0.5 mm. They started and ended as cosine-squared ramps with 50-ms rise/fall times, and duration of 0.5 s, as measured between half-power points.

### 4.2.3 Computational Model

Model diagram is shown in Figure 4.1. To generate input to the simulated excitatory (E) and inhibitory (I) neurons, we have also constructed a thalamic neuron model (Th) and calculated the average firing rate of each neuron in response to different mechanical stimulation. Cortical neurons are denoted as $E$ and $I$ whereas thalamic neurons is shown as $Th$. Each output of neurons are simulated as average firing rate per unit time.

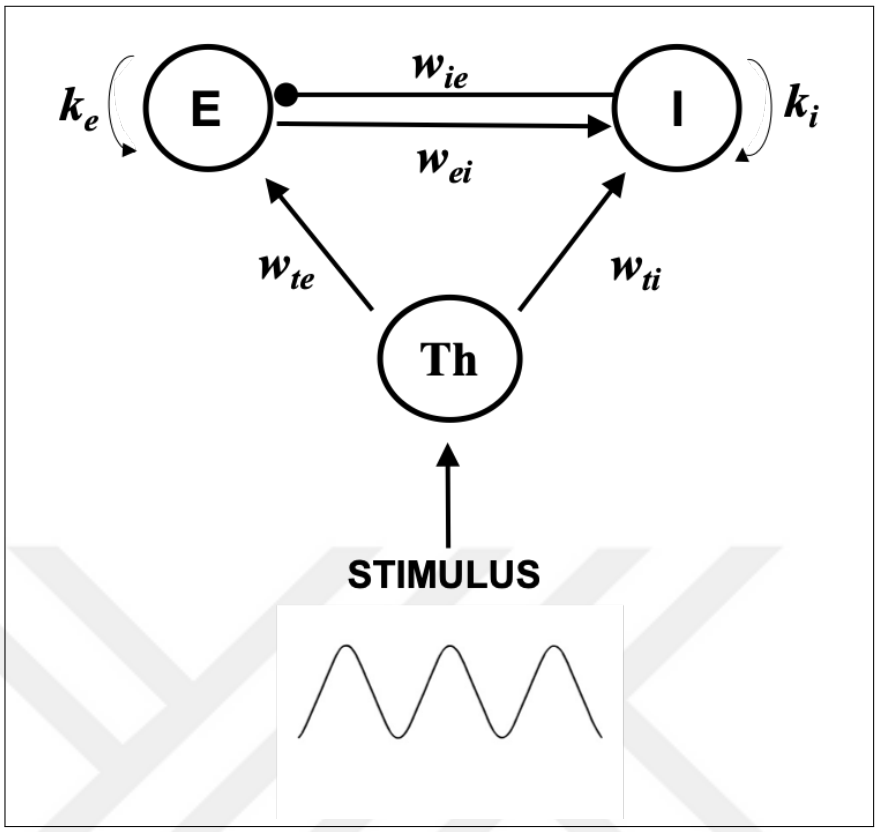


**Figure 4.1** Computational Model Diagram

• **Thalamic Model**

In this study, thalamic neuron model is constructed using experimental study in which thalamic neuron responses from rats were recorded during the sinusiodal mechanical stimulation to whiskers. [171, 257, 258]. Experimental data obtained using short air puffs show a single peaked thalamic response, about 50 ms long, which resembles the profile of a Gamma function [259]. Sinusoidal whisker stimulation produces a large onset peak response followed by a small offset response. We have neglected this small offset peak and have modeled the Th in both pulse and sinusoidal stimulation with a Gamma function defined as:

$$T = T_0 \ + \frac{C}{\sigma} \ t \ e^{\left(\frac{t}{\sigma} \ +1\right)} \tag{4.1}$$

Output of T neuron continues periodically in each cycle of the stimulus and gives the average firing rate per unit time. $T_0$, basal thalamic neuron rate, represents the tha-

lamic AP's spontaneously discharge rate in the absence of stimulation [42,196,260,261]. C defines the maximum peak response which stimulation can produce whereas $\sigma$ denotes the time-to-peak. The values of C and $\sigma$ are defined according to characteristic of stimulation frequency on the thalamic neuron. The parameters for each variable were given in Table 4.1 for each frequency.

**Table 4.1**
Values of each parameter for both thalamic and E/I model.

| Model Parameters | Values |
|---|---|
| $k_{1e}$, $k_{1i}$ | 0.7, 0.2 |
| $k_{2e}$, $k_{2i}$ | 7.4, 4.1 |
| $\tau_e$, $\tau_i$ | 5, 15 |
| $w_{ee}$, $w_{ei}$ | (1.0 ± 0.5), (1.0 ± 0.5) |
| $w_{ie}$, $w_{ii}$ | (2.05 ± 1.025), (3.5 ± 1.75) |
| $w_{te}$, $w_{ti}$ | (3.9 ± 1.95), (6.0 ± 3.0) |
| d | e:12.03, i: 11.62 |
| C | 5-Hz: 10, 40-Hz: 10 |
| $\sigma$ | 5-Hz: 10, 40-Hz: 2 |

• **Excitatory and Inhibitory Neuron Model**

E and I shown in Figure 4.1 represents excitatory and inhibitory cortical neurons, respectively in the hindpaw representation of the SI cortex. Neuronal activity of each neuron is represented by following differential equations (Equation 4.2, 4.3) and activation function P (Equation 4.4).

$$\tau_e \frac{dE}{dT} = -k_{1e}E + (1 - k_{2e}P_E(E))\ P_E(w_{ee}E + w_{te}Th - w_{ie}I) \tag{4.2}$$

$$\tau_i \frac{dI}{dT} = -k_{1i}I + (1 - k_{2i}P_I(I))\ P_E(w_{eb}E + w_{ti}Th - w_{ii}I) \tag{4.3}$$

$$P(Z) = 1 + erf\Big(\frac{Z-15}{d}\Big), erf(x) = \frac{2}{\pi}\int_0^x e^{-y^2}dy \tag{4.4}$$

All simulated neurons (E, I, and Th) are connected to each other with varying

synaptic weights ($w_{xy}$) (x: presynaptic neuron, y: postsynaptic neuron). In order to mimic the random variation among neurons, all synaptic weights were sampled from their particular probability distribution functions. Values of each synaptic weight which were given in Table 4.1 has their average and standard deviation from a Gauss distribution. Range of values for all synaptic weights except $w_{ti}$ were set to be half the mean. Variance of $w_{ti}$ was made large to reflect the marked heterogeneity that is known to exist in the numbers of corticothalamic synapses onto inhibitory neurons [262, 263]. Additionally, all synaptic weights were chosen according to anatomical and physiological studies in the literature [153, 240, 262, 264]. $k_{1e}$, $k_{1i}$ represent self-decay constants whereas $k_{2e}$, $k_{2b}$ represent refractory period. For all neurons, synaptic weights were passed through the activation function given in Equation 4.4. d given in the activation function P represents the varying parameter according to type of neuron.

### 4.2.4 Statistical Analysis

To compare with experimental data (n=55), we simulated same number of E (n=31) and I (n=24) neurons using the computational model. To model the effects of drugs microinjected into the cortex, synaptic weights were determined from its probabilistic distribution for each E and I neuron simulated. Synaptic weights are increased or decreased from the reference point according to the generic effects of drug. For example, to simulate the effects of biculline, inhibitory synaptic weights onto excitatory and inhibitory neuron ($w_{ie}$ and $w_{ii}$, respectively) were decreased. Moreover, to simulate the effects of AMPA and NMDA, excitatory synaptic weights onto excitatory and inhibitory neurons ($w_{ee}$ and $w_{ei}$, respectively) were increased. After drug microinjection, % change of the the average firing rates ($R_o$ (initial 100-ms of mechanical stimuli) and $R_d$ (500-ms of mechanical stimuli) for each frequency) in the experimental data were compared with simulated E and I. Statistical analysis was done with pair t-tests for each frequency and each drug condition.

## 4.3 Results

In order to compare the experimental data with the output of the simulation, we analyzed the data in terms of average firing rate. Moreover, we modelled the effects of the drugs and compared the results according to their "sham" condition in terms of percent change. Consistent with the existing literature and experimental work [245], tactile neurons mostly responded at the onset of the 40- and 250-Hz sinusoidal vibrations, but could be entrained (1:1 firing) at 5 Hz. Similar behaviors for E and I neurons were shown in Figure 4.2. Additionally, output of E and I neurons in the computational model shows other characteristics of RS and FS neurons, respectively. For example, average background firing rate of B neuron and its firing rate during mechanical stimuli are higher compared to those of E in the same time period. Moreover, we observed that the response to mechanical stimuli of B neuron are longer whereas response of E neuron is much sharper.

First, to understand the behavior of an E and I neuron depending on the probabilistic relative synaptic weight onto them, we investigated the effects of 15 different synaptic weights on the $R_d$ and $R_o$ of a simulated E and I neuron (Figure 4.3 and 4.4, respectively). Figure 4.3 shows how the different synaptic weights onto the excitatory neuron, E, modulate the $R_d$ and $R_o$. Consistent with the previous study (2, at 40-Hz, inhibitory synaptic weight onto E neuron was decreased (Figure 4.3(d)) or excitatory synaptic weight onto E neuron (Figure 4.3(c)), change in activity is higher for $R_d$ compared to $R_o$, in fact the change in $R_o$ was very small. This behavior was not observed at 5-Hz (Figure 4.3(a) and 4.3(b)). Additionally, we show that how the different synaptic weights onto the inhibitory neuron, I, modulate the $R_d$ and $R_o$ in Figure 4.4. For both frequencies, all synaptic weights onto I neuron did not have any effect for both $R_d$ and $R_o$. Furthermore, in the case of synaptic weights were decreased to their lowest value or increased to their highest value, change in average firing rate were much smaller compared to E neuron.

After simulation of neuron E and I in response to different mechanical stimuli, to model the effects of drugs injected, synaptic weights were probabilistically increased or decreased. To mimic the effects of bicuculline, inhibitory synaptic weights, $w_{ie}$ and $w_{ii}$, were decreased. To mimic the effects of NMDA or AMPA, the excitatory synaptic

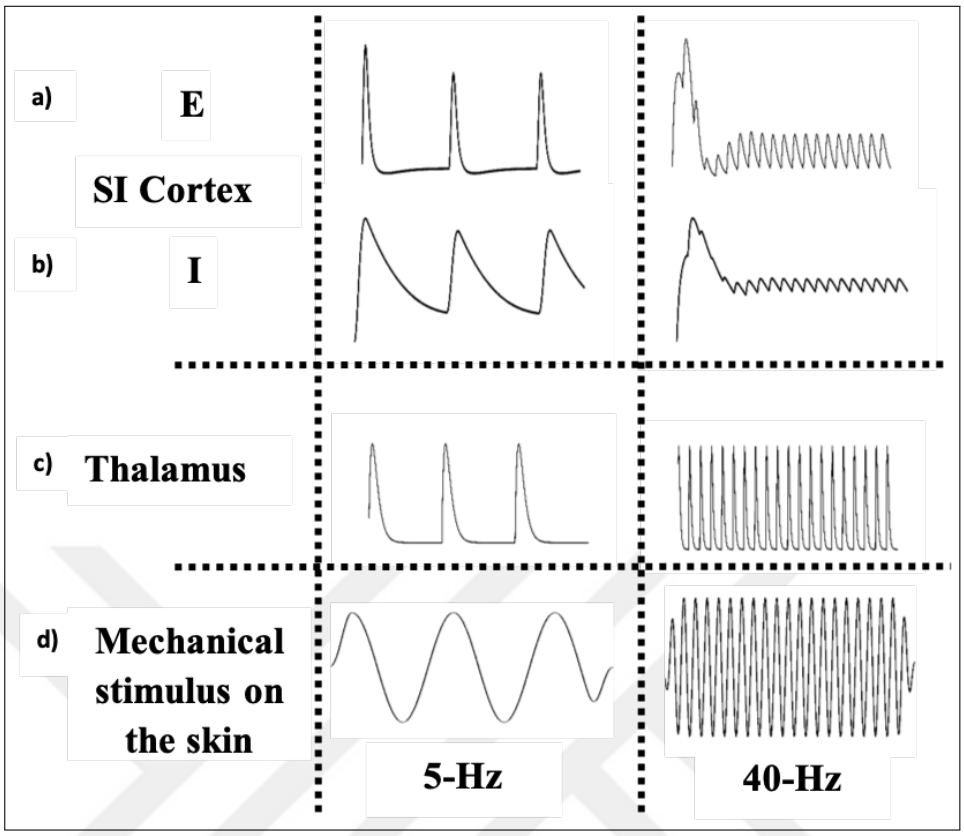


**Figure 4.2** Time histograms of each neuron to vibrotactile stimulation (E, I, Th). a) Response of E neuron to 5-Hz (left column) and 40-Hz stimulation (right column) in the cortex. b) Response of I neuron to 5-Hz (left column) and 40-Hz stimulation (right column) in the cortex. c) Response of Th neuron to 5-Hz (left column) and 40-Hz stimulation (right column) in the thalamus. d) Mechanical stimulation on the skin: 5-Hz (left column) and 40-Hz stimulation (right column).

weights, $w_{ei}$ and $w_{ee}$, were increased. Subsequently, change in average firing rates in two time periods ($R_d$ and $R_o$) were calculated for 31 E and 25 I neurons. 31 E and 25 I neurons. The results are shown in Figure 4.5. Left y-axis shows change in $R_d$ whereas right y-axis shows change in $R_o$. X-axes represent corresponding neuron type (E or I).

Statistical analyses to compare computational model and experimental data were summarized in Table 4.2. Although, average firing rates per unit time for E and I neurons were lower than the experimental data, change in average firing rate after drug effects were successfully simulated except one condition ($R_d$-5Hz-E-Bic).

Another result from the experimental work is that $R_d$ of RS neurons were statistically significant for both drug conditions at all frequencies; but this was not observed for $R_o$. On the other hand, the change in average firing rate after drug microinjection were not statistically different than sham conditions for FS neurons. As observed in the

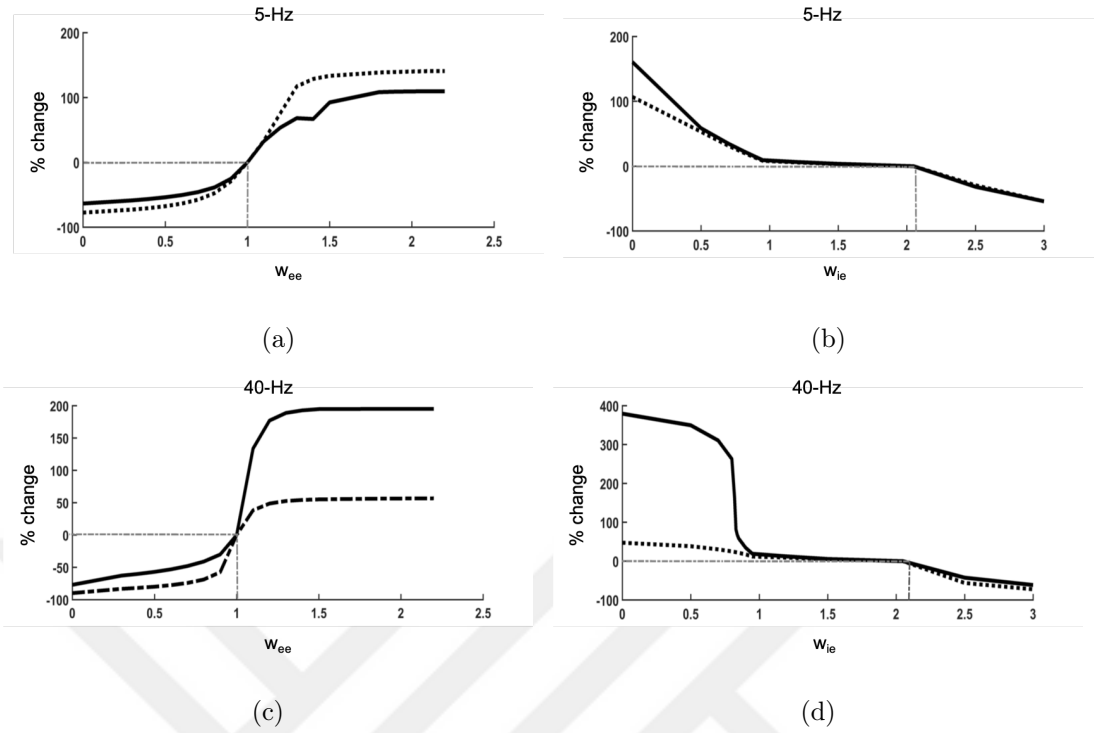


**Figure 4.3** Effect of synaptic weight change onto excitatory neuron in response to 5-Hz and 40-Hz mechanical stimuli. Black lines: $R_d$, Black dotted lines: $R_o$, Gray dotted lines: Reference point.

computational model, change in firing rate for I neuron were much smaller compared to E neuron and these results were consistent with the experimental data.

## 4.4 Discussion

The aim of this study was to simulate excitatory and inhibitory neurons found in the primary somatosensory cortex representing the hindlimb area and their change in activity during microinjection of bicuculline and NMDA/AMPA. This study also provides a preliminary model to simulate the effects of cholinergic inputs to SI and to improve the existing model for attentional modulation of tactile processing. However, this model is phenomenological model since it does not involve anatomical and physiological characteristics of the neurons. In general, although the output of the model is successful and consistent with experimental work, this model needs to be modified especially in the low frequency stimulation. The differences observed at 5-Hz is due

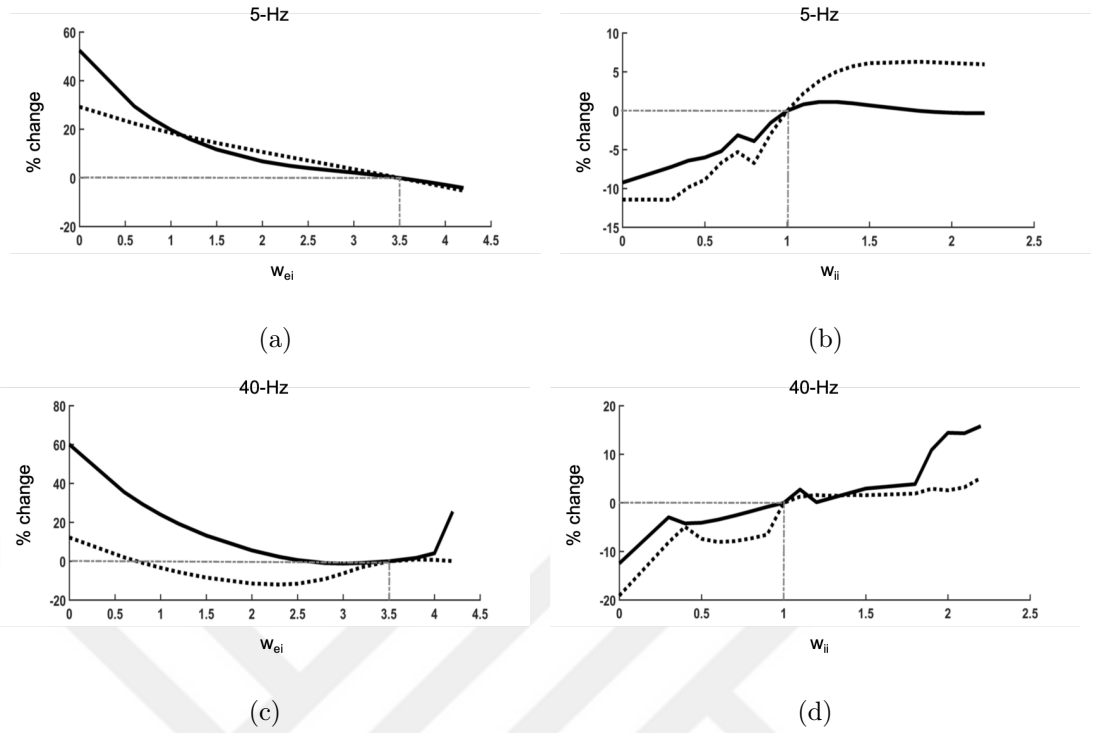


**Figure 4.4** Effect of synaptic weight change onto inhibitory neuron in response to 5-Hz and 40-Hz mechanical stimuli. Black lines: $R_d$, Black dotted lines: $R_o$, Gray dotted lines: Reference point.

to limitations of the previous model developed for the whisker stimulation. This limitation is due to difference in the cortical area (SI vs. barrel cortex) and stimulation method (vibrotactile vs. ramp-and-hold stimuli).

Some differences observed in $R_d$ and $R_o$ will be investigated in the future studies. By doing this, the synaptic weights such as $w_{ee}$, $w_{ei}$, $w_{te}$ and $w_{tb}$ can be modified to obtain more realistic results. For example, excitatory synaptic weights can be divided into sections representing different glutamate receptors (i.e AMPA and NMDA). The importance and their generic effects can be distributed to synaptic weights. Additionally, physiological data from the experimental studies can be incorporated into the model. Thus, absolute values of firing rates can be used instead of percent changes.

Another limitation of this study is the model is not suitable for high frequency stimulation. The output of the thalamic neuron for high frequency stimulation (i.e. 250-Hz) cannot be currently used for cortical model. In fact, the Pacinian corpuscles found in the glabrous skin mostly responds to 200-300-Hz mechanical vibrations [265]. Therefore, thalamic neuron model needs to modified especially for the high frequency

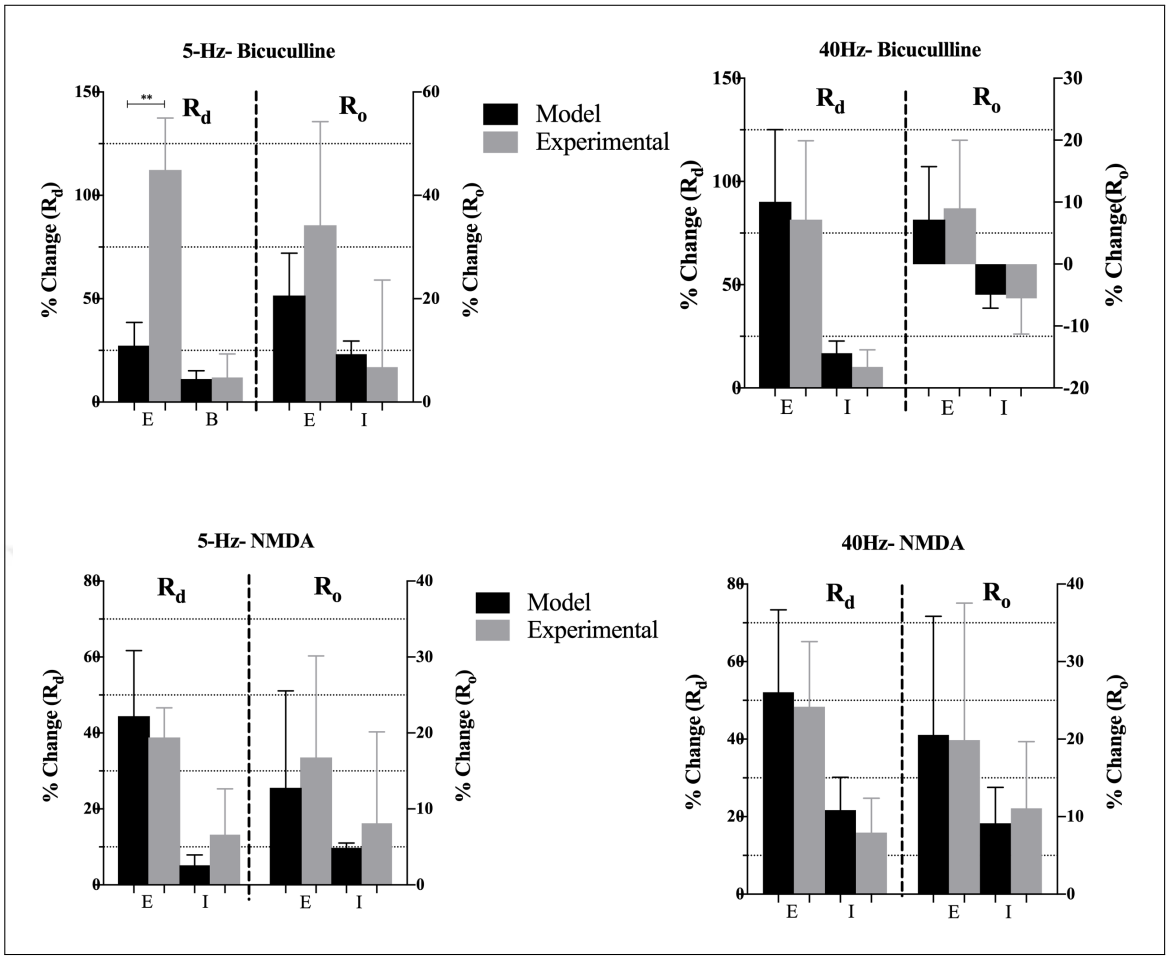


**Figure 4.5** Percent change in firing rates for each frequency and drug conditions in two time windows: $R_d$ and $R_o$. Comparison of the computational model and experimental data. Left y-axis shows % change in $R_d$ and right y-axis shows % change in $R_o$. x-axis shows E and I neurons affected by injected chemicals. Left column of the figure shows the results in 5-Hz mechanical stimulation whereas the right column of the figure shows 40-Hz mechanical stimulation.

stimulation.

## 4.5 Conclusion and future work

This study was a preliminary work of a computational model for attentional modulation of tactile processing. The proposed computational model will be simulating the vibrotactile responses of different type of neurons (i.e. excitatory (E) and inhibitory (I)) and their synaptic interactions in the hindpaw representation of the rat

**Table 4.2**
Paired t-test results. Abbreviations are as follow: Time Period ($R_d$ or $R_o$) - Frequency of stimuli (5 or 40-Hz)- Neuron type (E or I)- Drug.

| Model vs. Experimental (Time Window-Freq-Neuron-Drug) | p-values |
|---|---|
| $R_d$-5Hz-E-Biculline | 0.006 |
| $R_o$-5Hz-E-Biculline | 0.28 |
| $R_d$-5Hz-I-Biculline | 0.75 |
| $R_o$-5Hz-I-Biculline | 0.66 |
| $R_d$-40Hz-E-Biculline | 0.86 |
| $R_o$-40Hz-E-Biculline | 0.55 |
| $R_d$-40Hz-I-Biculline | 0.51 |
| $R_o$-40Hz-I-Biculline | 0.79 |
| $R_d$-5Hz-E-NMDA | 0.77 |
| $R_o$-5Hz-E-NMDA | 0.82 |
| $R_d$-5Hz-I-NMDA | 0.52 |
| $R_o$-5Hz-I-NMDA | 0.79 |
| $R_d$-40Hz-E-NMDA | 0.89 |
| $R_o$-40Hz-E-NMDA | 0.97 |
| $R_d$-40Hz-I-NMDA | 0.64 |
| $R_o$-40Hz-I-NMDA | 0.62 |

primary somatosensory cortex (Figure 4.6). This computational model will be based on simple firing rate model consisting of two layers: thalamic layer (T) and cortex (S1). Further, the cortex will be divided into 4 layers (layer II/III, layer IV, layer V and layer VI). Each will be consisting of two types of neuron (E and I) connected to each layer and other neurons with varying synaptic connections ($w_{ei}$, $w_{ie}$, $w_{ii}$, $w_{ee}$) according to existing literature and collected experimental data. This work will be combined with our previous experimental data in which we investigated the effects of NMDA, AMPA and bicuculline on vibrotactile responses of excitatory and inhibitory neurons. For each type of receptor (glutamate (NMDA, AMPA), $GABA_A$, nicotinic and muscarinic), there will be different synaptic weights onto each neuron which will be changing to simulate the effects of drugs injected. According to the hypothesis, each neuron located in each layer will be affected differentially by microinjected chemicals and/or electrical stimulation of BF because of three reasons. First, distribution of

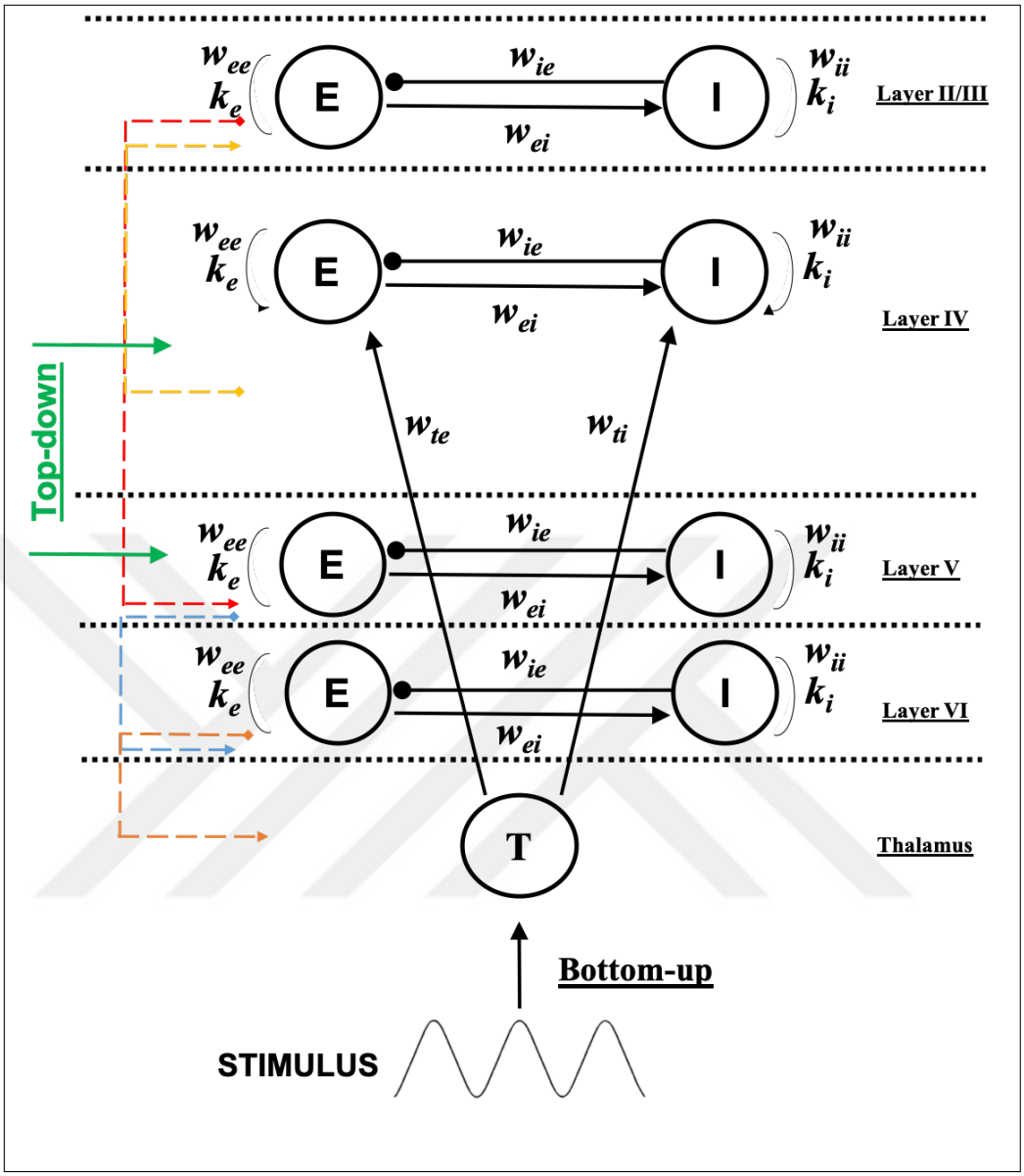


**Figure 4.6** Schematic diagram of the proposed computational model. Each component of model (E, I and T) represents a neuron in the given layer. E=excitatory neuron, I=inhibitory neuron, T=thalamic neuron. Each neuron is connected to other neuron(s) with varying weights ($w_{xy}$), x=pre-synaptic neuron, y=post-synaptic neuron. k represents each neuron's decay constant. Filled circle denotes inhibitory connection whereas the arrow denotes excitatory connections.

muscarinic and nicotinic receptors are not homogenous throughout the cortex. Second, BF projections to S1 is only through layer IV and V which will affect the spike rates of neurons located in other layers indirectly (depending on corticocortical connections). Third, the vibrotactile responses of E and I neurons is changing with frequency of mechanical stimuli. Detailed explanation of equations and parameters can be found in Materials and Methods section in Chapter 4.

# 5. GENERAL CONCLUSIONS AND FUTURE WORK

At the end of each chapter, general conclusions and the future work related with study discussed within the chapter were given. On top of that, after revealing the connections between different layers of SI cortex and the distribution of muscarinic and nicotinic receptor throughout the cortex, the computational model generated can be useful to test different hypotheses related with the electrophysiology. According to our knowledge, there is no study combining electrical stimulation and microinjection of drugs. For example, for further elucidation of the receptor characterization, microinjection of cholinergic drugs during ON conditions of BF stimulation would help us understand what kind of receptors mediate top-down modulation of attention.

Moreover, the behavioral tasks related with attention can be designed in the operant chamber specifically built for tactile stimulation [266]. Mechanical/electrical stimulation and cortical recording are possible during a behavioral task. In this case, chronic implant consisting of an electrode array can be placed in the hindpaw representation of SI cortex and cortical recording/ICMS can be performed.

It is such a hope that characterization of what kind of receptors are responsible for function of synaptic modulation would be helpful for the new drug discovery to assess cholinergic neurotransmission in treatment of diseases such as ADHD, AD. Moreover, electroceuticals have a long history in treatment of diseases and recently are in favor of PD treatment. They are devices using electric impulses to treat ailments [267]. It is possible to implant such devices to deliver impulses to certain brain regions to increase cholinergic transmission which in turns improves the sensation.

# APPENDIX A. Chapter 2 Supplementary Figures

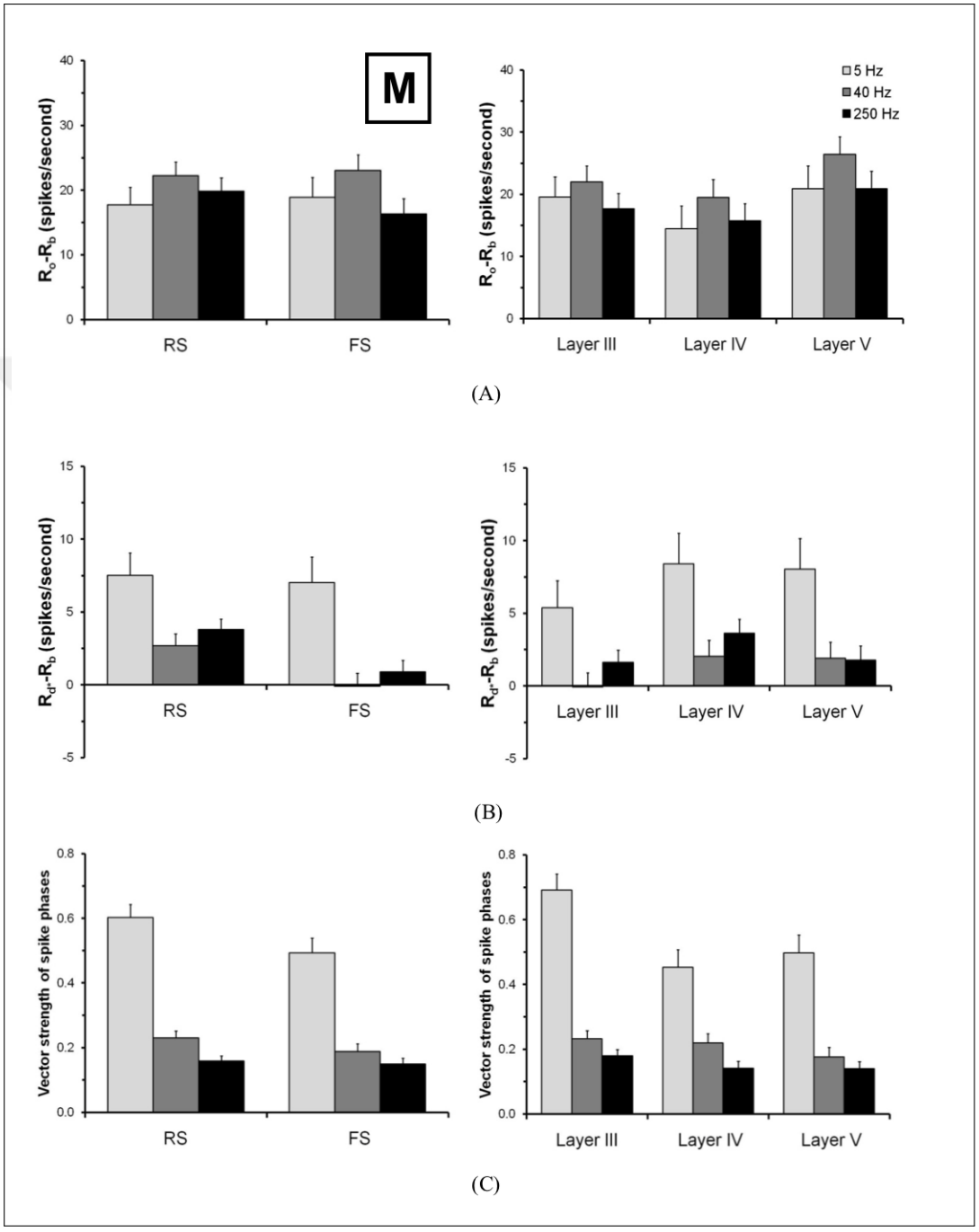


**Figure A.1** Average firing rates (AFRs) and vector strength (VS) values for the mechanical-only (M) condition. The graphs are given with respect to vibrotactile frequency, and represent averages across neurons pooled according to type (RS or FS) and cortical layer. (A) Change of AFR during the initial 100-ms period of the stimulus with respect to background ($R_o$-$R_b$). (B) Change of AFR during the remaining 400-ms period of the stimulus with respect to background ($R_d$*-$R_b$). (C) VS of spike phases from the entire stimulus duration (0.5 s). Error bars are the standard errors.

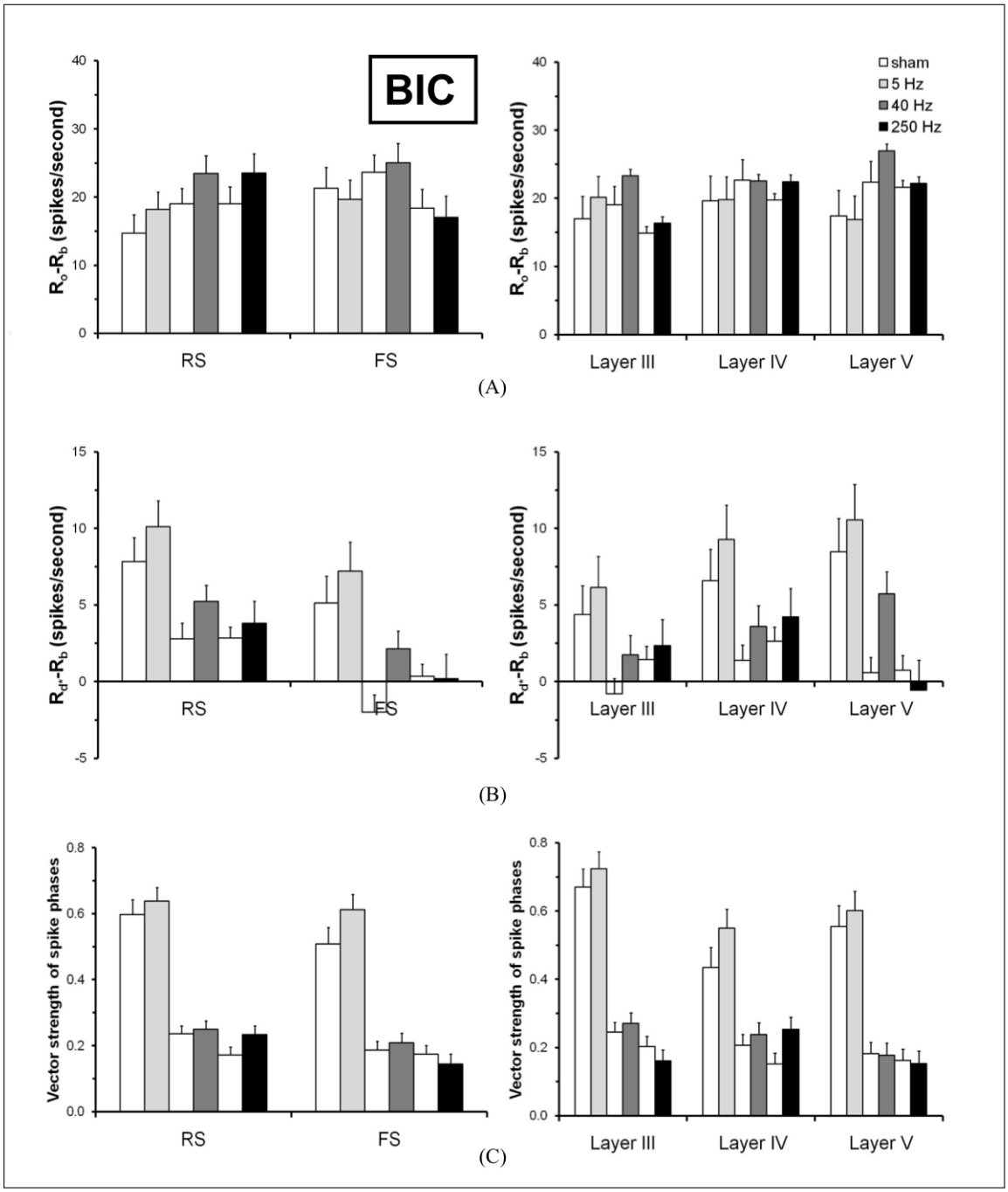


**Figure A.2** Average firing rates and vector strength values for the bicuculline condition. See Figure A.1 caption for details.

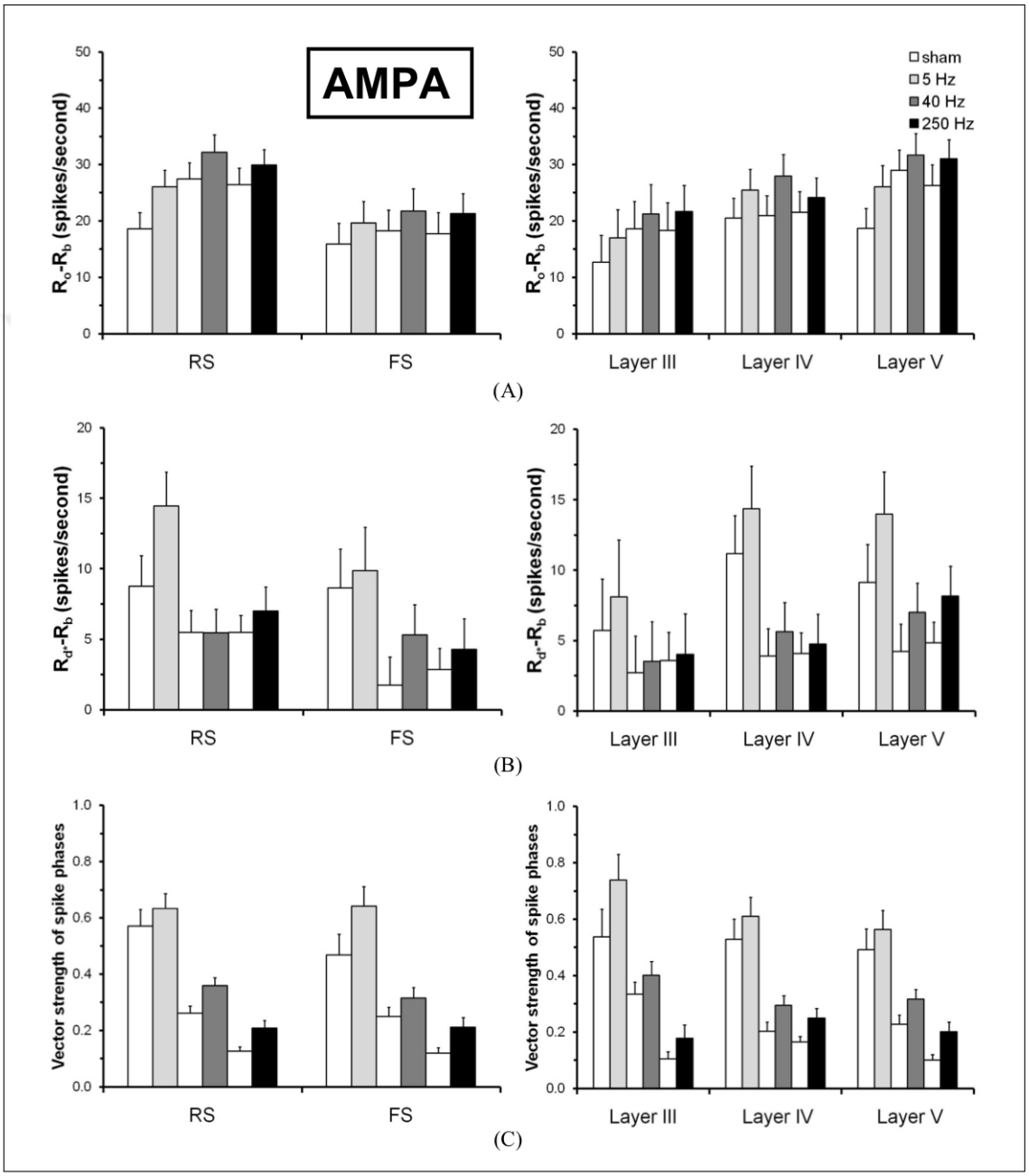


**Figure A.3** Average firing rates and vector strength values for the AMPA condition. See Figure A.1 caption for details.

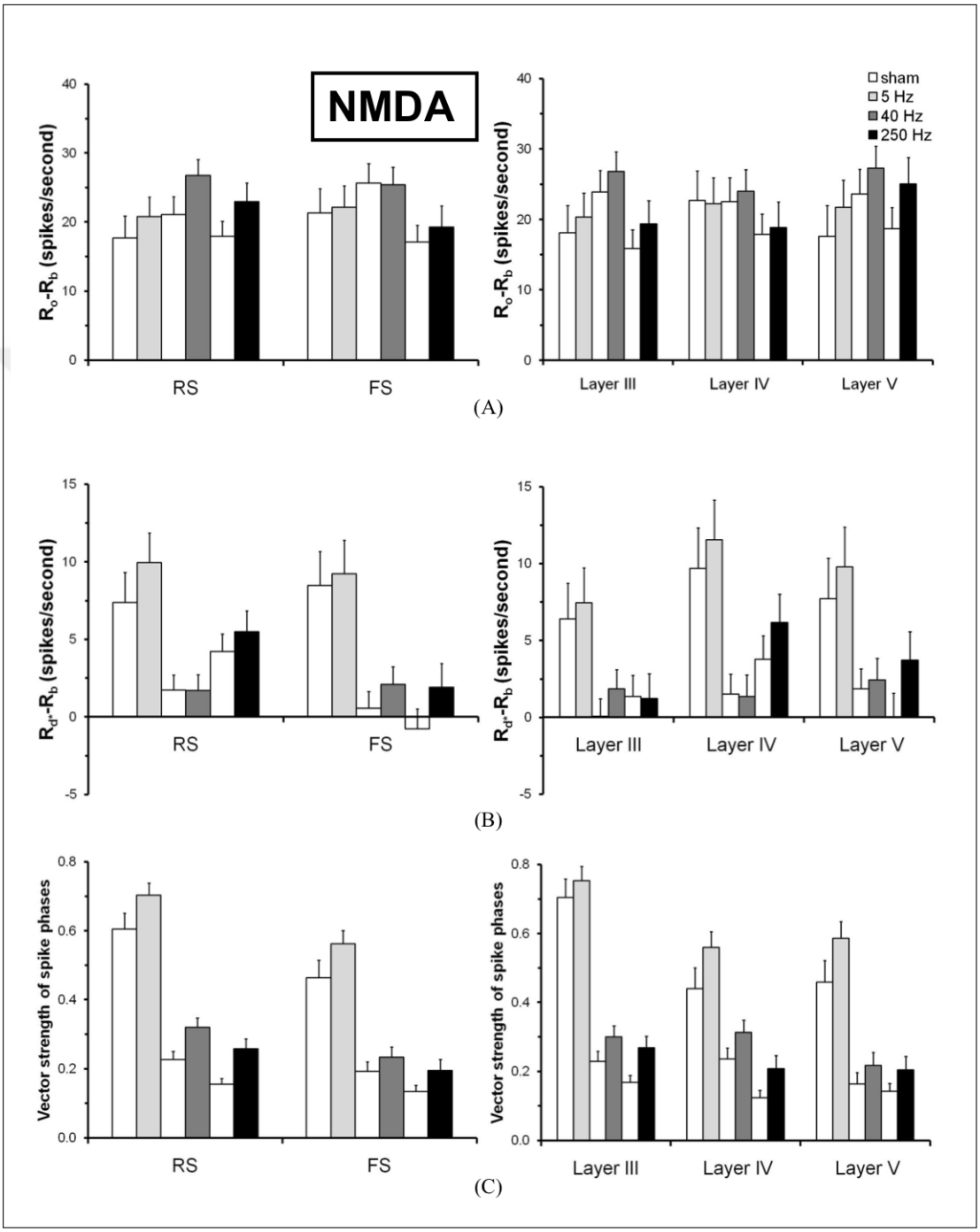


**Figure A.4** Average firing rates and vector strength values for the NMDA condition. See Figure A.1 caption for details.

# APPENDIX B. Publications

## Articles

- Vardar B. and Güçlü B., Non-NMDA receptor-mediated vibrotactile responses of neurons from the hindpaw representation in the rat SI cortex. *Somatosensory and Motor Research* 33:3 189-203, 2017.
- Vardar B. and Güçlü B., Effects of Basal Forebrain stimulation on the cortical neurons in the hindpaw representation of SI cortex *In progress.*

## Conference Proceedings

### *International Conference Proceedings*

- **Vardar B.** and Güçlü B., Basal forebrain stimulation modulates vibrotactile responses of rat SI neurons based on cell type, layer, and in a time-dependent manner. *Neuroscience 2018.* San Diego, CA, USA: Society for Neuroscience, 2018.
- **Vardar B.** and Güçlü B., Basal forebrain activation changes the vibrotactile responses of neurons in the hindpaw representation of rat SI cortex. *Neuroscience 2017.* Washington, DC, USA: Society for Neuroscience, 2017.
- **Vardar B.** and Güçlü B., Modeling the vibrotactile responses of excitatory and inhibitory neurons in the hindpaw representation of rat SI cortex. *Neuroscience 2016.* San Diego, CA, USA: Society for Neuroscience, 2016.
- **Vardar B.** and Güçlü B., Effects of bicuculline and NMDA on the vibrotactile responses of cortical neurons in the rat SI cortex. *Neuroscience 2015.* Chicago, IL, USA: Society for Neuroscience, 2015.

- **Vardar B.** and Güçlü B., Effects of bicuculline and NMDA on the vibrotactile responses of cortical neurons in the rat SI cortex. *The Third Joint Satellite Meeting of Turkey Chapter of Society for Neuroscience and Neuroscience Society of Turkey.* Chicago, IL. 2015.

***National Conference Proceedings***

- Devlet B., **Vardar B.**, Babür B. ve Güçlü B. Bazal önbeyin uyarımının sıçan beynindeki bedenduyusu ve motor kortekslerinde $\alpha 4/\alpha 7$ alt tipli nikotinik asetilkolin reseptör dağılımlarına etkisi. *Ulusal Sinirbilim Toplantısı*, 2019.

- Öztürk S., **Vardar B.** ve Güçlü B., Nöroprotezlerde davranışsal olayları öngörmek için S1 korteksindeki aksiyon potansiyellerinin sınıflandırılması. *Ulusal Sinirbilim Toplantısı*, 2018.

- Yusufoğulları S., **Vardar B.** ve Güçlü B., Sıçan beynindeki duyu-motor alanlarında muskarinik reseptör M2'nin katmansal dağılımı. *Ulusal Sinirbilim Toplantısı*, 2017.

- **Vardar B.** ve Güçlü B., Bikukulin ve N-metil-D-aspartik asitin Sıçan Bedenduyusu Korteksindeki Nöronlar üzerindeki Etkisi ve Bir Model Çalışması. *Biyomedikal Mühendisliği Ulusal Toplantısı*, 2016.

- **Vardar B.** ve Güçlü B., Asetilkolin ve atropinin arka ayak bölgesini temsil eden sıçan korteksindeki dokunma duyusu nöronlarına etkisi. *Ulusal Sinirbilim Toplantısı*, 2016.

- **Vardar B.** ve Güçlü B., Arka ayak bölgesiyle ilişkin sıçan korteksinde bikukulin ve N-metil-D-aspartik asitin III. ve IV. katman nöronları üzerindeki etkileri. *Ulusal Sinirbilim Toplantısı*, 2014.

- Dumlu S., Şahin D., **Vardar B.**, Duru A.D. ve Akın A., Motor Hareket ve Motor Hareketin Hayal Edilmesi Anlarsında Beyin Fonksiyonlarının EEG Yöntemiyle İncelenmesi. *Sinyal İşleme ve İletişim Uygulamaları Kurultayı*, 2014.

# REFERENCES


1. Tata, A., L. Velluto, C. D'Angelo, and M. Reale, "Cholinergic System Dysfunction and Neurodegenerative Diseases: Cause or Effect?," *CNS & Neurological Disorders - Drug Targets*, Vol. 13, pp. 1294–1303, 10 2014.

2. Müller, M. L. T. M., and N. I. Bohnen, "Cholinergic Dysfunction in Parkinson's Disease," *Current Neurology and Neuroscience Reports*, Vol. 13, p. 377, 9 2013.

3. Potter, A. S., G. Schaubhut, and M. Shipman, "Targeting the nicotinic cholinergic system to treat attention-deficit/hyperactivity disorder: Rationale and progress to date," *CNS Drugs*, Vol. 28, pp. 1103–1113, 12 2014.

4. Renard, P.-Y., and L. Jean, "Probing the cholinergic system to understand neurodegenerative diseases," *Future Medicinal Chemistry*, Vol. 9, pp. 131–133, 2 2017.

5. Hawkes, N., "Pfizer abandons research into Alzheimer's and Parkinson's diseases," *BMJ*, Vol. 122, no. January, 2018.

6. Polanczyk, G., M. S. De Lima, B. L. Horta, J. Biederman, and L. A. Rohde, "The worldwide prevalence of ADHD: A systematic review and metaregression analysis," *American Journal of Psychiatry*, Vol. 164, pp. 942–948, 6 2007.

7. Bartus, R. T., R. L. Dean, B. Beer, and A. S. Lippa, "The cholinergic hypothesis of geriatric memory dysfunction.," *Science*, Vol. 217, pp. 408–14, 7 1982.

8. BARTUS, R. T., R. L. DEAN, M. J. PONTECORVO, and C. FLICKER, "The Cholinergic Hypothesis: A Historical Overview, Current Perspective, and Future Directions," *Annals of the New York Academy of Sciences*, Vol. 444, no. 1, pp. 332–358, 1985.

9. Zimmerman, A., L. Bai, and D. D. Ginty, "The gentle touch receptors of mammalian skin," *Science*, Vol. 346, no. 6212, pp. 950–954, 2014.

10. K.Kandel, E., J. H. Schwatrz, T. M.Jessell, S. A.Siegelbaum, and A. Hudspeth, "Touch," in *Principles of Neural Science*, pp. 498–527, McGraw Hill, 2013.

11. Gardner, E. P., and K. O. Johnson, "Touch," in *Principles of Neural Science* (Kandel, E. R., J. H. Schwartz, T. M. Jessell, S. A. Siegelbaum, and A. Hudspeth, eds.), pp. 498–529, New York: McGraw-Hill, 5 ed., 2012.

12. Abraira, V. E., and D. D. Ginty, "The sensory neurons of touch," *Neuron*, Vol. 79, pp. 618–639, 8 2013.

13. Bliss, D., "Skin Anatomy: Image Details - NCI Visuals Online," 2010.

14. Johansson, R. S., and Ã. B. Vallbo, "Tactile sensory coding in the glabrous skin of the human hand," *Trends in Neurosciences*, Vol. 6, no. C, pp. 27–32, 1983.

15. Vega-Bermudez, F., and K. O. Johnson, "SA1 and RA receptive fields, response variability, and population responses mapped with a probe array," *Journal of Neurophysiology*, Vol. 81, no. 6, pp. 2701–2710, 1999.

16. Connor, C. E., S. S. Hsiao, J. R. Phillips, and K. O. Johnson, "Tactile roughness: neural codes that account for psychophysical magnitude estimates.," *The Journal of Neuroscience*, Vol. 10, no. 12, pp. 3823–36, 1990.

17. Phillips, J. R., K. O. Johnson, and S. S. Hsiao, "Spatial pattern representation and transformation in monkey somatosensory cortex.," *Proceedings of the National Academy of Sciences*, Vol. 85, no. 4, pp. 1317–21, 1988.

18. Phillips, J. R., and K. O. Johnson, "Tactile spatial resolution. II. Neural representation of Bars, edges, and gratings in monkey primary afferents," *Journal of Neurophysiology*, Vol. 46, no. 6, pp. 1192–1203, 1981.

19. Paré, M., R. Elde, J. E. Mazurkiewicz, A. M. Smith, and F. L. Rice, "The Meissner corpuscle revised: a multiafferented mechanoreceptor with nociceptor immunochemical properties.," *The Journal of Neuroscience*, Vol. 21, no. 18, pp. 7236–7246, 2001.

20. "Histology Slides/Dartmouth Univeristy."

21. Ridley, A., "Silver staining of nerve endings in human digital glabrous skin," *Journal of Anatomy*, Vol. 104, no. Pt 1, pp. 41–48, 1969.

22. Bolanowski, S. J., and L. Pawson, "Organization of Meissner corpuscles in the glabrous skin of monkey and cat," *Somatosensory and Motor Research*, Vol. 20, no. 3-4, pp. 223–31, 2003.

23. Cauna, N., and L. L. Ross, "The fine structure of Meissner's touch corpuscles of human fingers," *The Journal of Biophysical and Biochemical Cytology*, Vol. 8, pp. 467–482, 1960.

24. Purves, D., G. J. Augustine, and P. J. Fitzgerald, "Mechanoreceptors Specialized to Receive Tactile Information," in *Neuroscience*, Sunderland, Massachusetts: Sinauer Associates, 2nd ed., 2001.

25. Casserly, I., T. Thambipillai, M. Macken, and M. J. FitzGerald, "Innervation of the tylotrich-touch dome complexes in rat skin: changing patterns during postnatal development.," *Journal of Anatomy*, Vol. 185, pp. 553–563, 1994.

26. Severson, K. S., D. Xu, M. Van de Loo, L. Bai, D. D. Ginty, and D. H. O'Connor, "Active Touch and Self-Motion Encoding by Merkel Cell-Associated Afferents," *Neuron*, Vol. 94, no. 3, pp. 666–676, 2017.

27. Merians, A. S., H. Poizner, R. Boian, G. Burdea, and S. Adamovich, "Sensorimotor training in a virtual reality environment: does it improve functional recovery poststroke?," *Neurorehabilitation and Neural repair*, Vol. 20, pp. 252–67, 6 2006.

28. Pease, D. C., and T. A. Quilliam, "ELECTRON MICROSCOPY OF THE PACINIAN CORPUSCLE," *The Journal of Biophysical and Biochemical Cytology*, Vol. 3, no. 3, p. 331, 1957.

29. Spencer, P. S., and H. H. Schaumburg, "An ultrastructural study of the inner core of the Pacinian corpuscle," *Journal of Neurocytology*, Vol. 2, no. 2, pp. 217–235, 1973.

30. Paré, M., C. Behets, and O. Cornu, "Paucity of presumptive Ruffini corpuscles in the index finger pad of humans," *Journal of Comparative Neurology*, Vol. 456, pp. 260–266, 2 2003.

31. Lawson, R., "Morphological and biochemical cell types of sensory neurons," in *Sensory Neurons: Diversity, Development, and Plasticity* (Scott, S. A., ed.), pp. 27–59, Oxford: Oxford University Press, 1992.

32. Chen, T. L., C. Babiloni, A. Ferretti, M. G. Perrucci, G. L. Romani, P. M. Rossini, A. Tartaro, and C. Del Gratta, "Human secondary somatosensory cortex is involved in the processing of somatosensory rare stimuli: An fMRI study," *NeuroImage*, Vol. 40, pp. 1765–1771, 5 2008.

33. SWENSON, R. S., "Review of Clinical and Functional Neuroscience, chapter 9," *Educational Review Manual in Neurology*, 2006.

34. Joseph, R. G., "Parietal Area 5: Movement, Tactile Sensation and the Motor Areas," in *Neuropsychiatry, Neuropsychology, Clinical Neuroscience*, Academic Press, 2000.

35. Mountcastle, V. B., "Modality and topographic properties of single neurons of cat's somatic sensory cortex," *Journal of Neurophysiology*, Vol. 20, no. 4, pp. 408–434, 1957.

36. Mountcastle, V. B., "The columnar organization of the neocortex.," *Brain*, Vol. 120, pp. 701–722, 1997.

37. Hubel, D., and T. Wiesel, "Receptive fields, binocular interaction and functional architecture in the cat' s visual cortex," *The Journal of Physiology*, Vol. 160, no. 1, pp. 106–154, 1962.

38. Staiger, J. F., R. Kötter, K. Zilles, and H. J. Luhmann, "Laminar characteristics of functional connectivity in rat barrel cortex revealed by stimulation with caged-glutamate.," *Neuroscience Research*, Vol. 37, no. 1, pp. 49–58, 2000.

39. Katzel, D., B. V. Zemelman, C. Buetfering, M. Wolfel, and G. Miesenbock, "The columnar and laminar organization of inhibitory connections to neocortical excitatory cells," *Nature Neuroscience*, Vol. 14, no. 1, pp. 100–107, 2011.

40. Chapin, J. K., "Laminar differences in sizes, shapes, and response profiles of cutaneous receptive fields in the rat SI cortex.," *Experimental Brain Research*, Vol. 62, no. 3, pp. 549–59, 1986.

41. Chapin, J. K., M. Sadeq, and J. L. Guise, "Corticocortical connections within the primary somatosensory cortex of the rat," *The Journal of Comparative Neurology*, Vol. 263, no. 3, pp. 326–46, 1987.

42. Castro-alamancos, M. a., T. Bezdudnaya, C. Deleuze, F. David, S. Béhuret, G. Sadoc, H.-s. Shin, and N. Victor, "Properties of primary sensory (lemniscal) synapses in the ventrobasal thalamus and the relay of high-frequency sensory inputs.," *Journal of Neurophysiology*, Vol. 87, no. 2, pp. 946–953, 2002.

43. Castro-Alamancos, M. A., "Dynamics of sensory thalamocortical synaptic networks during information processing states," *Progress in Neurobiology*, Vol. 74, no. 4, pp. 213–247, 2004.

44. Fox, K., *Barrel Cortex*, Leiden: Cambridge University Press, 2008.

45. Lee, L. J., and R. S. Erzurumlu, "Altered parcellation of neocortical somatosensory maps in N-methyl-D-aspartate receptor-deficient mice," *Journal of Comparative Neurology*, Vol. 485, no. 1, pp. 57–63, 2005.

46. Tracey, D., "Somatosensory System," *The Rat Nervous System*, pp. 797–815, 1 2004.

47. Chapin, J. K., and C. S. Lin, "Mapping the body representation in the SI cortex of anesthetized and awake rats," *Journal of Comparative Neurology*, Vol. 229, no. 2, pp. 199–213, 1984.

48. Perry, E., M. Walker, J. Grace, and R. Perry, "Acetylcholine in mind: a neurotransmitter correlate of consciousness?," *Trends in Neurosciences*, Vol. 22, pp. 273–280, 6 1999.

49. Sarter, M., M. E. Hasselmo, J. P. Bruno, and B. Givens, "Unraveling the attentional functions of cortical cholinergic inputs: interactions between signal-driven and cognitive modulation of signal detection.," *Brain Research Reviews*, Vol. 48, pp. 98–111, 2 2005.

50. Klinkenberg, I., A. Sambeth, and A. Blokland, "Acetylcholine and attention.," *Behavioural Brain Research*, Vol. 221, pp. 430–42, 8 2011.

51. Arnold, H. M., J. A. Burk, E. M. Hodgson, M. Sarter, and J. P. Bruno, "Differential cortical acetylcholine release in rats performing a sustained attention task versus behavioral control tasks that do not explicitly tax attention," *Neuroscience*, Vol. 114, no. 2, pp. 451–460, 2002.

52. Himmelheber, A. M., M. Sarter, and J. P. Bruno, "Increases in cortical acetylcholine release during sustained attention performance in rats.," *Cognitive Brain Research*, Vol. 9, pp. 313–325, 6 2000.

53. Himmelheber, A. M., M. Sarter, and J. P. Bruno, "The effects of manipulations of attentional demand on cortical acetylcholine release.," *Cognitive Brain Research*, Vol. 12, pp. 353–70, 12 2001.

54. McGaughy, J., and M. Sarter, "Sustained attention performance in rats with intracortical infusions of 192 IgG-saporin-induced cortical cholinergic deafferentation: effects of physostigmine and FG 7142.," *Behavioral Neuroscience*, Vol. 112, pp. 1519–1525, 12 1998.

55. Sarter, M., J. P. Bruno, and J. Turchi, "Basal forebrain afferent projections modulating cortical acetylcholine, attention, and implications for neuropsychiatric disorders," in *Annals of the New York Academy of Sciences*, Vol. 877, pp. 368–382, 6 1999.

56. Turchi, J., and M. Sarter, "Cortical acetylcholine and processing capacity: Effects of cortical cholinergic deafferentation on crossmodal divided attention in rats," *Cognitive Brain Research*, Vol. 6, pp. 147–158, 10 1997.

57. Oldford, E., and M. Castro-Alamancos, "Input-specific effects of acetylcholine on sensory and intracortical evoked responses in the "barrel cortex" in vivo," *Neuroscience*, Vol. 117, pp. 769–778, 3 2003.

58. Levin, E. D., F. J. McClernon, and A. H. Rezvani, "Nicotinic effects on cognitive function: behavioral characterization, pharmacological specification, and anatomic localization.," *Psychopharmacology*, Vol. 184, pp. 523–39, 3 2006.

59. Poranen, A., and J. Hyvarinen, "Effects of Attention on Multiunit Responses to Vibration in the Somatosensory regions of the monkey's brain," *Electroencephalography and clinical neurophysiology*, Vol. 53, pp. 525–537, 1982.

60. Hyvärinen, J., A. Poranen, and Y. Jokinen, "Influence of attentive behavior on neuronal responses to vibration in primary somatosensory cortex of the monkey.," *Journal of Neurophysiology*, Vol. 43, pp. 870–882, 1980.

61. Hsiao, S. S., D. M. O'Shaughnessy, and K. O. Johnson, "Effects of selective attention on spatial form processing in monkey primary and secondary somatosensory cortex.," *Journal of Neurophysiology*, Vol. 70, pp. 444–447, 1993.

62. Steinmetz, P. N., A. Roy, P. J. Fitzgerald, S. S. Hsiao, K. O. Johnson, and E. Niebur, "Attention modulates synchronized neuronal firing in primate somatosensory cortex.," *Nature*, Vol. 404, pp. 187–190, 2000.

63. Burton, H., R. J. Sinclair, S. G. Hon, J. R. Pruett, and K. C. Whang, "Tactile-spatial and cross-modal attention effects in the second somatosensory and 7b cortical areas of rhesus monkeys," *Somatosensory and Motor Research*, Vol. 14, no. 4, pp. 237–267, 1997.

64. McKenna, T. M., J. H. Ashe, G. K. Hui, and N. M. Weinberger, "Muscarinic agonists modulate spontaneous and evoked unit discharge in auditory cortex of cat.," *Synapse*, Vol. 2, no. 1, pp. 54–68, 1988.

65. Sillito, A. M., and J. A. Kemp, "Cholinergic modulation of the functional organization of the cat visual cortex.," *Brain Research*, Vol. 289, pp. 143–155, 1983.

66. Sato, H., Y. Hata, H. Masui, and T. Tsumoto, "A functional role of cholinergic innervation to neurons in the cat visual cortex.," *Journal of Neurophysiology*, Vol. 58, pp. 765–780, 1987.

67. Lamour, Y., P. Dutar, A. Jobert, and R. W. Dykes, "An iontophoretic study of single somatosensory neurons in rat granular cortex serving the limbs: a laminar analysis of glutamate and acetylcholine effects on receptive-field properties," *Journal of Neurophysiology*, Vol. 60, no. 2, pp. 725–750, 1988.

68. Metherate, R., N. Tremblay, and R. W. Dykes, "The Effects of Acetylcholine on Response Properties of Cat Somatosensory Cortical Neurons," *Journal of Neurophysiology*, Vol. 59, no. 4, pp. 1231–1252, 1988.

69. Donoghue, J. P., and K. L. Carroll, "Cholinergic modulation of sensory responses in rat primary somatic sensory cortex," *Brain Research*, Vol. 408, pp. 367–371, 1987.

70. Tremblay, N., R. A. Warren, and R. W. Dykes, "Electrophysiological studies of acetylcholine and the role of the basal forebrain in the somatosensory cortex of the cat. I. Cortical neurons excited by glutamate.," *Journal of Neurophysiology*, Vol. 64, pp. 1199–1211, 1990.

71. Tremblay, N., R. A. Warren, and R. W. Dykes, "Electrophysiological studies of acetylcholine and the role of the basal forebrain in the somatosensory cortex of the cat. II. Cortical neurons excited by somatic stimuli.," *Journal of Neurophysiology*, Vol. 64, pp. 1212–1222, 1990.

72. Descarries, L., K. Krnjevic, and M. Steriade, *Acetylcholine in the Cerebral Cortex*, Elsevier Inc., 2003.

73. Verdier, D., and R. W. Dykes, "Long-term cholinergic enhancement of evoked potentials in rat hindlimb somatosensory cortex displays characteristics of long-term potentiation.," *Experimental Brain Research*, Vol. 137, pp. 71–82, 2001.

74. Torres, E. M., T. A. Perry, A. Blockland, L. S. Wilkinson, R. G. Wiley, D. A. Lappi, and S. B. Dunnet, "Behavioural, histochemical and biochemical consequences of selective immunolesions in discrete regions of the basal forebrain cholinergic system.," *Neuroscience*, Vol. 63, pp. 95–122, 1994.

75. Herrero, J. L., M. J. Roberts, L. S. Delicato, M. A. Gieselmann, P. Dayan, and A. Thiele, "Acetylcholine contributes through muscarinic receptors to attentional modulation in V1.," *Nature*, Vol. 454, pp. 1110–1114, 2008.

76. Herremans, A. H. J., T. H. Hijzen, P. F. E. Welborn, B. Olivier, and J. L. Slangen, "Effects of infusion of cholinergic drugs into the prefrontal cortex area on delayed matching to position performance in the rat," *Brain Research*, Vol. 711, pp. 102–111, 1996.

77. Fournier, G. N., K. Semba, and D. D. Rasmusson, "Modality- and region-specific acetylcholine release in the rat neocortex.," *Neuroscience*, Vol. 126, pp. 257–62, 1 2004.

78. Wang, N., A. Orr-Urtreger, and A. D. Korczyn, "The role of neuronal nicotinic acetylcholine receptor subunits in autonomic ganglia: Lessons from knockout mice," *Progress in Neurobiology*, Vol. 68, no. 5, pp. 341–360, 2002.

79. Clarke, P. B., R. D. Schwartz, S. M. Paul, C. B. Pert, and A. Pert, "Nicotinic binding in rat brain: autoradiographic comparison of [3H]acetylcholine, [3H]nicotine, and [125I]-alpha-bungarotoxin.," *The Journal of Neuroscience*, Vol. 5, pp. 1307–1315, 5 1985.

80. Tribollet, E., D. Bertrand, A. Marguerat, and M. Raggenbass, "Comparative distribution of nicotinic receptor subtypes during development, adulthood and aging: an autoradiographic study in the rat brain.," *Neuroscience*, Vol. 124, pp. 405–420, 1 2004.

81. Houser, C. R., G. D. Crawford, P. M. Salvaterra, and J. E. Vaughn, "Immunocytochemical localization of choline acetyltransferase in rat cerebral cortex: a study of cholinergic neurons and synapses.," *The Journal of Comparative Neurology*, Vol. 234, pp. 17–34, 4 1985.

82. Sahin, M., W. D. Bowen, and J. P. Donoghue, "Location of nicotinic and muscarinic cholinergic and u-opiate receptors in rat cerebral neocortex: Evidence from thalamic and cortical lesions," *Brain Research*, Vol. 579, pp. 135–147, 1992.

83. Levy, R. B., A. D. Reyes, and C. Aoki, "Nicotinic and muscarinic reduction of unitary excitatory postsynaptic potentials in sensory cortex; dual intracellular recording in vitro.," *Journal of Neurophysiology*, Vol. 95, pp. 2155–66, 4 2006.

84. Christophe, E., A. Roebuck, J. F. Staiger, D. J. Lavery, E. Audinat, A. J. Lee, G. Wang, X. Jiang, S. M. Johnson, E. T. Hoang, R. L. Stornetta, M. P. Beenhakker, Y. Shen, J. J. Zhu, A. Brombas, L. N. Fletcher, and S. R. Williams, "Two Types of Nicotinic Receptors Mediate an Excitation of Neocortical Layer I Interneurons," *Journal of Neurophysiology*, Vol. 88, pp. 1318–1327, 2002.

85. Xiang, Z., J. R. Huguenard, and D. A. Prince, "Cholinergic switching within neocortical inhibitory networks.," *Science*, Vol. 281, pp. 985–988, 8 1998.

86. Nuñez, A., S. Domínguez, W. Buño, and D. Fernández de Sevilla, "Cholinergic-mediated response enhancement in barrel cortex layer V pyramidal neurons.," *Journal of Neurophysiology*, Vol. 108, pp. 1656–68, 9 2012.

87. Albuquerque, E. X., E. F. R. Pereira, M. Alkondon, and S. W. Rogers, "Mammalian Nicotinic Acetylcholine Receptors: From Structrue to Function," *Physiology Review*, Vol. 89, no. 1, pp. 73–120, 2009.

88. Levey, A. I., C. A. Kitt, W. F. Simonds, D. L. Price, and M. R. Brann, "Identification and localization of muscarinic acetylcholine receptor proteins in brain with subtype-specific antibodies.," *The Journal of Neuroscience*, Vol. 11, pp. 3218–3226, 1991.

89. Hammer, R., C. P. Berrie, N. J. Birdsall, A. S. Burgen, and E. C. Hulme, "Pirenzepine distinguishes between different subclasses of muscarinic receptors.," *Nature*, Vol. 283, no. 5742, pp. 90–92, 1980.

90. Buckley, N. J., T. I. Bonner, and M. R. Brann, "Localization of a Family of Muscarinic Receptor mRNAs in Rat Brain," *The Journal of Neuroscience*, Vol. 8, no. 12, pp. 4646–4652, 1988.

91. Bonner, T. I., N. J. Buckley, A. C. Young, and M. R. Brann, "Identification of a family of muscarinic acetylcholine receptor genes," *Science*, Vol. 237, pp. 527–532, 7 1987.

92. Zee, A. V. D., C. Streefland, A. D. Strosberg, H. Schrder, and P. G. M. Luiten, "Visualization of cholinoceptive neurons in the rat neocortex : colocalization of muscarinic and nicotinic acetylcholine receptors," *Molecular Brain Research*, Vol. 14, pp. 326–336, 1992.

93. Parikh, V., and M. Sarter, "Cholinergic Mediation of Attention," *Annals of the New York Academy of Sciences*, Vol. 1129, pp. 225–235, 2008.

94. Tian, M. K., C. D. C. Bailey, and E. K. Lambe, "Cholinergic excitation in mouse primary vs. associative cortex: region-specific magnitude and receptor balance.," *The European Journal of Neuroscience*, Vol. 40, pp. 2608–18, 8 2014.

95. Levy, R. B., A. D. Reyes, and C. Aoki, "Cholinergic modulation of local pyramid-interneuron synapses exhibiting divergent short-term dynamics in rat sensory cortex.," *Brain research*, Vol. 1215, pp. 97–104, 6 2008.

96. Levin, E. D., S. R. McGurk, D. South, and L. L. Butcher, "Effects of combined muscarinic and nicotinic blockade on choice accuracy in the radial-arm maze.," *Behavioral and Neural Biology*, Vol. 51, pp. 270–277, 3 1989.

97. Levin, E. D., J. E. Rose, S. R. McGurk, and L. L. Butcher, "Characterization of the cognitive effects of combined muscarinic and nicotinic blockade.," *Behavioral and Neural Biology*, Vol. 53, pp. 103–112, 1 1990.

98. Mesulam, M. M., E. J. Mufson, B. H. Wainer, and A. I. Levey, "Central cholinergic pathways in the rat: an overview based on an alternative nomenclature (Ch1-Ch6).," *Neuroscience*, Vol. 10, pp. 1185–1201, 1983.

99. Mechawar, N., C. Cozzari, L. Descarries, and B. Cellulare, "Cholinergic Innervation in Adult Rat Cerebral Cortex : A Quantitative," *The Journal of Comparative Neurology*, Vol. 428, no. March, pp. 305–318, 2000.

100. Mash, D. C., W. F. White, and M. M. Mesulam, "Distribution of muscarinic receptor subtypes within architectonic subregions of the primate cerebral cortex.," *The Journal of Comparative Neurology*, Vol. 278, pp. 265–74, 12 1988.

101. Kristt, D. A., R. A. McGowan, N. Martin-MacKinnon, and J. Solomon, "Basal forebrain innervation of rodent neocortex: Studies using acetylcholinesterase histochemistry, Golgi and lesion strategies," *Brain Research*, Vol. 337, no. 1, pp. 19–39, 1985.

102. Mesulam, M. M., and E. J. Mufson, "Neural inputs into the nucleus basalis of the substantia innominata (ch4) in the rhesus monkey," *Brain*, Vol. 107, no. 1, pp. 253–274, 1984.

103. Russchen, F. T., D. G. Amaral, and J. L. Price, "The afferent connections of the substantia innominata in the monkey, Macaca fascicularis.," *The Journal of Comparative Neurology*, Vol. 242, no. 1, pp. 1–27, 1985.

104. Baluch, F., and L. Itti, "Mechanisms of top-down attention," *Trends in Neurosciences*, Vol. 34, no. 4, pp. 210–224, 2011.

105. Gilbert, C. D., and M. Sigman, "Brain States: Top-Down Influences in Sensory Processing," *Neuron*, Vol. 54, no. 5, pp. 677–696, 2007.

106. Güçlü, B., S. J. Bolanowski, and L. Pawson, "End-to-end linkage (EEL) clustering algorithm: A study on the distribution of Meissner corpuscles in the skin," *Journal of Computational Neuroscience*, Vol. 15, no. 1, pp. 19–28, 2003.

107. Greenspan, J. D., and S. J. Bolanowski, "The psychophysics of tactile perception and its peripheral physiological basis," in *Pain and touch* (Kruger, L., ed.), pp. 25–104, San Diego, CA: Acedemic Press, 1996.

108. Güçlü, B., G. K. Mahoney, L. J. Pawson, A. K. Pack, R. L. Smith, and S. J. Bolanowski, "Localization of Merkel cells in the monkey skin: an anatomical model," *Somatosensory and Motor Research*, Vol. 25, no. 2, pp. 123–138, 2008.

109. Jones, L. A., and S. J. Lederman, *Human Hand Function*, Oxford University Press, 2006.

110. Mountcastle, V. B., *The Sensory Hand: neural mechanisms of somatic sensation*, Cambridge,Mass.: Harvard University Press, 2005.

111. Feldmeyer, D., M. Brecht, F. Helmchen, C. C. Petersen, J. F. Poulet, J. F. Staiger, H. J. Luhmann, and C. Schwarz, "Barrel cortex function," 2013.

112. Dykes, R. W., and Y. Lamour, "An electrophysiological study of single somatosensory neurons in rat granular cortex serving the limbs: a laminar analysis," *Journal of Neurophysiology*, Vol. 60, pp. 703–724, 6 1988.

113. Moxon, K. A., L. L. Hale, J. Aguilar, and G. Foffani, "Responses of infragranular neurons in the rat primary somatosensory cortex to forepaw and hindpaw tactile stimuli," *Neuroscience*, Vol. 156, no. 4, pp. 1083–1092, 2008.

114. Leem, J. W., W. D. Willis, and J. M. Chung, "Cutaneous sensory receptors in the rat foot," *Journal of Neurophysiology*, Vol. 69, no. 5, pp. 1684–1699, 1993.

115. Leem, J. W., W. D. Willis, S. C. Weller, and J. M. Chung, "Differential activation and classification of cutaneous afferents in the rat," *Journal of Neurophysiology*, Vol. 70, no. 6, pp. 2411–2424, 1993.

116. Devecioğlu, I., and B. Güçlü, "Asymmetric response properties of rapidly adapting mechanoreceptive fibers in the rat glabrous skin," *Somatosensory and Motor Research*, Vol. 30, no. 1, pp. 16–29, 2013.

117. Kolb, B., and R. C. Tees, *The cerebral cortex of the rat*, Cambridge,Mass.: The MIT Press, 1990.

118. Güçlü, B., and S. J. Bolanowski, "Distribution of the intensity-characteristic parameters of cat rapidly adapting mechanoreceptive fibers," *Somatosensory & Motor Research*, Vol. 20, no. 2, pp. 149–155, 2003.

119. Güçlü, B., and S. J. Bolanowski, "Frequency responses of cat rapidly adapting mechanoreceptive fibers," *Somatosensory and Motor Research*, Vol. 20, no. 3-4, pp. 249–263, 2003.

120. Güçlü, B., and S. J. Bolanowski, "Probability of stimulus detection in a model population of rapidly adapting fibers," *Neural Computation*, Vol. 16, no. 1, pp. 39–58, 2004.

121. Güçlü, B., and S. J. Bolanowski, "Tristate Markov Model for the Firing Statistics of Rapidly-Adapting Mechanoreceptive Fibers," *Journal of Computational Neuroscience*, Vol. 17, pp. 107–126, 2004.

122. Güçlü, B., "Deviation from Weber's law in the Non-Pacinian I tactile channel: A psychophysical and simulation study of intensity discrimination," *Neural Computation*, Vol. 19, pp. 2638–2664, 2007.

123. Güçlü, B., and S. M. Dinçer, "Neural coding in the Non-Pacinian i tactile channel: A psychophysical and simulation study of magnitude estimation," *Somatosensory and Motor Research*, Vol. 30, pp. 1–15, 3 2013.

124. Zilles, K., "Anatomy of the neocortex: cytoarchitecture and myeloarchitecture," in *The cerebral cortex of the rat* (Kolb, B., and R. C. Tees, eds.), pp. 77–112, Cambridge: MIT Press, 1990.

125. Chapin, J. K., and C. S. Lin, "The somatic sensory cortex of the rat," in *The cerebral cortex of the rat* (Kolb, B., and R. C. Tees, eds.), pp. 341–380, Cambridge: MIT Press, 1990.

126. Woolsey, T. A., and H. Van der Loos, "The structural organization of layer IV in the somatosensory region (SI) of mouse cerebral cortex. The description of a cortical field composed of discrete cytoarchitectonic units.," *Brain Research*, Vol. 17, pp. 205–42, 1 1970.

127. Angel, A., and R. N. Lemon, "Sensorimotor cortical representation in the rat and the role of the cortex in the production of sensory myoclonic jerks.," *The Journal of Physiology*, Vol. 248, pp. 465–88, 6 1975.

128. Armstrong James, M., "The functional status and columnar organization of single cells responding to cutaneous stimulation in neonatal rat somatosensory cortex S1.," *The Journal of Physiology*, Vol. 246, pp. 501–538, 4 1975.

129. Haupt, S. S., F. Spengler, R. Husemann, and H. R. Dinse, "Receptive field scatter, topography and map variability in different layers of the hindpaw representation of rat somatosensory cortex," *Experimental Brain Research*, Vol. 155, pp. 485–499, 4 2004.

130. Tracey, D., "Ascending and descending pathways in the spinal cord," in *The Rat Nervous System* (Paxinos, G., ed.), ch. 7, pp. 149–164, San Diego, CA: Elsevier Academic Press, 3 ed., 2004.

131. McAllister, J. P., and J. Wells, "The structural organization of the ventral posterolateral nucleus in the rat," *Journal of Comparative Neurology*, Vol. 197, no. 2, pp. 271–301, 1981.

132. Shin, H. C., and J. K. Chapin, "Mapping the effects of motor cortex stimulation on single neurons in the dorsal column nuclei in the rat: Direct responses and afferent modulation," *Brain Research Bulletin*, Vol. 22, no. 2, pp. 245–252, 1989.

133. Keller, A., E. L. White, and P. B. Cipolloni, "The identification of thalamocortical axon terminals in barrels of mouse Sml cortex using immunohistochemistry of anterogradely transported lectin (Phaseolus vulgaris-leucoagglutinin)," *Brain Research*, Vol. 343, no. 1, pp. 159–165, 1985.

134. Agmon, A., and B. W. Connors, "Correlation between intrinsic firing patterns and thalamocortical synaptic responses of neurons in mouse barrel cortex.," *The Journal of Neuroscience*, Vol. 12, no. 1, pp. 319–329, 1992.

135. Connors, B. W., and M. J. Gutnick, "Intrinsic firing patterns of diverse neocortical neurons," *Trends in Neurosciences*, Vol. 13, no. 3, pp. 99–104, 1990.

136. Schubert, D., J. F. Staiger, N. Cho, R. Kötter, K. Zilles, and H. J. Luhmann, "Layer-specific intracolumnar and transcolumnar functional connectivity of layer V pyramidal cells in rat barrel cortex.," *The Journal of Neuroscience*, Vol. 21, pp. 3580–92, 5 2001.

137. Beierlein, M., J. R. Gibson, and B. W. Connors, "Two dynamically distinct inhibitory networks in layer 4 of the neocortex.," *Journal of Neurophysiology*, Vol. 90, pp. 2987–3000, 7 2003.

138. Porter, J. T., C. K. Johnson, and A. Agmon, "Diverse types of interneurons generate thalamus-evoked feedforward inhibition in the mouse barrel cortex.," *The Journal of Neuroscience*, Vol. 21, pp. 2699–710, 4 2001.

139. Eaton, S. A., and T. E. Salt, "Role of N-methyl-D-aspartate and metabotropic glutamate receptors in corticothalamic excitatory postsynaptic potentials in vivo," *Neuroscience*, Vol. 73, pp. 1–5, 1996.

140. Salin, P. A., and D. A. Prince, "Electrophysiological mapping of GABAA receptor-mediated inhibition in adult rat somatosensory cortex," *Journal of Neurophysiology*, Vol. 75, no. 4, pp. 1589–1600, 1996.

141. Cotman, C. W., D. T. Monaghan, and O. P. Ottersen, "Anatomical organization of excitatory amino acid receptors and their pathways," *Trends in Neurosciences*, Vol. 10, no. 7, pp. 273–280, 1987.

142. Monaghan, D. T., R. Bridges, and C. W. Cotman, "The Excitatory Amino Acid Receptors: Their Classes, Pharmacology, and Distinct Properties in the Function of the Central Nervous System," *Annual Review Pharmacology and Toxicology*, Vol. 29, pp. 365–402, 1989.

143. Jaarsma, D., J. B. Sebens, and J. Korf, "Localization of NMDA and AMPA receptors in rat barrel field," *Neuroscience Letters*, Vol. 133, pp. 233–236, 12 1991.

144. Zhu, J. J., and B. W. Connors, "Intrinsic Firing Patterns and Whisker-Evoked Synaptic Responses of Neurons in the Rat Barrel Cortex," *Journal of Neurophysiology*, Vol. 81, pp. 1171–1183, 3 1999.

145. Gabernet, L., S. P. Jadhav, D. E. Feldman, M. Carandini, and M. Scanziani, "Somatosensory integration controlled by dynamic thalamocortical feed-forward inhibition," *Neuron*, Vol. 48, no. 2, pp. 315–327, 2005.

146. Armstrong-James, M., E. Welker, and C. A. Callahan, "The contribution of NMDA and non-NMDA receptors to fast and slow transmission of sensory information in the rat SI barrel cortex.," *The Journal of Neuroscience*, Vol. 13, no. 5, pp. 2149–2160, 1993.

147. Wilent, W. B., and D. Contreras, "Synaptic Responses to Whisker Deflections in Rat Barrel Cortex as a Function of Cortical Layer and Stimulus Intensity," *Journal of Neuroscience*, Vol. 24, pp. 3985–3998, 4 2004.

148. Ling, D. S., and L. S. Benardo, "Recruitment of GABAA inhibition in rat neocortex is limited and not NMDA dependent," *Journal of Neurophysiology*, Vol. 74, no. 6, pp. 2329–2335, 1995.

149. Hicks, T. P., and R. W. Dykes, "Receptive field size for certain neurons in primary somatosensory cortex is determined by GABA-mediated intracortical inhibition," *Brain Research*, Vol. 274, no. 1, pp. 160–164, 1983.

150. Dykes, R. W., R. Metherate, T. P. Hicks, P. Landry, R. Metherate, and T. P. Hicks, "Functional Role of GABA in Cat Primary Somatosensory Cortex : Shaping Receptive Fields of Cortical Neurons," *Journal of Neurophysiology*, Vol. 52, pp. 1066–1093, 12 1984.

151. Alloway, K. D., and H. Burton, "Differential effects of GABA and bicuculline on rapidly- and slowly-adapting neurons in primary somatosensory cortex of primates," *Experimental Brain Research*, Vol. 85, pp. 598–610, 1991.

152. Alloway, K., P. Rosenthal, and H. Burton, "Quantitative measurements of receptive field changes during antagonism of GABAergic transmission in primary somatosensory cortex of cats," *Experimental Brain Research*, Vol. 78, pp. 514–532, 12 1989.

153. Kyriazi, H. T., G. E. Carvell, J. C. Brumberg, and D. J. Simons, "Quantitative effects of GABA and bicuculline methiodide on receptive field properties of neurons in real and simulated whisker barrels.," *Journal of Neurophysiology*, Vol. 75, no. 2, pp. 547–560, 1996.

154. Kyriazi, H., G. E. Carvell, J. C. Brumberg, and D. J. Simons, "Laminar differences in bicuculline methiodide's effects on cortical neurons in the rat whisker/barrel system," *Somatosensory and Motor Research*, Vol. 15, pp. 146–156, 1 1998.

155. Lo, F.-S., F. Akkentli, V. Tsytsarev, and R. S. Erzurumlu, "Functional significance of cortical NMDA receptors in somatosensory information processing," *Journal of Neurophysiology*, Vol. 110, pp. 2627–2636, 12 2013.

156. Salt, T. E., "Mediation of thalamic sensory input by both NMDA receptors and non-NMDA receptors," *Nature*, Vol. 322, no. 6076, pp. 263–265, 1986.

157. Vahle-Hinz, C., O. Detsch, M. Siemers, and E. Kochs, "Contributions of GABAergic and glutamatergic mechanisms to isoflurane-induced suppression of thalamic somatosensory information transfer," *Experimental Brain Research*, Vol. 176, no. 1, pp. 159–172, 2007.

158. Duncan, G. H., D. A. Dreyer, T. M. McKenna, and B. L. Whitsel, "Dose- and time-dependent effects of ketamine on SI neurons with cutaneous receptive fields.," *Journal of Neurophysiology*, Vol. 47, pp. 677–99, 4 1982.

159. Antkowiak, B., "Different actions of general anesthetics on the firing patterns of neocortical neurons mediated by the GABA(A) receptor," *Anesthesiology*, Vol. 91, pp. 500–511, 8 1999.

160. Whitsel, B. L., O. Favorov, K. A. Delemos, C. Lee, M. Tommerdahl, G. K. Essick, and B. Nakhle, "SI neuron response variability is stimulus tuned and NMDA receptor dependent.," *Journal of Neurophysiology*, Vol. 81, pp. 2988–3006, 6 1999.

161. Gil, Z., and Y. Amitai, "Adult thalamocortical transmission involves both NMDA and non-NMDA receptors," *Journal of Neurophysiology*, Vol. 76, no. 4, pp. 2547–2553, 1996.

162. Güçlü, B., "Vibrotactile intensity coding by cortical neurons from the hindpaw representation in the rat SI cortex," in *Society for Neuroscience Annual Meeting*, (Chicago,IL,USA), 2015.

163. Vardar, B., and B. Güçlü, "Effects of bicuculline and NMDA on the vibrotactile responses of cortical neurons in the rat SI cortex," in *Society for Neuroscience Annual Meeting*, (Chicago,IL,USA), 2015.

164. Vardar, B., and B. Güçlü, "Modeling the vibrotactile responses of excitatory and inhibitory neurons in the hindpaw representation of rat SI cortex," in *Society for Neuroscience Annual Meeting*, (San Diego, CA, USA), 2016.

165. Chapin, J. K., B. D. Waterhouse, and D. J. Woodward, "Differences in cutaneous sensory response properties of single somatosensory cortical neurons in awake and halothane anesthetized rats," *Brain Research Bulletin*, Vol. 6, pp. 63–70, 1 1981.

166. Gibson, J. M., and W. I. Welker, "Quantitative studies of stimulus coding in first-order vibrissa afferents of rats. 2. Adaptation and coding of stimulus parameters," *Somatosensory Research*, Vol. 1, no. 2, pp. 95–117, 1983.

167. Simons, D. J., "Response properties of vibrissa units in rat SI somatosensory neocortex," *Journal of Neurophysiology*, Vol. 41, no. 3, pp. 798–820, 1978.

168. Simons, D. J., and G. E. Carvell, "Thalamocortical response transformation in the rat vibrissa/barrel system.," *Journal of Neurophysiology*, Vol. 61, no. 2, pp. 311–30, 1989.

169. Shoykhet, Donald Doherty, D. J. M., "Coding of deflection velocity and amplitude by whisker primary afferent neurons: implications for higher level processing," *Somatosensory and Motor Research*, Vol. 17, no. 2, pp. 171–180, 2000.

170. Garabedian, C. E., S. R. Jones, M. M. Merzenich, A. Dale, and C. I. Moore, "Band-Pass Response Properties of Rat SI Neurons," *Journal of Neurophysiology*, Vol. 90, pp. 1379–1391, 5 2003.

171. Arabzadeh, E., R. S. Petersen, and M. E. Diamond, "Encoding of whisker vibration by rat barrel cortex neurons: implications for texture discrimination.," *The Journal of Neuroscience*, Vol. 23, no. 27, pp. 9146–9154, 2003.

172. Zhang, M., and K. D. Alloway, "Stimulus-induced intercolumnar synchronization of neuronal activity in rat barrel cortex: a laminar analysis," *Journal of Neurophysiology*, Vol. 92, no. 3, pp. 1464–1478, 2004.

173. Paxinos, G., and C. Watson, *The Rat Brain in Stereotaxic Coordinates*, Academic Press, 3 ed., 1997.

174. Haidarliu, S., D. Shulz, and E. Ahissar, "A multi-electrode array for combined microiontophoresis and multiple single-unit recordings," *Journal of Neuroscience Methods*, Vol. 56, pp. 125–31, 2 1995.

175. Haidarliu, S., R. Sosnik, and E. Ahissar, "Simultaneous multi-site recordings and iontophoretic drug and dye applications along the trigeminal system of anesthetized rats," *Journal of Neuroscience Methods*, Vol. 94, pp. 27–40, 12 1999.

176. Akaoka, H., C. F. Saunier, K. Chergui, P. Charléty, M. Buda, and G. Chouvet, "Combining in vivo volume-controlled pressure microejection with extracellular unit recording," *Journal of Neuroscience Methods*, Vol. 42, pp. 119–128, 4 1992.

177. Hupé, J. M., G. Chouvet, and J. Bullier, "Spatial and temporal parameters of cortical inactivation by GABA.," *Journal of Neuroscience Methods*, Vol. 86, pp. 129–43, 1 1999.

178. Paul, C., B. Beltz, and J. Berger-Sweeney, *Discovering Neurons: The Experimental Basis of Neuroscience*, New York: Cold Spring Harbor Laboratory Press, 1997.

179. Cohen, J. C., J. C. Makous, and S. J. Bolanowski, "Under which conditions do the skin and probe decouple during sinusoidal vibrations?," *Experimental Brain Research*, Vol. 129, no. 2, pp. 211–217, 1999.

180. Güçlü, B., "Vibrotactile Responses of Cortical Neurons from Hindpaw Representation in the rat SI Cortex," in *Society for Neuroscience Annual Meeting*, (Washington, DC, USA), 2013.

181. Mountcastle, V. B., W. H. Talbot, H. Sakata, and J. Hyvarinen, "Cortical Neuronal mechanisms in flutter-vibration studied in unanethetized monkeys. Neuronal periodicity and frequency discrimination," *Journal of Neurophysiology*, Vol. 32, pp. 452–484, 1969.

182. Whitsel, B. L., E. F. Kelly, K. A. Delemos, M. Xu, and P. M. Quibrera, "Stability of rapidly adapting afferent entrainment vs responsivity," *Somatosensory and Motor Research*, Vol. 17, no. 1, pp. 13–31, 2000.

183. Grün, S., and S. Rotter, *Analysis of Parallel Spike Trains*, New York: Springer, 7 ed., 2010.

184. van Hemmen, J. L., A. Longtin, and A. N. Vollmayr, "Testing resonating vector strength: auditory system, electric fish, and noise.," *Chaos*, Vol. 21, p. 047508, 12 2011.

185. Berens, P., "CircStat: A MATLAB toolbox for circular statistics," *Journal of Statistical Software*, Vol. 31, no. 10, pp. 1–21, 2009.

186. Ferrington, D., and M. Rowe, "Differential contributions to coding of cutaneous vibratory information by cortical somatosensory areas I and II," *Journal of Neurophysiology*, Vol. 43, no. 2, pp. 310–331, 1980.

187. Salinas, E., A. Hernandez, A. Zainos, R. Romo, A. Hernández, A. Zainos, and R. Romo, "Periodicity and firing rate as candidate neural codes for the frequency of vibrotactile stimuli," *Journal of Neuroscience*, Vol. 20, no. 14, pp. 5503–5515, 2000.

188. Whitsel, B. L., E. F. Kelly, M. Xu, M. Tommerdahl, and M. Quibrera, "Frequency-dependent response of SI RA-class neurons to vibrotactile stimulation of the receptive field.," *Somatosensory and Motor Research*, Vol. 18, no. 4, pp. 263–285, 2001.

189. Pei, Y.-C., P. V. Denchev, S. S. Hsiao, J. C. Craig, and S. J. Bensmaia, "Convergence of submodality-specific input onto neurons in primary somatosensory cortex," *Journal of Neurophysiology*, Vol. 102, pp. 1843–1853, 9 2009.

190. Harvey, M. A., H. P. Saal, J. F. Dammann, and S. J. Bensmaia, "Multiplexing Stimulus Information through Rate and Temporal Codes in Primate Somatosensory Cortex," *PLoS Biology*, Vol. 11, p. e1001558, 5 2013.

191. Foffani, G., B. Tutunculer, and K. A. Moxon, "Role of spike timing in the forelimb somatosensory cortex of the rat," *Journal of Neuroscience*, Vol. 24, no. 33, pp. 7266–7271, 2004.

192. Hartings, J. A., and D. J. Simons, "Thalamic relay of afferent responses to 1- to 12-Hz whisker stimulation in the rat.," *Journal of Neurophysiology*, Vol. 80, pp. 1016–1019, 1998.

193. Diamond, M. E., M. Armstrong James, M. J. Budway, and F. F. Ebner, "Somatic sensory responses in the rostral sector of the posterior group (POm) and in the ventral posterior medial nucleus (VPM) of the rat thalamus: Dependence on the barrel field cortex," *The Journal of Comparative Neurology*, Vol. 319, pp. 66–84, 5 1992.

194. Ahissar, E., R. Sosnik, and S. Haidarliu, "Transformation from temporal to rate coding in a somatosensory thalamocortical pathway.," *Nature*, Vol. 406, no. 6793, pp. 302–306, 2000.

195. Stüttgen, M. C., and C. Schwarz, "Integration of Vibrotactile Signals for Whisker-Related Perception in Rats Is Governed by Short Time Constants: Comparison of Neurometric and Psychometric Detection Performance," *Journal of Neuroscience*, Vol. 30, no. 6, pp. 2060–2069, 2010.

196. Fanselow, E. E., and M. A. Nicolelis, "Behavioral modulation of tactile responses in the rat somatosensory system.," *The Journal of Neuroscience*, Vol. 19, no. 17, pp. 7603–7616, 1999.

197. Derdikman, D., C. Yu, S. Haidarliu, K. Bagdasarian, A. Arieli, and E. Ahissar, "Layer-Specific Touch-Dependent Facilitation and Depression in the Somatosensory Cortex during Active Whisking," *Journal of Neuroscience*, Vol. 26, pp. 9538–9547, 9 2006.

198. Poggio, G. F., and V. B. Mountcastle, "The Functional Properties Of Ventrobasal Thalamic Neurons Studied In Unanestithetized Monkeys.," *Journal of Neurophysiology*, Vol. 26, no. 5, pp. 775–806, 1963.

199. Diamond, M. E., M. Armstrong-James, and F. F. Ebner, "Somatic sensory responses in the rostral sector of the posterior group (POm) and in the ventral posterior medial nucleus (VPM) of the rat thalamus," *Journal of Comparative Neurology*, Vol. 318, pp. 462–476, 4 1992.

200. Swadlow, H. A., and A. G. Gusev, "The influence of single VB thalamocortical impulses on barrel columns of rabbit somatosensory cortex.," *Journal of Neurophysiology*, Vol. 83, no. 5, pp. 2802–13, 2000.

201. Bruno, R. M., and D. J. Simons, "Feedforward mechanisms of excitatory and inhibitory cortical receptive fields.," *Journal of Neuroscience*, Vol. 22, no. 24, pp. 10966–10975, 2002.

202. Kyriazi, H. T., G. E. Carvell, J. C. Brumberg, and D. J. Simons, "Effects of baclofen and phaclofen on receptive field properties of rat whisker barrel neurons," *Brain Research*, Vol. 712, no. 2, pp. 325–328, 1996.

203. Kim, H. G., K. Fox, and B. W. Connors, "Properties of excitatory synaptic events in neurons of primary somatosensory cortex of neonatal rats," *Cerebral Cortex*, Vol. 5, pp. 148–57, 1995.

204. Markram, H., M. Toledo-Rodriguez, Y. Wang, A. Gupta, G. Silberberg, and C. Wu, "Interneurons of the neocortical inhibitory system.," *Nature reviews. Neuroscience*, Vol. 5, no. 10, pp. 793–807, 2004.

205. Headley, P. M., and S. Grillner, "Excitatory amino acids and synaptic transmission: the evidence for a physiological function.," *Trends in Pharmacological Sciences*, Vol. 11, no. 5, pp. 205–11, 1990.

206. Collingridge, G., and T. Bliss, "NMDA receptors - their role in long-term potentiation," *Trends in Neurosciences*, Vol. 10, no. 7, pp. 288–293, 1987.

207. Fox, K., H. Sato, and N. Daw, "The location and function of NMDA receptors in cat and kitten visual cortex," *Journal of Neuroscience*, Vol. 9, no. 7, pp. 2443–2454, 1989.

208. Armstrong-James, M., C. A. Callahan, and M. A. Friedman, "Thalamo-cortical processing of vibrissal information in the rat. I. Intracortical origins of surround but not centre-receptive fields of layer IV neurones in the rat S1 barrel field cortex," *Journal of Comparative Neurology*, Vol. 303, no. 2, pp. 193–210, 1991.

209. Armstrong-James, M., and C. A. Callahan, "Thalamo-cortical processing of vibrissal information in the rat. II. spatiotemporal convergence in the thalamic ventroposterior medial nucleus (VPm) and its relevance to generation of receptive fields of S1 cortical "barrel" neurones," *Journal of Comparative Neurology*, Vol. 303, no. 2, pp. 211–224, 1991.

210. Salt, T. E., and S. A. Eaton, "Function of non-NMDA receptors and NMDA receptors in synaptic responses to natural somatosensory stimulation in the ventrobasal thalamus," *Experimental Brain Research*, Vol. 77, pp. 646–652, 1989.

211. Mayer, M. L., G. L. Westbrook, and P. B. Guthrie, "Voltage-dependent block by Mg2+ of NMDA responses in spinal cord neurones.," *Nature*, Vol. 309, no. 5965, pp. 261–3, 1984.

212. Monaghan, D. T., and C. W. Cotman, "Distribution of N-methyl-D-aspartate-sensitive L-[3H]glutamate-binding sites in rat brain.," *The Journal of Neuroscience*, Vol. 5, no. 11, pp. 2909–2919, 1985.

213. Feldmeyer, D., J. Lübke, R. A. Silver, and B. Sakmann, "Synaptic connections between layer 4 spiny neurone-layer 2/3 pyramidal cell pairs in juvenile rat barrel cortex: physiology and anatomy of interlaminar signalling within a cortical column.," *The Journal of Physiology*, Vol. 538, no. Pt 3, pp. 803–22, 2002.

214. Fox, K., and M. Armstrong-James, "The role of the anterior intralaminar nuclei and N-methyl D-aspartate receptors in the generation of spontaneous bursts in rat neocortical neurones," *Experimental Brain Research*, Vol. 63, no. 3, pp. 505–518, 1986.

215. Erchova, I. A., M. A. Lebedev, and M. E. Diamond, "Somatosensory cortical neuronal population activity across states of anaesthesia," *European Journal of Neuroscience*, Vol. 15, pp. 744–752, 2 2002.

216. Stryker, M. P., W. M. Jenkins, and M. M. Merzenich, "Anesthetic state does not affect the map of the hand representation within area 3b somatosensory cortex in owl monkey," *Journal of Comparative Neurology*, Vol. 258, pp. 297–303, 4 1987.

217. Kohrs, R., and M. E. Durieux, "Ketamine: teaching an old drug new tricks.," *Anesthesia and Analgesia*, Vol. 87, pp. 1186–93, 11 1998.

218. Schwarz, C., H. Hentschke, S. Butovas, F. Haiss, M. C. Stüttgen, T. V. Gerdjikov, C. G. Bergner, and C. Waiblinger, "The head-fixed behaving rat-procedures and pitfalls.," *Somatosensory and Motor Research*, Vol. 27, no. 4, pp. 131–48, 2010.

219. Robert, A., and J. R. Howe, "How AMPA receptor desensitization depends on receptor occupancy.," *The Journal of Neuroscience*, Vol. 23, pp. 847–58, 2 2003.

220. Tutunculer, B., G. Foffani, B. T. Himes, and K. A. Moxon, "Structure of the excitatory receptive fields of infragranular forelimb neurons in the rat primary somatosensory cortex responding to touch," *Cerebral Cortex*, Vol. 16, no. 6, pp. 791–810, 2006.

221. Lamour, Y., and A. Jobert, "Laminar distribution and convergence of deep and superficial peripheral inputs in the forelimb representation of rat SI somatosensory cortex.," *Journal de physiologie*, Vol. 78, pp. 158–62, 8 1982.

222. Hummelsheim, H., and M. Wiesendanger, "Neuronal responses of medullary relay cells to controlled stretches of forearm muscles in the monkey," *Neuroscience*, Vol. 16, no. 4, pp. 989–996, 1985.

223. Neafsey, E. J., E. L. Bold, G. Haas, K. M. Hurley-Gius, G. Quirk, C. F. Sievert, and R. R. Terreberry, "The organization of the rat motor cortex: A microstimulation mapping study," *Brain Research Reviews*, Vol. 11, no. 1, pp. 77–96, 1986.

224. Tsodyks, M., T. Kenet, A. Grinvald, and A. Arieli, "Linking spontaneous activity of single cortical neurons and the underlying functional architecture," *Science*, Vol. 286, pp. 1943–1946, 12 1999.

225. Fiser, J., C. Chiu, and M. Weliky, "Small modulation of ongoing cortical dynamics by sensory input during natural vision," *Nature*, Vol. 431, pp. 573–578, 9 2004.

226. Poulet, J. F., and C. C. Petersen, "Internal brain state regulates membrane potential synchrony in barrel cortex of behaving mice," *Nature*, Vol. 454, pp. 881–885, 8 2008.

227. Hasselmo, M. E., E. Schnell, and E. Barkai, "Dynamics of learning and recall at excitatory recurrent synapses and cholinergic modulation in rat hippocampal region CA3.," *The Journal of Neuroscience*, Vol. 15, pp. 5249–62, 7 1995.

228. Everitt, B. J., and T. W. Robbins, "CENTRAL CHOLINERGIC SYSTEMS AND COGNITION," *Annual Review of Psychology*, Vol. 48, pp. 649–684, 2 1997.

229. Kilgard, M. P., and M. M. Merzenich, "Cortical map reorganization enabled by nucleus basalis activity," *Science*, Vol. 279, pp. 1714–1718, 3 1998.

230. Froemke, R. C., M. M. Merzenich, and C. E. Schreiner, "A synaptic memory trace for cortical receptive field plasticity," *Nature*, Vol. 450, pp. 425–429, 11 2007.

231. Metherate, R., N. Tremblay, and R. W. Dykes, "Acetylcholine permits long-term enhancement of neuronal responsiveness in cat primary somatosensory cortex," *Neuroscience*, Vol. 22, pp. 75–81, 7 1987.

232. Lin, Y., and J. W. Phillis, "Muscarinic agonist-mediated induction of long-term potentiation in rat cerebral cortex," *Brain Research*, Vol. 551, pp. 342–345, 6 1991.

233. Metherate, R., and J. H. Ashe, "Basal forebrain stimulation modifies auditory cortex responsiveness by an action at muscarinic receptors.," *Brain Research*, Vol. 559, pp. 163–7, 9 1991.

234. Talbot, W. H., I. Darian-Smith, H. H. Kornhuber, and V. B. Mountcastle, "The sense of flutter-vibration: comparison of the human capacity with response patterns of mechanoreceptive afferents from the monkey hand," *Journal of Neurophysiology*, Vol. 31, no. 2, pp. 301–334, 1968.

235. Johansson, R. S., U. Landstrom, and R. Lundstrom, "Sensitivity to edges of mechanoreceptive afferent units innervating the glabrous skin of the human head," *Brain Research*, Vol. 244, no. 1, pp. 27–35, 1982.

236. Goodwin, A. W., and H. E. Wheat, "Effects of nonuniform fiber sensitivity, innervation geometry, and noise on information relayed by a population of slowly adapting type I primary afferents from the fingerpad," *The Journal of Neuroscience*, Vol. 19, no. 18, pp. 8057–8070, 1999.

237. Harris, J. A., R. S. Petersen, and M. E. Diamond, "Distribution of tactile learning and its neural basis," *Proceedings of the National Academy of Sciences of the United States of America*, Vol. 96, no. 13, pp. 7587–7591, 1999.

238. Vega-Bermudez, F., and K. O. Johnson, "Surround suppression in the responses of primate SA1 and RA mechanoreceptive afferents mapped with a probe array," *Journal of Neurophysiology*, Vol. 81, no. 6, pp. 2711–2719, 1999.

239. Welker, C., and T. A. Woolsey, "Structure of layer IV in the somatosensory neocortex of the rat: description and comparison with the mouse," *Journal of Comparative Neurology*, Vol. 158, no. 4, pp. 437–453, 1974.

240. Kyriazi, H. T., and D. J. Simons, "Thalamocortical response transformations in simulated whisker barrels.," *The Journal of Neuroscience*, Vol. 13, no. 4, pp. 1601–1615, 1993.

241. Pinto, D. J., J. C. Brumberg, and D. J. Simons, "Circuit dynamics and coding strategies in rodent somatosensory cortex," *Journal of Neurophysiology*, Vol. 83, no. 3, pp. 1158–1166, 2000.

242. Semba, K., "Multiple output pathways of the basal forebrain: Organization, chemical heterogeneity, and roles in vigilance," *Behavioural Brain Research*, Vol. 115, no. 2, pp. 117–141, 2000.

243. Constantinople, C. M., and R. M. Bruno, "Effects and mechanisms of wakefulness on local cortical networks," *Neuron*, 2011.

244. Vardar, B., and B. Güçlü, "Differential effects of acetylcholine and atropine on vibrotactile responses of neurons in the hindpaw representation of rat SI cortex," in *Turkish National Neuroscience Congress*, 2016.

245. Vardar, B., and B. Güçlü, "Non-NMDA receptor-mediated vibrotactile responses of neurons from the hindpaw representation in the rat SI cortex," *Somatosensory and Motor Research*, Vol. 34, no. 3, pp. 189–203, 2017.

246. Rasmusson, D. D., and R. W. Dykes, "Long-term enhancement of evoked potentials in cat somatosensory cortex produced by co-activation of the basal forebrain and cutaneous receptors," *Experimental Brain Research*, Vol. 70, pp. 276–286, 1988.

247. Devlet, B., B. Vardar, B. Babür, and B. Güçlü, "Effects of basal forebrain stimulation on the distribution of nicotinic acetylcholine receptors with alpha4 and alpha7 subunits in the somatosensory and motor cortex of rat brain," in *National Neuroscience Congress Turkey*, (Trabzon,Turkey), 2019.

248. Yusufoğullari, S., B. Vardar, and B. Güçlü, "Layer-specific distribution of muscarinic receptor M2 in the sensorimotor areas of rat brain," in *National Neuroscience Congress Turkey*, (Istanbul, Turkey), 2017.

249. Iggo, A., and H. H. Kornhuber, "A quantitative study of C-mechanoreceptors in hairy skin of the cat.," *Journal of Physiology*, Vol. 271, no. 2, pp. 549–65, 1977.

250. Wessberg, J., H. Olausson, K. W. Fernstrom, and A. B. Vallbo, "Receptive field properties of unmyelinated tactile afferents in the human skin," *Journal of Neurophysiology*, Vol. 89, no. 3, pp. 1567–1575, 2003.

251. Lumpkin, E. A., K. L. Marshall, and A. M. Nelson, "The cell biology of touch," *Journal of Cell Biology*, Vol. 191, no. 2, pp. 237–248, 2010.

252. Kandel, E., J. Schwartz, and T. Jessell, *Principles of Neural Science*, 2000.

253. Staiger, J. F., M. Möck, A. Proenneke, and M. Witte, "What types of neocortical GABAergic neurons do really exist?," *e-Neuroforum*, Vol. 6, no. 2, pp. 49–56, 2015.

254. Lubke, J., and D. Feldmeyer, "Excitatory signal flow and connectivity in a cortical column: focus on barrel cortex," *Brain Struct Funct*, Vol. 212, no. 1, pp. 3–17, 2007.

255. Vardar, B., and B. Güçlü, "Effects of Bicuculline and NMDA on the excitatory and inhibitory neurons in the rat somatosensory cortex: A Preliminary Model," in *20th National Biomedical Engineering Meeting (BIYOMUT)*, (IZMIR, TURKEY), 2016.

256. Pinto, D. J., J. C. Brumberg, D. J. Simons, and G. B. Ermentrout, "A quantitative population model of whisker barrels: re-examining the Wilson-Cowan equations.," *Journal of Computational Neuroscience*, Vol. 3, no. 3, pp. 247–64, 1996.

257. Hartings, J. A., "Processing of Periodic Whisker Deflections By Neurons in the Ventroposterior Medial and Thalamic Reticular Nuclei," *Journal of Neurophysiology*, Vol. 90, no. 5, pp. 3087–3094, 2003.

258. Khatri, V., J. a. Hartings, and D. J. Simons, "Adaptation in thalamic barreloid and cortical barrel neurons to periodic whisker deflections varying in frequency and velocity.," *Journal of Neurophysiology*, Vol. 92, no. 6, pp. 3244–54, 2004.

259. Sosnik, R., S. Haidarliu, and E. Ahissar, "Temporal Frequency of Whisker Movement. I. Representations in Brain Stem and Thalamus," *Journal of Neurophysiology*, 2011.

260. Swadlow, H. A., and A. G. Gusev, "The impact of 'bursting' thalamic impulses at a neocortical synapse," *Nature Neuroscience*, 2001.

261. Bruno, R. M., and B. Sakmann, "Cortex is driven by weak but synchronously active thalamocortical synapses," *Science*, Vol. 312, no. 5780, pp. 1622–1627, 2006.

262. Keller, A., and E. L. White, "Synaptic organization of GABAergic neurons in the mouse SmI cortex.," *The Journal of Comparative Neurology*, Vol. 262, no. 1, pp. 1–12, 1987.

263. White, E. L., G. Benshalom, and S. M. Hersch, "Thalamocortical and other synapses involving nonspiny multipolar cells of mouse SmI cortex," *Journal of Comparative Neurology*, Vol. 229, pp. 311–320, 11 1984.

264. Jensen, K. F., and H. P. Killackey, "Terminal arbors of axons projecting to the somatosensory cortex of the adult rat. II. The altered morphology of thalamocortical afferents following neonatal infraorbital nerve cut.," *The Journal of Neuroscience*, Vol. 7, pp. 3544–3553, 1987.

265. Yildiz, M. Z., and B. Güçlü, "Relationship between vibrotactile detection threshold in the Pacinian channel and complex mechanical modulus of the human glabrous skin," *Somatosensory and Motor Research*, Vol. 30, no. 1, pp. 37–47, 2013.

266. Devecioğlu, I., and B. Güçlü, "A novel vibrotactile system for stimulating the glabrous skin of awake freely behaving rats during operant conditioning," *Journal of Neuroscience Methods*, Vol. 242, pp. 41–41, 2015.

267. Ling, G., and C. E. Lathan, "Electroceuticals," 2018.